THE INVESTIGATION OF IONOSPHERIC IRREGULARITIES

by

A.C. Beresford B.Sc. (Hons)

A Thesis

presented for the degree of

Doctor of Philosophy

at the

University of Adelaide

Physics Department

March 1973

CONTENTS

SUMMARY

Chapter 1 reviews the historical development of the various ways of studying ionospheric irregularities.

Chapter 2 describes the solar cycle, seasonal and daily changes of spread F in the Australian region. It also shows that spread F is not related to magnetic activity.

Chapter 3 describes the instrumentation and data handling methods used in this thesis. Chapter 4 describes the observation of large scale ionospheric irregularities, as observed using total electron content observations with low orbit satellites.

Chapter 5 reviews the observations of total electron content using geostationary satellites. The results of observations are given and compared in Chapter 6.

Chapter 7 studies three facets of the diffraction of radio waves and the statistics and properties of the field strength pattern observed. These are, the minimum in the power spectrum of the amplitude fluctuations, the occurrence of small very dense irregularities, and the investigation into full correlation analysis applied to satellite records.

Chapter 8 reviews the diurnal and seasonal variations in scintillation at mid-latitudes. The observations made during eight months, September 1969 to May 1970 are presented and compared with previous observations. No correlation with magnetic activity is found and there is a strong seasonal variation of scintillation index for both daytime and night time scintillations.

Chapter 8 summarizes the conclusions of previous chapters and suggests lines for further investigation.

PREFACE

Here is given a chronological account of the events involved in my research. It is tendered as a part explanation of the variety of work presented. Originally more work was intended on irregularity heights using the triangle of receivers established by Parkin. Some modifications to the equipment were necessary for this. After some observations were made, none of any use, two of the three antennae were stolen for the copper. Replacing these took some time. At about this time the transmissions from satellites BEB and BEC were not continuous due to power supply problems. At this point it was decided that observations with them would be impossible, so it was decided to observe the geo-stationary satellite Syncom 3 and obtain drift velocities with the triangle. Observations on 40 MHz were to continue on a single receiver when signals were available.

Converters were ordered, from overseas, to convert from the satellite telemetry band down to the 20.005 MHz frequency of the receivers already possessed. Some difficulty was experienced in adjusting the frequency of the oscillators in these converters and there was a problem of thermal drift. At about this time public irrigation work at the westerly triangle site displaced the receiver and, because of potential electrical interference, made that site unusable. Meanwhile more suitable converters had been purchased

and some scintillation observations made at the St. Kilda field station using Syncom 3.

The building of the rotating aerial system for total content observations was started and the mechanical part finished in good time. At this time it was intended to use it on Syncom 3. The electrical interference at St. Kilda was rising however so a movement of all the equipment to the Buckland Park field station was decided upon. This included the 40 MHz equipment for one site, the rotating aerial and the equipment for the three sites for observing Syncom 3. Resiting the equipment and laying out the communications lines occupied three months. During this time Syncom 3 exhausted the fuel supply for the small rockets which kept it at a fixed longitude and it drifted westwards, relative to the earth's surface. This was not realised until the cause of the weak signal was investigated.

At this time the authorities concerned decided to switch off Syncom 3. This necessitated choosing a new satellite, and ATS1 was chosen. Although this was at a very low elevation, which was why it had not been considered before, it turned out to be more suitable. However, new converters had to be obtained and this caused a delay of several months. The first observations of ATS1 concentrated on obtaining scintillation occurrence and index observations. It was

decided to purchase a circularly polarized antenna for this work. Testing this involved two months because of the discovery that the signal appeared linearly polarized anyway, due to ground effects. This is discussed in Chapter 2. Then the rotating aerial was set up. Some difficulty was experienced with inductively coupled coils used to feed the signal to the converter. It was found necessary to tune them in situ which was awkward and made them sensitive to the weather. The work on the triangle of receivers for drift work could not go on at this time because of occupation with the rotating aerial.

On completing this, work started on siting the converters and receivers at the remote sites at Buckland Park. This involved a certain amount of electronics, and of field work at each site. This work was nearing completion when the equipment at the two remote sites of the intended triangle was stolen. That event largely terminated the observations, as it was decided to finish then and write up the material already obtained.

DECLARATION

To the best of the author's knowledge this thesis contains no material previously published or written by another person, except where due reference is made. It contains no material which has been accepted for the award of any other degree or diploma in any University, except where due reference is made.

A. C. Beresford

Adelaide University
March, 1973.

ACKNOWLEDGEMENTS

I must first acknowledge the help and encouragement of my supervisor Dr. B.H. Briggs.

I owe help in data analysis and in diffraction theory to former colleagues and colleagues in the Radiophysics group of the Physics Department, particularly Dr. I. A. Parkin and Dr. E. M. Doyle and Dr. M. G. Golley.

The work would have been impossible without the technical help of Mr. L. A. Hettner who constructed the rotating aerial system and built most of the antennae and many other things besides. My thanks to Mr. J. Smith, Research Officer, whose unfailing help with the electronic aspects contributed to the success of the work and the personal knowledge of the author.

Lastly I must thank my parents for support and encouragement during the work involved in this thesis. Without their help it would have been impossible for me to complete it.

CHAPTER 1

A SURVEY OF RADIO METHODS

1.0 Historical

The exploration of the ionosphere by the use of radio waves began with the work of Appleton in the 1930's.

An early advance, the use of pulsed transmissions, was pioneered by Breit and Tuve in America and taken up by Appleton in England. This work led to the development of the ionosonde, with which echoes from a series of heights in the ionosphere are obtained by means of a progressive change in radio frequency. The output (usually on photographic film) is a plot of group delay versus frequency, and is called an ionogram. A world wide network of these ionosondes has been in operation since the 1930's. The study of ionograms from these stations has allowed the main global features of the ionosphere to be studied. This investigation has now been extended to the region above the electron density maximum using ionosondes carried in satellites. The electron density versus height curve can be computed from the ionogram, but before the development of computers such a calculation was far too time-consuming to be routine. Now the use of computers means routine calculation of the electron density profile is possible.

During the development of this method, some information was also obtained about "fine scale" structure of the ionosphere. It was seen that the pulse returned from the ionosphere was at times much longer in duration than the transmitted pulse. The different parts of the lengthened echo varied randomly in strength, in such a way as to suggest a scattering process. For echoes returned from the F region the phenomenon was particularly marked, being visible on ionograms as well as fixed frequency transmissions, it has become known as "spread F".

It was also found that successive members of a train of returned pulses often varied in strength, in a random way, even if no obvious spreading was present. This phenomenon, known as "fading" was studied extensively by Ratcliffe and Pawsey in the late 1930's. Studies using spaced receivers led to a "random screen" model of the reflection process. In this model the ionosphere is assumed to behave like an irregular diffracting screen which moves horizontally due to the action of a wind or electromagnetic force. Developments of this idea led to extensive studies of world-wide ionospheric drifts by the spaced receiver fading technique, and to the development of quite sophsticated methods of analysis of the records by correlation techniques. Similar methods are applied to receiver records of satellite signals later in this thesis.

The development of radio-astronomy allowed, for the first time, the study of the effects of the ionosphere on a radio wave transmitted through it. In the range of frequencies first used, it was found that the intensity of discrete radio sources sometimes varied in a random manner. The phenomenon is the radio analogue of the "scintillation" or "twinkling" of stars in the visual region of the spectrum. Cooperative work at Cambridge and Jodrell Bank showed the effect to be due to irregularities of ionization in the ionosphere. Scintillation was found to be present mainly at night, but did not occur every night. For mid-latitudes a close correlation was established with the occurrence of spread F, suggesting that the same irregularities were responsible for both phenomena. Spaced receiver observations carried out at Cambridge showed that these F region irregularities are anisotropic, being elongated along the direction of the geomagnetic field. Their scale was about one kilometre perpendicular to the field direction, and averaged about five kilometres along the field. Earlier work at Cambridge had already shown that the irregularities causing scintillation were mainly in the F region. Indeed, because of the mechanism, irregularities in the E region cannot usually cause intense s cintillation since the wave cannot propagate far enough from the screen for interference of the diffracted waves to cause much amplitude scintillation. One exception to this rule is the auroral zone E region where scintillation causing irregularities have been observed. The other exception

is daytime scintillation in lower middle latitudes which has been shown to be correlated with sporadic E.

Observations by Gardner and Pawsey in the1930's using powerful transmitters revealed yet another type of irregularity. Echoes were detected from the D region between fifty and ninety kilometres. Total reflection was impossible because the transmitted frequency exceeded the D region critical frequency by at least an order of magnitude. The observed echoes are due to scattering from gradients in electron density or collision frequency between neutral atoms and electrons. The scattering at a given range usually exhibits the characteristics of being formed from independently moving scatterers. However this was not always the case. An important method of determining D region electron density is based on measurements of the ratio of the scattered signal amplitude for ordinary and extraordinary polarization of the transmitted wave.

At the same time as the "fading" and "spreading" of reflected echoes was being studied another phenomenon was first observed. This was what was later to be called the "Travelling Ionospheric Disturbance" (T.I.D.). T.I.D.'s were first observed as distortions and additions to the normal F region reflection on an ionogram. These travelled downward in apparent range with time. On fixed frequency records they appeared as a variation of reflection height with time. The weaker examples seem similar to some categories of spread F,

particularly the "satellite traces" observed by workers in Brisbane. Observations of these disturbances at widely separated places showed that they sometimes travelled several thousand kilometres before losing identity, although most only travelled several hundred kilometres. They also appeared to have a size of the order of fifty to two hundred kilometres, and a horizontal velocity of the order of seventy metres per second. The apparent downward movement was shown to occur because the disturbance is in the form of forward tilted wavefronts moving horizontally. It is the phase velocity which is observed because one is following the changes in electron density as the disturbance propagates. A characteristic of the disturbance is their "frontal character," i.e. they are larger perpendicular to the direction of propagation. The disturbances showed a tendency to propagate towards the equator in both hemispheres, although poleward movement has been observed and Munro found a seasonal change in the direction of propagation.

2.0 More Recent Observations

2.1 Ground Based Satellite Techniques

With the advent of man-made satellites observing techniques developed earlier could be applied to the radio transmitters carried on these vehicles; at first only "orbitting" satellites were available: but since 1964 "geostationary" satellites have also become

available. This has lead to much published work on satellite "scintillation", analogous to radio star scintillation. The use of satellites has enabled a better picture of the large scale features of the irregularity distribution to be obtained because of the high time resolution possible using satellites in medium altitude orbits.

A picture emerges of a region around the magnetic equator,on the nightside, where irregularities are strong and two regions around the magnetic poles, bounded by the auroral oval where the irregularities are also strong. The equatorward boundary of the disturbed polar regions is usually sharply bounded. In common with other phenomena, the boundary moves equator-wards during increased magnetic activity.

The use of geostationary satellites for scintillation work allows a fixed part of the ionosphere to be continuously observed for the occurrence of irregularities. This is very helpful in studying the average diurnal and seasonal behaviour separately. With either radio stars or low altitude satellites diurnal and seasonal effects are confused by the slowly changing local time when such sources are observable.

Scintillation observations using a geostationary satellite are discussed in Chapter 8.

Observations of the ground pattern of satellite scintillation enable the height of the irregularities to be determined. The elongation along the magnetic field has been confirmed. In fact observations suggest a larger elongation than found by radio star work.

It is a fairly common phenomenon for the intensity of scintillation to increase as the line of sight to an "orbitting"satellite approaches the geomagnetic field. This confirms the irregularities are field aligned. Thus most satellite observations support a model of irregularity structure of randomly placed, highly elongated increases or decreases in electron density.

There are however quite a number of observations of signal amplitude which cannot be explained by such a "random phase screen" model. An example is shown in Chapter 7. Other examples often exhibit patterns reminiscent of the diffraction pattern of a sharp edge or an opaque strip. Still others just show a quasi-periodic structure suggesting two ray interference. The most plausible model to explain this type of record is the presence of an isolated, very dense irregularity, usually of somewhat larger size than the "scale size" of the random screen model. Quite random"scintillation-like" patterns could be produced by a succession of several such irregularities.

Another use of satellite radio transmitters is the observation of the integrated electron content from the observing point to the satellite. This is usually converted to an equivalent vertical total electron content for purposes of intercomparison. Two properties of the propagation are used. The first is the change in the refractive index, for radio waves, with frequency. This enables the Doppler shift caused by the changing optical path to be found by comparing Doppler shifts at coherent, harmonically related frequencies. A related technique is to use the difference in group path, by comparing the time delay of the modulation on a high and a low frequency carrier.

The second property used is the fact that for upper HF and VHF frequencies the presence of the geomagnetic field causes the refractive indices for oppositely polarized arcular polarizations to be different. This in turn means that the plane of polarization of a linear polarized wave will rotate as it travels. This rotation can be shown to be proportional to the integrated product of the electron density and the component of the field along the line of sight. This is different from the Doppler shift, discussed previously,which is proportional to the total electron content. It is called Faraday rotation after the original discoverer of the effect M. Faraday. He discovered the effect with visible light in glas subject to a strong magnetic field.

Observations of the total electron content by both methods have contributed to knowledge of the average diurnal behaviour of the ionosphere, and to knowledge of the ion chemistry involved in the growth and decay of the ionosphere. Geostationary satellites are particularly suitable for such observations because the part of the ionosphere that is observed is the same, and it is easy to get continuous records. A summary of some work in this area and a few observations are given in Chapter 5.

Observations using satellites in orbits such that a "slice" of the ionosphere is sampled enable profiles of the spatial structure to be investigated independent on any motions on the medium itself. Such work has complemented and extended ground based observation of T.I.D.'s. Many of the T.I.D.'s have been shown to be of a quasi-periodic nature. Observations by Russian workers using the Doppler effect have shown that a complete spectrum of irregularity sizes exists from the range of the smallest observable size (about 5 kilometre wavelength) up to several hundred kilometers. T.I.D.'s and their probable cause, internal gravity waves, are discussed more fully in Chapters 4, 5 and 6.

T.I.D.'s can also be observed using total electron content techniques and stationary satellites. Spaced receivers enable the velocity and direction of the disturbance to be calculated. One

particular type of T.I.D. shown by these observations is the type originating in the auroral zone E region when the auroral electrojet intensities. The resultant rapid heating causes a long period T.I.D. to appear in the mid-latitude F region. The intensification of the current in the electrojet occurs during a certain phase of the auroral sub-storm. An observation of such an event is reported in Chapter 6. Related phenomena are abrupt and large increases in total electron content are observed at some places during some storms. The effect seems to be due to a lifting of the whole ionosphere by a change in the F region wind systems caused by the heating mentioned above. Whether an increase is observed depends on the local time of day of the start of the heating. An observation of such an event is also reported in Chapter 6.

Another important use of total electron content observations is in connection with the study of the global morphology of the ionosphere. Work in this field has involved two regions. Firstly the shape and behaviour of the equatorial anomaly can be studied. This anomaly is in the behaviour of the latitudinal profile of electron density. There are two maxima either side of the equator instead of one maximum underneath the sun.

The other feature, first observed with the topside sounder, is

the polar trough in electron density. This is an annular region of lower electron density about each pole. It is about five degrees of latitude wide. The position is dependent on the level of magnetic disturbance. It has been shown to be related to the boundary of the plasmasphere, called the plasmapause. This is a surface in the magnetosphere across which the density of plasma drops rapidly. The troughs are the intersection of this surface with the F region. No observations of this phenomenon are discussed here, because the trough is not observable from Adelaide.

2.2 Topside Sounding

Since satellites have been launched which carry ionosondes, ionograms of the region of the ionosphere above the F region peak have become available. Spread F phenomena are visible on such ionograms in the three main regions of the equator and the two polar regions. Certain types of spread F can be explained by the capture of radio waves in field aligned waveguides. Other types have been explained by scattering. The occurrence of topside spread F is higher than bottomside spread F. In the polar regions it usually occurs all the time.

Many other peculiarities occur on topside ionograms. These are mostly resonances, occurring in the plasma near the satellite. These usually occur at a frequency formed from combinations of the plasma

frequency, the gyrofrequency and the transmitter frequency. They are useful diagnostics of the state of the plasma.

T.I.D.'s have been observed using topside sounder ionograms but not much work has been done. If appreciable horizontal gradients exist it is often difficult to analyse ionograms properly because of the possibility of non-vertical propagation.

2.3 Satellite Observations

Several satellites, notably Explorer 20 and Allouette 1,2,3 and Explorer 33, have carried instruments capable of making extensive observations of electron density and temperature, and ionic composition. This has led to a major improvement of the knowledge of the physics and chemistry of the ionosphere and the inner magnetosphere. Most experiments have been looking for the average properties, and the sampling rates have not been fast enough to study small irregularities. Some results from Allouette 2 show that the region of occurrence at one thousand kilometre altitude is confined to the polar regions.

Phenomena thought to be T.I.D.'s have been seen using electron density measurements. The most extensive experiment for such studies consisted of some joint observations made using satellite 1966 44A. This utilized the electron density measurements and the

neutral atmosphere density measurements for the study of which the satellite was specially launched. This was the first time such waves had been detected in the neutral atmosphere, rather than by their indirect effects.

3.0 Recent Ground Based Observations

Several new techniques have been developed for observing T.I.D.'s and other ionospheric movements. The presence of T.I.D.'s causes the changes in ground back-scattered signals. With appropriate large antennas this can be seen. There is some difficulty in exact interpretation of the observed signals because of the complexity of ground backscatter phenomena in general. The best approach has been through computer modelling using simplified models of the disturbance.

Another very useful technique is the use of moderately oblique fixed frequency CW signals. The frequency is monitored and the Doppler shift caused by the changing phase path recorded. Using spaced transmitters and either single or spaced receivers, T.I.D.'s have been extensively observed. The optimum spacing seems to be about one hundred kilometres. The method is a very useful one for monitoring snd studying the spatial structure of T.I.D.'s since the

transmitter can have fairly low power because the receiver bandwidth is small, lessening interference problems.

Another technique which should be mentioned is the phase-path method. This method measures the changes in the phase of the returned echo ehen using a pulse transmitter. The phase standard is related to the frequency controlling the transmitter. Thus the equipment measures changes in the total "phase path" to the ionosphere and back to the ground. The technique can be used on all ionospheric regions but has been most extensively applied to the D and E regions. Use of the technique has shown that D region scattered echoes are sometimes coherent. Occasionally periodic changes in phase path have been seen indicating the presence of gravity waves in this region. Using moderate (one kilometre) spacing of receivers the method has been used for spaced receiver work. This has indicated the presence of disturbances in the E region which are probably internal gravity waves. These disturbances are relatively large (twenty to fifty kilometres) and it is suggested that some of the fading of reflected waves is due to the interference of the several possible rays under such conditions.

Other recent related work has been to give the normal ionosonde a directional capability by using an interferometer as an antenna. By this means off vertical echoes can be distinguished, and errors due to this cause eliminated in the determination of electron

density profiles, reflection height determinations, and in studies of spread F and sporadic E.

The spaced receiver method has been applied to many different ionospheric phenomena. The theory of the method has been extended to cover the case of more than three receivers. If a large number of antennae are used as in Buckland Park array, the spatial and temporal characteristics of the pattern can be separated and such things as pattern velocity can be found independently of assumptions about the form of the pattern.

The only important observing technique not mentioned so far is the incoherent scatter radar. This technique utilizes a very high power radar, with large gain receiver and transmitter antennae to detect the incoherently scattered signal from electrons. Adequate height resolution is usually obtained by using a pulse transmission system, although bistatic systems can obtain height resolution by using narrow antenna beams. By observing the characteristics of the returned signal as a function of height, several important parameters of the ionosphere can be deduced. These are electron density, electron and ion temperatures and ion composition. The electron belocity component along the beam direction can also be observed. For some sites this enables neutral atmosphere winds to be calculated. In this thesis some observations using these

techniques are discussed to support arguments about T.I.D.'s. No new observations are reported.

4.0 Other Methods

Since the early 1950's an important technique for finding the neutral atmospheric motion in the D and E region has been the motion of self luminous or sunlit trails of contaminants released from sounding rockets. The small scale vertical structure shown in the wind profiles obtained has two causes. The first is the fact that the tidally induced winds predominate at ionospheric heights and some of the allowable modes have quite small vertical wavelengths. The other cause is either internal gravity waves or turbulent flow. It could possibly be both. A characteristic of the trail itself, visible on the photographs used to measure motion, is the occurrence below a nearly fixed height of small irregularities. These are due to turbulence. At a height of about 105 km turbulent motion is damped out by increasing molecular viscosity. The height at which this happens is called the turbopause. It is important as defining the height above which hydrodynamic turbulence cannot compete with viscosity.

Contaminants can be released in the F region. The one usually used is barium. This partially ionizes in sunlight and so two clouds

of matter form. Both are visible by fluouresence. The ionized cloud drifts under the joint influence of the ambient electric field and the neutral atmosphere wind. The neutral cloud drifts in the wind. The ionized cloud becomes elongated along the magnetic field because diffusion across the field lines is unhibited for charged particles. This cloud often becomes irregular, breaking up into a collection of fluted columns. A form of plasma instability is thought to be the cause.

5.0 Theory of Origin

Many theories have been put forward to explain the cause of the several forms of irregularities studied. Thus far no theory has offered a reasonable explanation of all the characteristics of any given type of irregularity. It is likely that several different causes exist, if only because of the large differences in scale. The matching of theory and observation is continually being complicated because most methods of observation cannot observe a wide enough range of scale size.

CHAPTER 2

"SPREAD F" AND MAGNETIC ACTIVITY

1. Introduction

"Spread F" is defined as a spread in the F region trace on ionograms. Ionograms show a display of apparent reflection height against frequency. There are two main types of spread F, illustrated in Figure 2.1(a) and 2.1(b). Figure 2.1(a) illustrates "range spreading", where the same frequency is reflected at different ranges. "Frequency spreading" is illustrated in Figure 2.1(b) where, near the critical frequency, reflection at a given range occurs over a spread of frequencies. The phenomenon is also divided into equatoral and mid-latitude types, which have different solar cycle and seasonal behaviour. Equatorial spread F occurs at stations within about twenty degrees of the magnetic equator. It is predominantly range-spreading. It will not be discussed any further as it appears to be a separate phenomenon from spread F at non-equatorial stations.

The two outstanding characteristics of mid-latitude spread F are its occurrence mainly at night, and its negative correlation with indicators of solar activity.

(a)

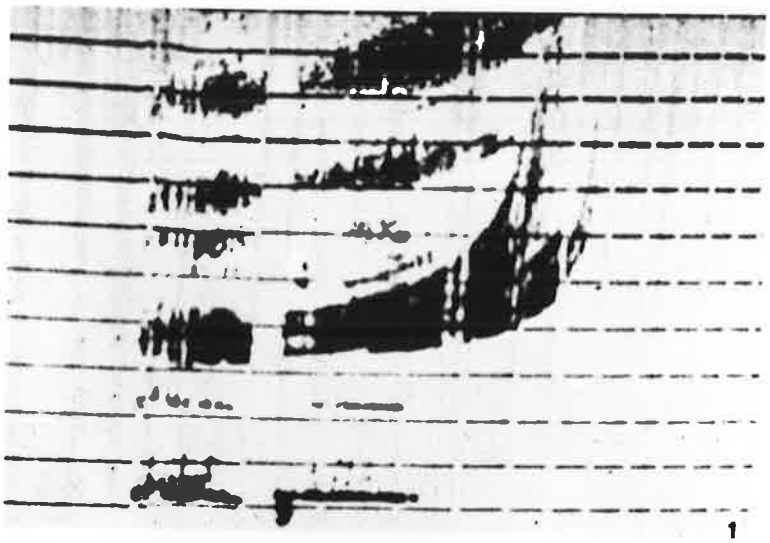

(b)

Figure 2.1 Types of Spread F. (a) Range spreading. (b) Frequency spreading.

2. Causes of Spread F

One possible cause of spread F is partial reflection by irregularities aligned along the lines of force of the magnetic field. This was put forward by Booker (1956). However King (1970) has shown that ionosondes have such a small dynamic range that partial reflections would not be detected. That there are field aligned irregularities cannot be disputed, from the observations of the ground pattern of satellite scintillation (e.g. Parkin, 1967). The second possible cause of spread F is a wave guide mode of reflection whereby the radio waves are trapped in a field aligned waveguide. They propagate to the reflection height and then back along the same path to the receiver. This produces a spread in range. Bowman (1960a, b) has shown that both range and frequency spreading at Brisbane (dip 57^{o}S) were due to total reflection from an ionosphere in which the iso-ionic contours had ripples of wavelengths between twenty and a hundred km. The only difference between range spreading and frequency spreading was that the maximum plasma density varied more for the latter. McNicol et al. (1956) had suggested that a kink or step in the iso-ionic contours was a better explanation, particularly for situations where separate traces could be resolved. King (1970) takes this up and suggests that all types of spread F are related. Frequency spreading is merely the decay of range spreading. He shows that if something

causes a local movement of ionization down a tube of force, then range spreading develops near the bottom of the F region. As the recombination smoothes out the irregularities at the bottom, variations in electron density still exist near the peak of the layer and above. King (1970) proposes that the forces that give the downward movement are local small scale electric fields, derived from the E region.

3. Effect of Magnetic Activity

The relation between spread F and magnetic activity, for a range of latitudes, was investigated by Shimazak (1969). He found that, for mid-latitudes, there was a positive correlation between the probability of occurrence of spread F and magnetic activity. For the occurrence of Spread F he used the appearance of the qualifier F in the tabulated data of f_oF2. This is easier than using the amount of spreading of the trace, but the latter is obviously a better and more quantitative index of spread F. However considering the difference between ionosondes, such a choice is the only one possible if many stations are to be compared. Otherwise many hundreds of thousands of ionograms would have to be read. Briggs (1965), using ionograms, showed that for Slough, spread F lagged behind magnetic activity (as given by the K index). The

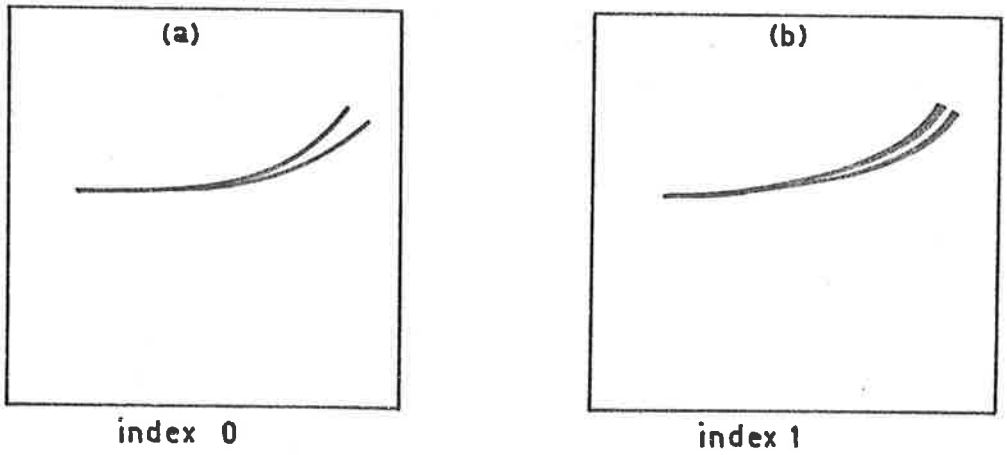

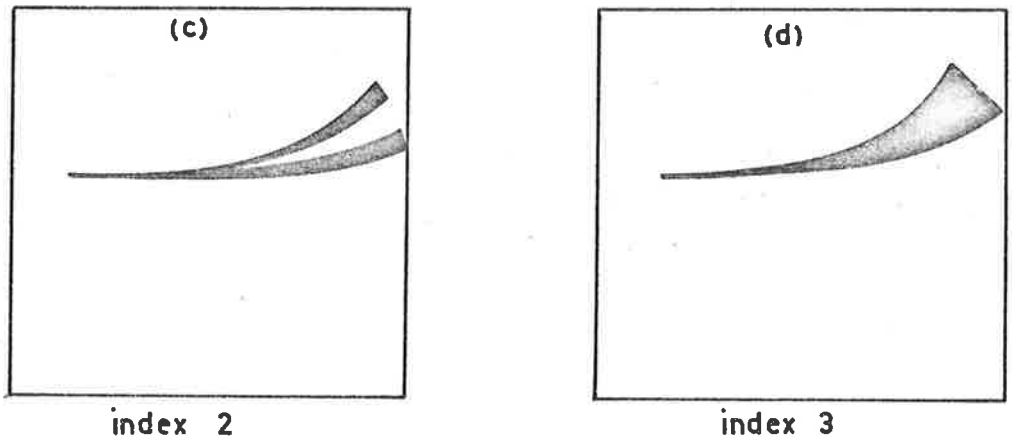

Figure 2.2 Assigning the spread F index.

amount of the lag was dependent on the phase of the sunspot cycle. Raju et al. (1969) have shown that the lag varies with latitude. Their results for Slough agree with those of Briggs (1965) for the previous cycle. Such an agreement is not trivial because Raju et al. used the occurrence of the qualifier F in the tabulated data, rather than an index of the amount of spread present near f_oF2 as used by Briggs. Bowman (1971) showed that the planetary index Ap reached a maximum three days before epoch in a superposed epoch analysis, using days of high spread F as zero epoch. Bowman also found that spread F showed a peak three days after days of low sunspot number.

Equatorial zone Spread F behaves differently, being negatively correlated with the magnetic activity index Kp.

4. Seasonal and Solar Cycle Variation

Briggs (1965) showed that the intensity of spread F at Slough had a winter maximum and a summer minimum. Reber (1956) and Singleton (1962) have given examples of stations where there is more spread F in summer than in winter. Outstanding among these are the Japanese stations. Reber (1956) defined a "spread F equator", which is different from either the geomagnetic or the geographic equator. It also appears to shift during the solar cycle.

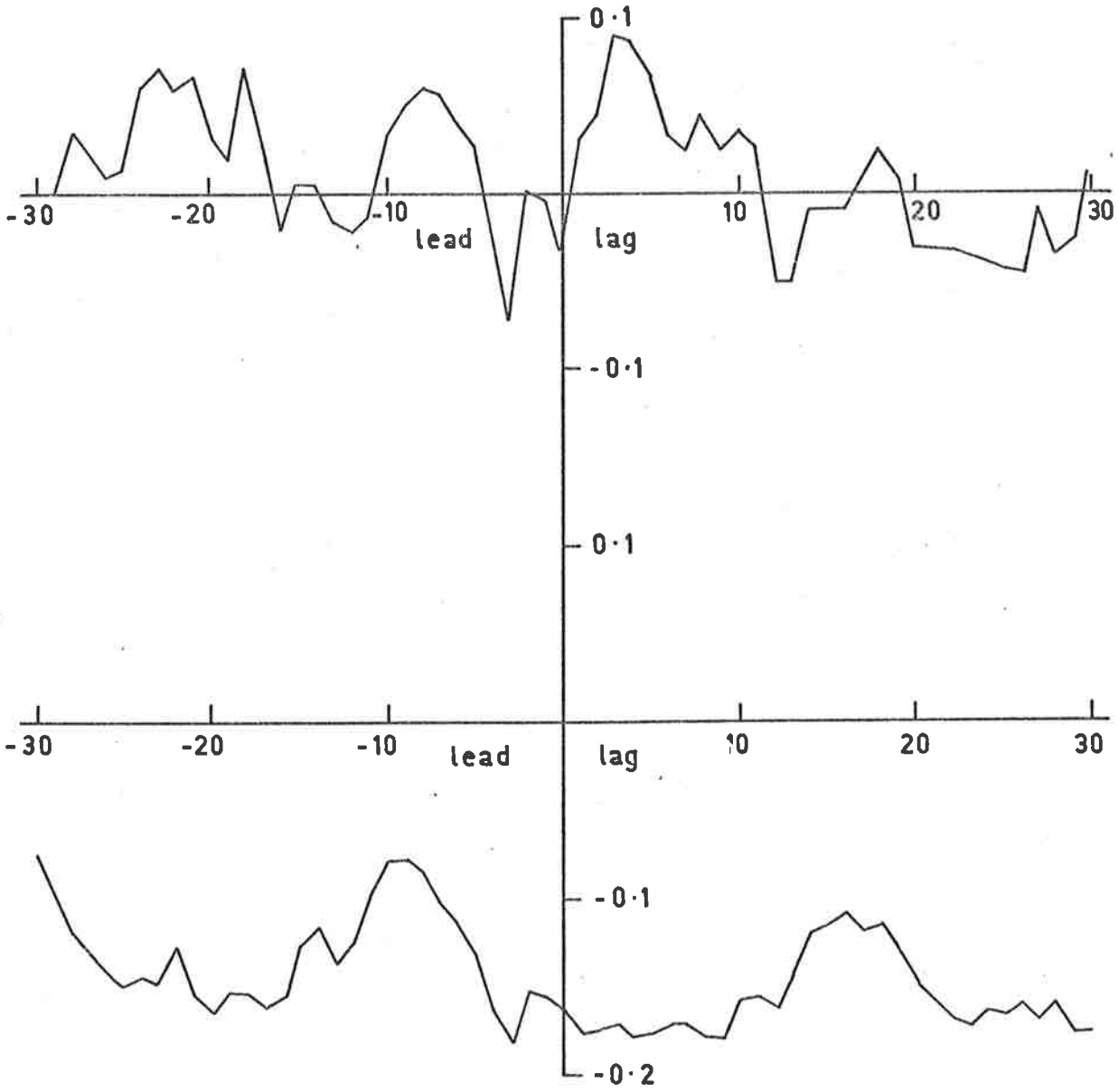

Figure 2.3(a) Cross-correlation between Woomera Spread F index and the daily sum of Kp.

Figure 2.3(b) Cross-correlation between Woomera spread F index and exospheric temperature

The work of Shimizaki (1959) also shows which stations have a summer maximum of probability of occurrence. These researchers all lump together the data in the months November, December and January, and May, June and July, to get seasonal variations. If the variation is not a simple one from a maximum in winter to a minimum in summer such a grouping can be misleading as to the form of the variation.

Bowman (1964) had suggested that there is a relation between spread F occurrence and the semi-annual variation in neutral particle density, maximum spread F occurring when density is a minimum. This was derived from long term averages of occurrence probability for three Japanese and three Australian stations. This hypothesis seems doubtful because not all ionosphere stations show such a variation. In Bowman's own diagram the result for Canberra shows hardly any sub-peak in summer.

5. Spread F at Woomera

To find out more about the occurrence of spread F, indices used by Briggs (1958a) were obtained from Woomera ionograms. A value of 0, 1, 2 or 3, was assigned to each hourly ionogram to indicate the spread of the trace near the F region critical frequancy. Sketches of representative ionograms for the indices are

shown in Figure 2.2. Ionograms for most days June 1, 1961 to December 31, 1963 were available, except for the whole of March 1963. From these hourly values an average was taken over the night-time, defined as 2000 LT to 0400 LT. This was used as a "daily" index of spread F for the date of the morning section of the interval. This interval of local time was chosen because spread F is a night-time phenomenon. Magnetic activity was indexed using the partial daily sum of the planetary K index. This was taken over the interval 0900-2100 UT. The date was assigned to be consistent with the spread F index. Other methods for calculating a daily magnetic index were tried, e.g. the 0 to 24 hr UT sum, and the 12 hr to 12 hr sum, but results were not significantly different. When an index of more local activity was used, such as K index for Toolangi, summed over the night-time, again the results were not significantly different. Atmospheric density was indexed using the global temperature minimum, T_N, as a single parameter. This was obtained from published values of Jacchia and Slowey (1963). The temperature was derived from density measurements using the air drag on 1961 Delta One, converted to exospheric temperature using the Jacchia 1965 model atmosphere (Jacchia, 1965). The daily time series formed in these ways were cross-correlated for shifts of $\pm$ 54 days using a programme which allowed for missing values in the time series.

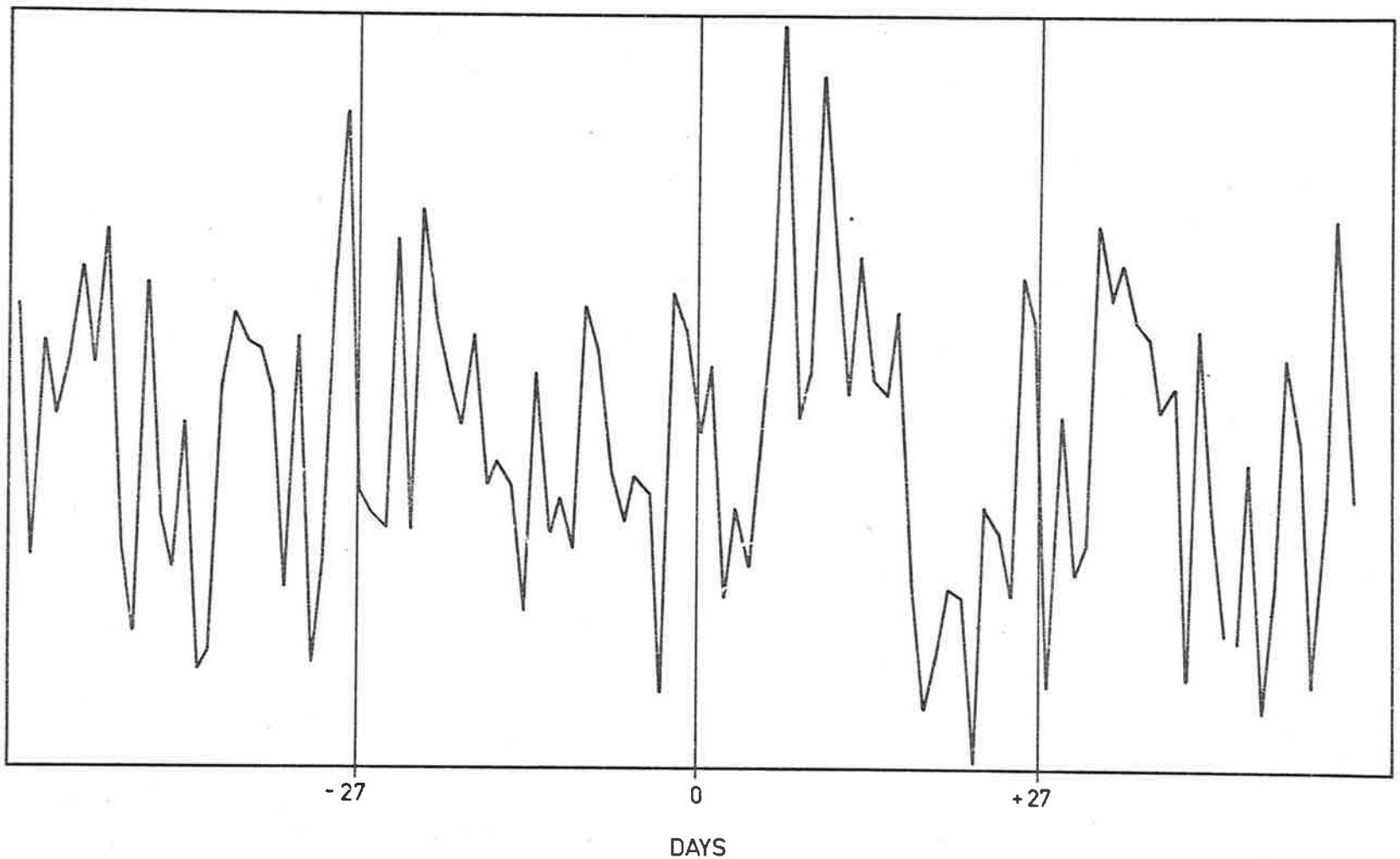

Figure 2.3(c) Superposed epoch analysis of Woomera spread F index using days of low 10.7 cm flux as epochs.

The probability of occurrence of spread F was investigated for Woomera, Canberra and Brisbane using the percentage occurrence of the qualifier F in the tabulated midnight values of f_oF2 for each month. Although this is not the best method for studying spread F, as explained earlier, it is the only practicable method if long periods of time are to be covered without excessive amounts of ionogram analysis. Table 1 shows the geographic and geomagnetic coordinates of the ionospheric stations used (WDC-A, 1970).

TABLE 1

Station	Geographic		Geomagnetic	Dip Angle
	Latitude	Longitude E	Latitude	
Woomera	-31.0	136.3	-41.2	-63^o
Canberra	-35.3	149.0	-44.0	-65.9
Brisbane	-27.5	152.9	-35.70	-57.4

The long series of percentage occurrence for Brisbane was compared with the shorter length of data for Woomera.

6. Results

The maximum correlation between the spread F index and magnetic activity was $0.089 \pm .035$. This is barely significant, especially

if one looks at the cross-correlation curve itself (Figure 2.3a). The data was split in two and cross correlated. No significant correlation was found. The cross-correlation between spread F and the exospheric temperature is given in Figure 2.3b. The reason for the constant negative cross correlation is discussed in the next section. The superposed epoch analysis of the index, using days of low 10.7 cm flux as epochs is given in Figure 2.3c. This does not show any peak near +3 days as in the results of Bowman (1971). Neither is any 27 day recurrence visible. The auto-correlation function of the index gives some useful results about the tendency of spread F to occur in groups of days. Table 2 gives the values of the auto-correlation for the first five shifts.

TABLE 2

Shift	Auto-Correlation
1	.291 ± .03
2	.197 ± .03
3	.197 ± .03
4	.169 ± .03
5	.175 ± .03

The significant values at shifts four and five represent the effect of the long term trends in the index. Because the seasonal effect

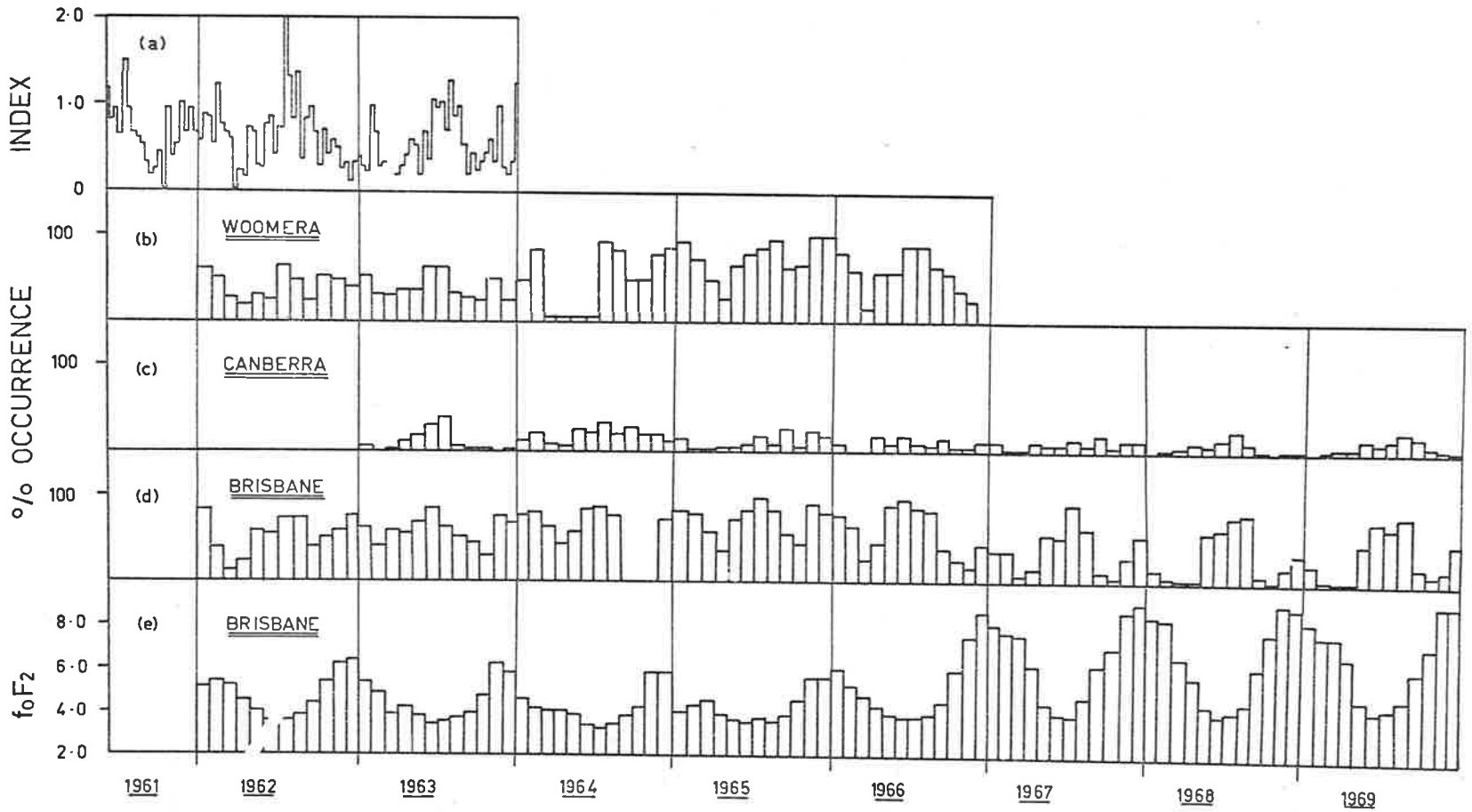

Figure 2.4 (a) to (d) Spread F occurrence and index. 4(e) FoF_2 monthly midnight median.

is so strong there is a significant component in the auto-correlation that would peak at one year. Any shorter term effects we are looking for are added onto this base line. The result suggests that there is significant correlation between one night and the next, but not any significant correlation between a night and the second night after it, other than the general effect of the seasonal variation.

A plot of the ten day averages of the nightly spread F index is shown in Figure 2.4(a). For comparison purposes the monthly percentage occurrence of spread F at midnight for Woomera, Canberra and Brisbane are given in Figures 2.4(b), 2.4(c) and 2.4(d) respectively. The semi-annual tendency for the spread F index for Woomera is noticeable. This is also evident in the percentage occurrence plots for Woomera for 1965 and 1966. Brisbane shows a clear semi-annual variation of occurrence of spread F. Canberra shows no such semi-annual variation and shows much less spread F than Woomera. To illustrate the effect of the solar cycle, Figure 2.4(e) shows the monthly median value of f_oF2 at midnight for Brisbane for the same time interval. This shows that the summer peak of occurrence gets smaller as summer midnight critical frequencies increase.

7. Discussion

There seems to be no correlation between spread F at Woomera and magnetic activity. There is also no day to day correlation between spread F and the neutral atmospheric density. The nearly constant negative correlation occurs because there is a semi-annual component in the spread F index, (Figure 2.4(a)) which is in antiphase to the semi-annual variation in atmospheric density. The lack of any peak in the cross-correlation function shows that there is no detailed day to day correlation. It is well known that just because two variables have an antiphase or inphase variation, they need not be directly related. Therefore there is probably no direct physical connection between variations of spread F and variations in atmospheric density. The auto-correlation function of the spread F index shows that there is only a slight grouping of nights of high spread F. This is similar to the results of Briggs (1958a) for Slough.

The plot of 10 day averages, Figure 2.4(a) shows a peak in winter for all the 3 years shown. A peak also exists in summer for 1961-1962. There is a suggestion of a peak for summer 62-63 but nothing definite. There seems to be a peak near the end of 1963. The occurrence probability shows a similar tendency for Woomera for 1964 to 1966, and so the lack of spread F in the summer of 1962-1963 is surprising, and is possibly of instrumental origin. Similar behaviour is shown by the monthly occurrence proability at Brisbane. Figure

2.4(d) Canberra shows no such behaviour, especially during 1968 and 1969 where the only peak is a strong winter one.

The southern summer peak is strongly influenced by the increase in f_oF2 at night as solar activity increases. Figure 2.4(e) shows themonthly median midnight critical frequency for Brisbane. This shows that the summer peak dropped in magnitude as soon as summer night-time critical frequency increased. Winter night-time critical frequency does not vary nearly so much, so that the change in the annual variation only shows that spread F occurs when critical frequency is least. This is a result that agrees with Singleton (1962).

Canberra clearly shows a different behaviour during 1968 and 1969 with only a peak in winter. The behaviour is more variable in 1963 and 1964. However the occurrence probability clearly differs from Brisbane.

At Woomera spread F is not found to occur preferentially three days after a day of low solar activity. The finding by Bowman (1971) of the peak in occurrence three days after low sunspot number is rather hard to explain. His explanation seems rather ad hoc. In any case the effect is rather marginal in significance when it is observed that the variation in his Figure 1 is about two percent on either side of the average. The selection of stations is suspect, as mentioned before, while the use of such large amounts of data for such varying

conditions could confuse the result. Perhaps the correlation between F_oF_2 and solar activity is the cause, since low sunspot number might mean lower f_oF_2. This is known to cause a greater occurrence of spread F.

8. Conclusion

There is no significant correlation between spread F at Woomera and magnetic activity. Since there is a positive correlation at higher latitudes and a negative correlation near the equator, perhaps Woomera is near the transition. No correlation was found between spread F at Woomera and changes in atmospheric density.

The seasonal variation of spread F occurrence and intensity at Woomera had two peaks, one in local summer and another stronger one in local winter. There are minima near the equinoxes. The annual variation of spread F occurrence at Canberra is different, showing no summer peak. Brisbane shows a definite summer peak of occurrence, which is suppressed when solar activity is high.

TABLE 7

Co-ordinates of Observing Sites

	Latitude (°)	Longitude (°E)
Buckland Park	-34.50	138.41
St. Kilda	-34.60	138.40

CHAPTER 3

INSTRUMENTATION AND METHODS

1. Introduction

The observations of satellite signals discussed in this thesis were obtained at two field stations of the Physics Department. These are known as St. Kilda and Buckland Park. Table 7 shows their co-ordinates. The equipment was moved to Buckland Park, which is about 15 km north of St. Kilda, because of increasing interference. The equipment will be described in three sections:

(i) Low orbit satellites

(ii) Geostationary satellites

(iii) Faraday rotation using stationary satellites.

2. Low Orbit Satellites

The equipment used for this work was constructed and used by Parkin (1967). My work consisted in further analysis of the records obtained and some new observations. Only a broad summary of the equipment will be given. The total electron content observations used Magnavox Model B receivers, on 40.010 and 41.010 MHz, fed from

the same dipole antenna via a 1 to 1 balun. The A.G.C. circuit of these receivers had been modified so that the gain only responded with a 5 second time constant. Thus the recorded voltage was a linear function of signal strength during scintillation, but the response for the slower Faraday fading was logarithmic. The voltage was recorded on a chart recorder with a paper speed of 2.5mm per second.

The ground pattern observations were made with 3 receivers, at the corners of a right-angled triangle, illustrated in Figure 3.1 from Parkin (1967). These receivers were also Magnavox Model B receivers, modified so that their response was linear for signals of periods less than 10 seconds. They were fed from folded dipole turnstile aerials to remove Faraday fading as far as possible. The output voltage was buffered and made push-pull, and then sent along a twisted pair line to the recording site. Problems due to mains pickup, mentioned by Parkin (1967) were completely solved by using a differential amplifier at the recording site, since the mains induced pickup was similar on both wires. Selected parts of satellite passes were recorded on a 3 channel chart recorder with a high paper speed (25 or 5mm per second) and were afterwards digitized manually.

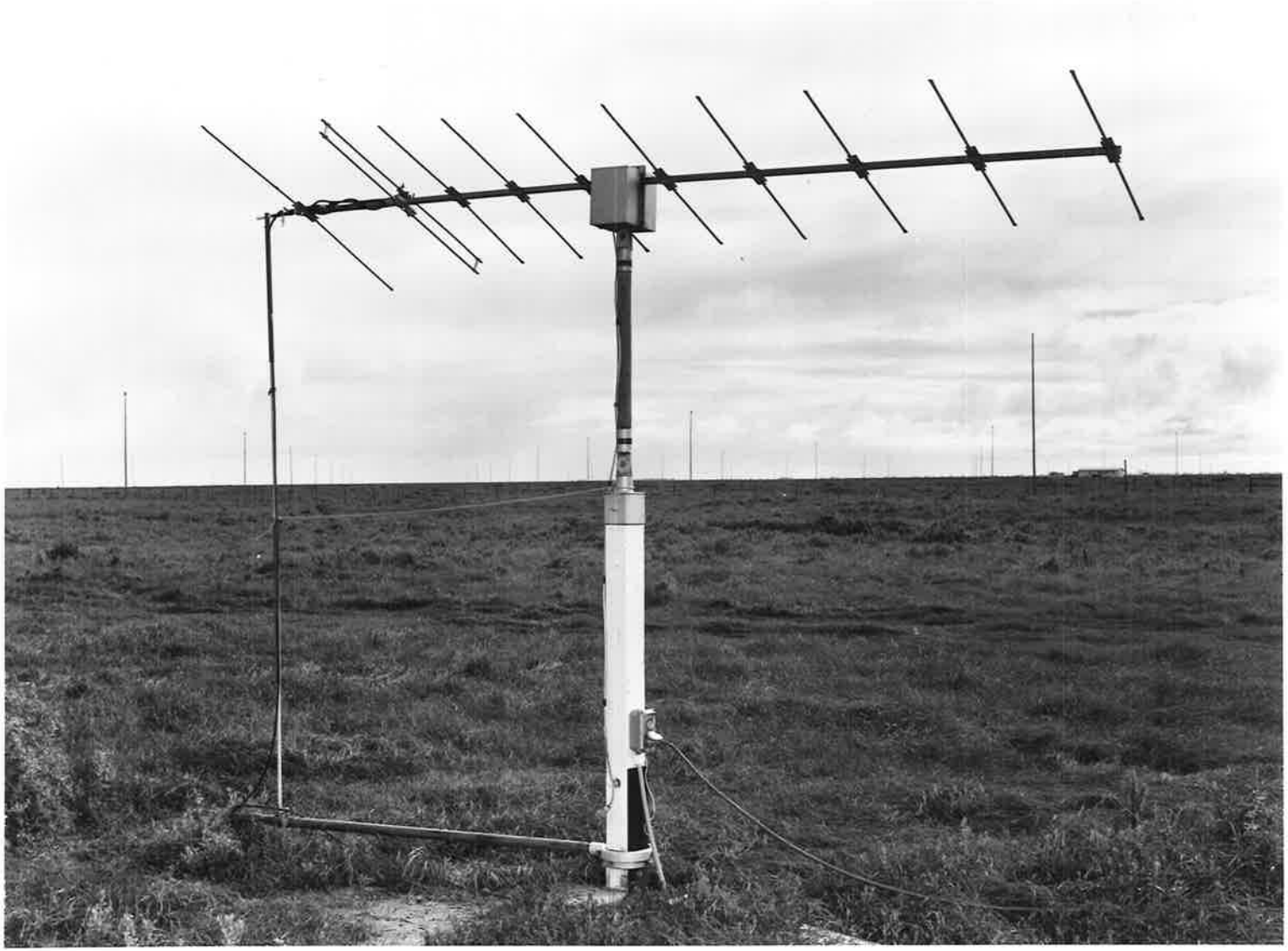

PLATE 1. The Rotating Antenna

3. Satellites

The satellites observed were the beacon satellites BEB and BEC (1964 64A and 1965 32A). The ground pattern observations used signals transmitted at 40.01 MHz. A description of these satellites can be found in Bordeau (1962). Satellite BEC was more useful for ground pattern observations because the particular inclination, when combined with the station latitude, meant that up to 6 successive passes could be observed during any one day. This satellite's path was such that the fading due to Faraday rotation had a long period. This was because the angle between the line of sight and the magnetic field in the ionosphere was not changing rapidly for passes to the south of the station.

Both satellites transmitted coherently related signals at 20.005 MHz, 40.010 MHz and 41.010 MHz derived from a crystal oscillator. The transmitting antennas were half-wave dipoles attached to extended panels supporting the solar cells. The transmitted power was .250 watts. The satellite's attitude was controlled by a bar magnet situated along the axis of greatest angular momentum. This forced the satellite spin axis to align to the magnetic field within a few days of launch. Rotation about this axis was halted by using rods of magnetic material perpendicular to the magnet which caused hysteresis damping of the rotation. Thus the axis of symmetry of the satellite was kept aligned to the direction of the

magnetic field. This meant that the observed transmitted polarization did not change much during a pass over the observing station. The small rotation due to changing geometry (Webster, 1967) has been neglected.

4. Geostationary Satellite Instrumentation

4.1 Aerials

Two types of aerials were used for observations of geostationary satellite beacons. The first was a commercially obtained antenna for Australian T.V. Channel 5A (137-144 MHz). This had a gain of 10 db and a nominal impedance of 300 ohms. The match to 70 ohms cable was achieved using a half-wave balun. The other antenna was a pair of crossed Yagi antennas, custom built and adjusted. Each individual Yagi had a gain of 13 db and an impedance of 70 ohms. The matching circuit is a gamma match which was adjusted with the antenna in position. This antenna was used to receive circularly polarized signals by inserting a quarter wavelength extra of cable in the line from one Yagi to the port of the hybrid network used to ensure isolation between the two Yagis.

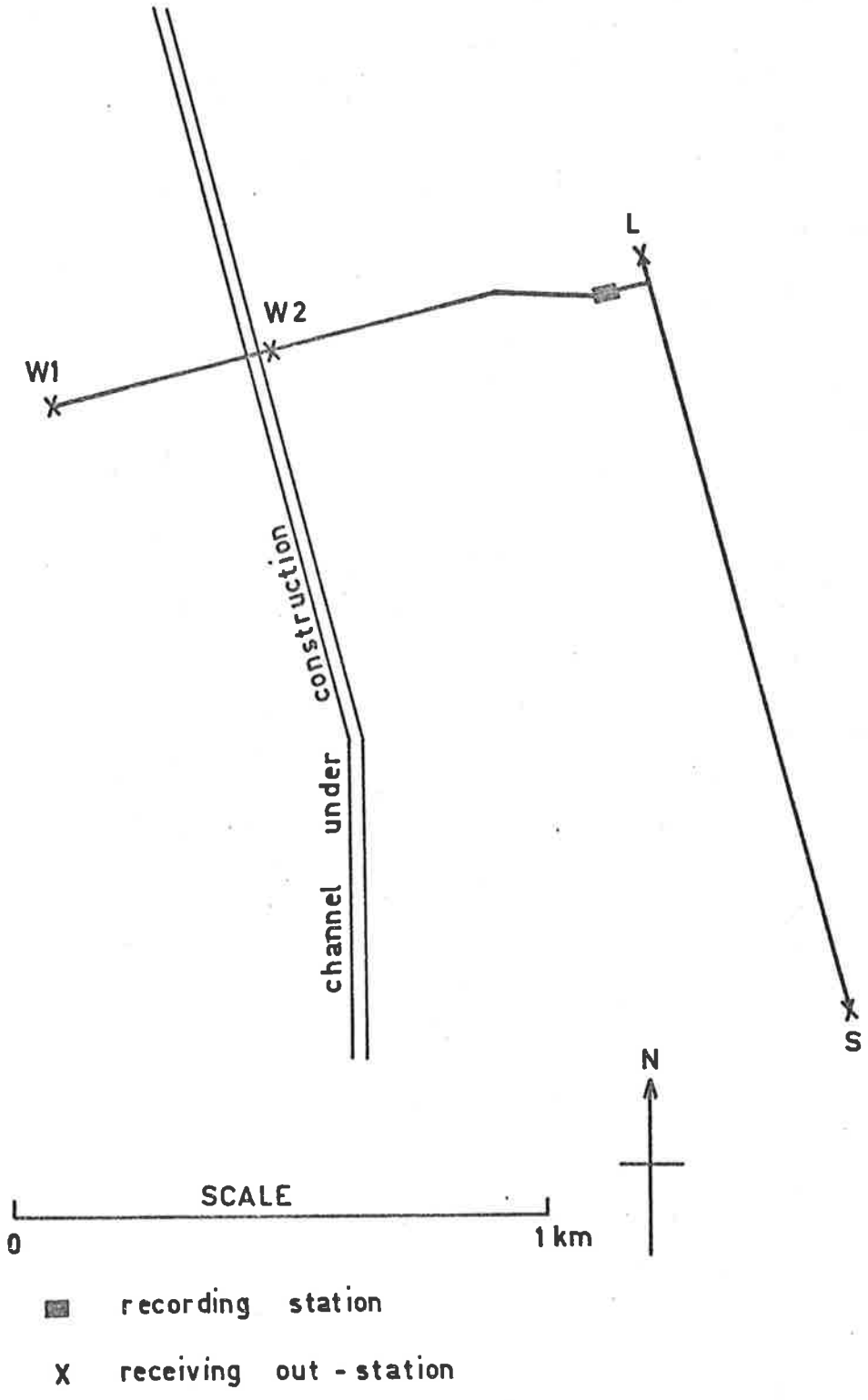

Figure 3.1 Plan of receiver sites, from Parkin (1967).

4.2 R.F. Instrumentation

The signal was converted down to 20.005 MHz using various converters, all of which used F.E.T. input stages, and did not degrade the noise figure of the following receivers. This was always a Magnavox Model B receiver with a plug-in converter for 20.005 MHz.

4.2 Signal Strength Measurement

For observing Syncom 3, the B.F.O. on the receiver was used to get an audio-frequency beat note, which was filtered, rectified and the filtered D.C. recorded for signal strength variations. This method was susceptible to frequency drift in the various crystal oscillators in the system, mainly in the converters. The drift, due to temperature variations, was reduced by burying the converter about 1 metre in the earth beneath the antenna. Manual adjustment of the B.F.O. compensated for drifts of a long term nature.

There was also a problem when the satellite switched itself off during either equinox, to conserve power. There was a noticeable drift in frequency for several hours while the transmitter "warmed up". During the solstices transmission was uninterrupted. In later observations on another satellite (A.T.S.1. 1966 110A) the receiver A.G.C. voltage was recorded as a means of determining signal strength. Because the additional voltage due to the satellite was a fraction

of the voltage due to receiver noise and the galactic background, a recording system was devised where this nearly constant voltage was backed off, and the wanted signal filtered with a time constant of 1 second and recorded on a chart recorder at a speed of 18 cm per hour. Time marks were provided by a cam operated microswitch, using a 1 revolution per hour synchronous motor to interrupt the input to the chart recorder every hour (Figure 3.2).

4.4 Polarization Measurement

A Channel 5A Yagi was split in the centre and a motor drive inserted at this point, using an electric motor with a chain drive. This motor also drove a two pole bicycle generator. This provided an electric signal of twice the rotation frequency. A photograph of the antenna is shown in Plate I. The signal was taken from the antenna using inductively coupled tuned circuits, and fed to a converter. The output of the converter at 20.005 MHz was fed to a Magnavox Model B receiver. The receiver output was passed through an active bandpass filter, centred at twice the rotation frequency. It was then put through a zero crossing detector, which produced a square wave with sharp transitions at the zero crossing points.

It was found necessary to put two zero crossing detectors in cascade to get a sharp enough edge. This is because of the low

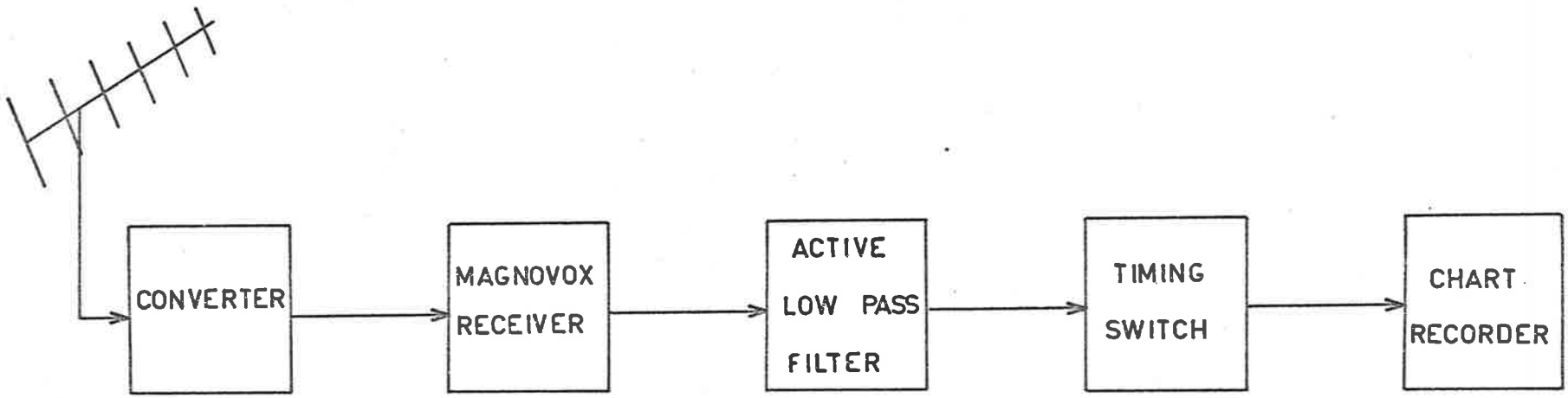

Figure 3.2 : System used to record signal strength of ATS1.

frequency of the input signal (2.6 Hz) and the consequent slow rate of change of signal with time.

After differentiating and clipping this square wave, a single polarity pulse train is produced. This is fed to one input of a discrete component R-S flip-flop. The other input is fed by a similar pulse train from the reference signal, treated in an identical manner. The resultant output at the collectors of the transistors is a waveform whose "on" duration is directly proportional to the phase difference between the input pulses. To get better ripple reduction, the collector voltage of both transistors was filtered separately and the difference taken, using a differential amplifier. This output was then further filtered with a time constant of 20 seconds and recorded on a three channel chart recorder. Figure 3.3 shows a block diagram. The other channel was the signal strength record described previously. Hourly time marks were provided. The recorded speed was 18 cm per hour. This is the method of recording described by Titheridge (1966).

5.0 Geostationary Satellites

This thesis contains observations of two different satellites Syncom 3 (1964 44A) and Applications Technology Satellite I. Table 3 shows the geometrical properties of the line of sight to these

satellites.

TABLE 3

Satellite	Azimuth	Elevation	Subionospheric Lat.(0) 300 km	Long (°E) height	Angle to Geomagnetic field
Syncom 3	57.5	30.5	-32.2°	142.6°	40°
A.T.S.1	80°	6°	-31.25°	154.1°	59°

The transmission from Syncom 3 was elliptically polarized. Interfering signals were often present because the Allouette satellites transmit telemetry on the same frequency (136-980 MHz). The nominal transmitter power was 2 watts. As mentioned earlier, to conserve the batteries, Syncom 3 was turned off for a few hours each night when it passed through the earth's shadow. This only happens around the equinoxes. At the two solstices it is sunlit all night.

The A.T.S.1 telemetry transmitter on 137.35 MHz is linearly polarized. The transmitter power is also nominally 2 watts. This satellite's beacon is on all the time. If there is telemetry on the carrier, all the effective sidebands appear to be within the bandpass of the receiver.

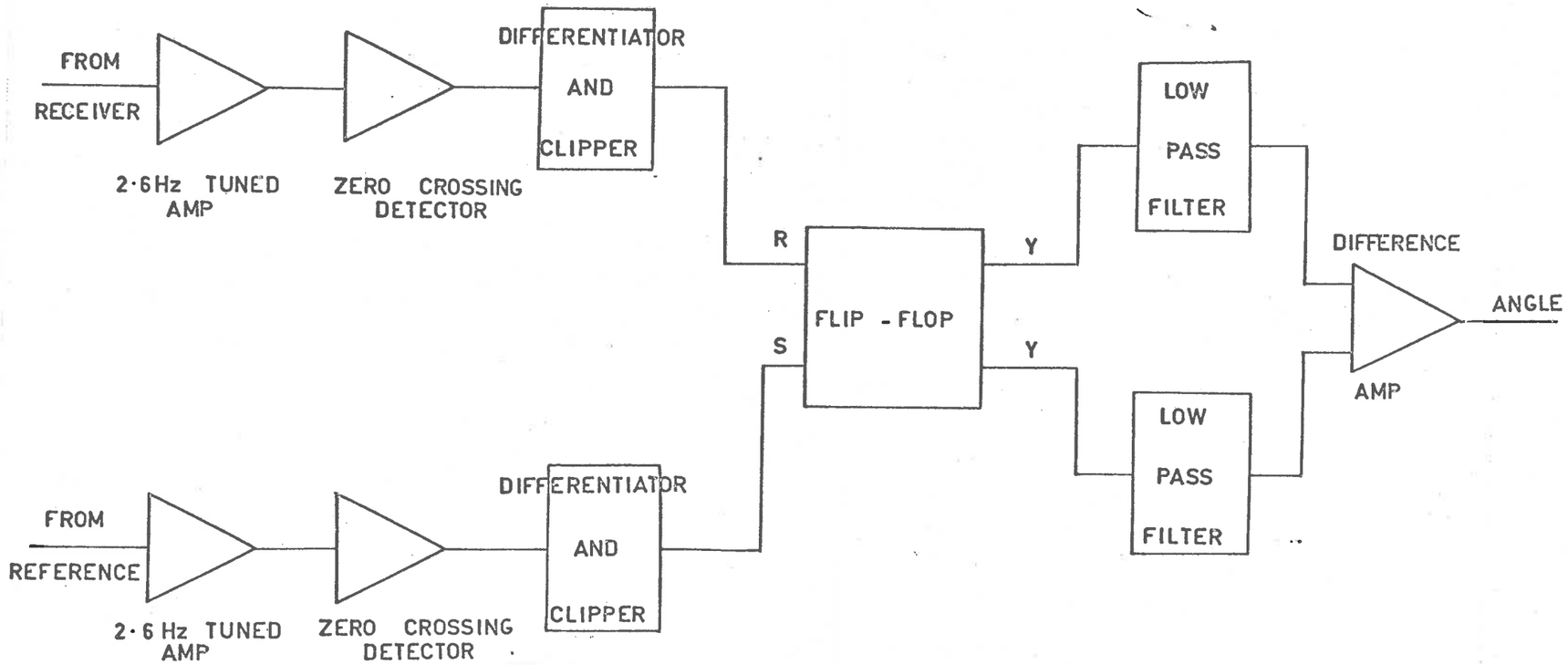

Figure 3.3 Block diagram of phase meter

A problem was experienced with this satellite because of its low elevation. With the particular aerial height chosen for the crossed Yagi, the vertically polarized ground reflected signal, cancelled out the direct vertically polarized signal. Thus the antenna behaved as though it was horizontally polarized, though it was really circularly polarized. The problem was not solvable by changing aerial height, because an appreciably higher position for the antenna was impracticable at the observing site, without making the antenna inaccessible for adjustment of the gamma match.

The lack of interference from other satellites was the main reason for using A.T.S.1 for most of the observations. From about August 1969 another satellite (Intellsat II F2) transmitting on 136.980 MHz was available. However it suffered from the same problem of interference from other satellites. Some of this had much the same form as a certain type of scintillation, of a more regular type than usual. To avoid any confusion it was thus necessary to study a satellite which could not be interfered with.

6.0 Methods of Data Analysis

6.1 Scintillation Index

For every hour, centred on the hour, the third highest (STH)

and the third from bottom (STL) scintillation peaks were scaled. Scintillation index as a percentage was then calculated using the formula:

$$S.I. = \frac{STH-STL}{STH+STL}$$

This is the recommended index of Allen (1967). The index can be converted to other indices using the formula for the A.G.C. voltage index given in the above paper.

6.2 Faraday

The differential Faraday rotation method used by Parkin (1967) involved measuring the angle between the planes of polarization of the 40 and 41 MHz transmission, using the displacement between the nulls, as shown in Figure 3.4. Then the total rotation for 40 MHz at a null is calculated using the formula. This calculation needs a value for n, which is the unknown multiple of π radians in the difference in rotation between the two frequencies. This unknown was established by calculating the electron content for each 40 MHz null for n = 0,1,2 and sometimes 3. Criteria were then applied to these curves to determine which value of n fitted best. Firstly, values of n which gave negative electron content at one end of the pass could be ignored. Secondly, an electron content was also calculated by the

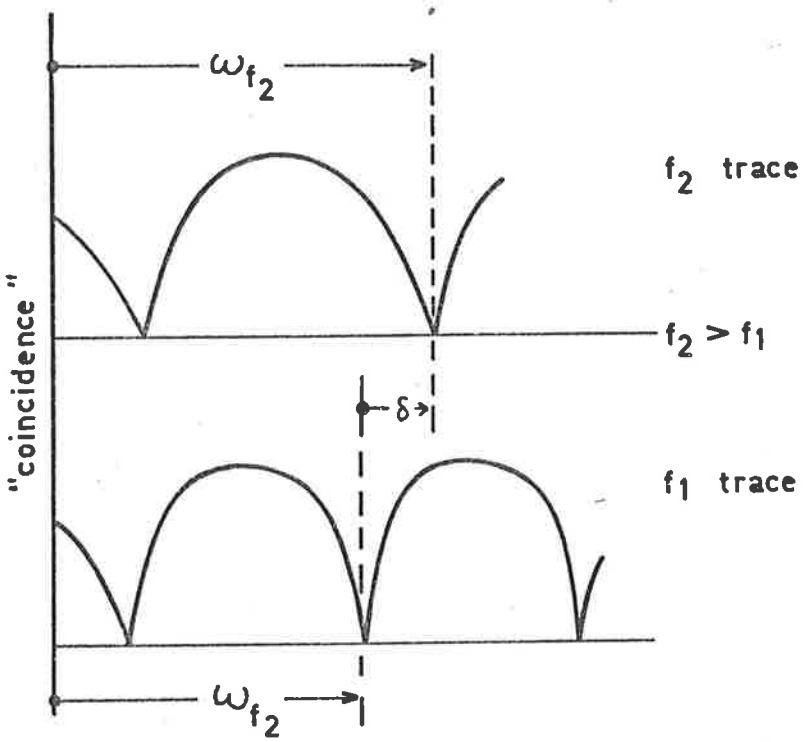

Figure 3.4 Illustrating the "Vernier method of finding the angle of rotation of the plane of polarization when two radio frequencies are used.

rotation rate method. If at any time during a pass the two estimates agreed, the value of n was determined as that whose curve agreed with the rotation rate method. This agreement had to be over several rotation periods to make sure the agreement was not due to an irregular gradient in electron content. Thirdly, high values of electron content were not allowed during the night. Lastly, the gradient of electron content was expected to be such that the higher content occurred to the north near midday. When the proper value of n had been chosen the appropriate plot was studied for irregularities, and the deviations and average electron content were tabulated.

The output of the rotating aerial system was studied in two different ways. To study relationship between scintillation and irregularities in electron content, the original records were studied. An example of such a record is shown in Figure 7.2 (Chapter 7). To study the daily changes in electron content it was necessary to digitize the record at 1 cm intervals. At each transition it was determined whether the electron content was increased or decreasing, and subsequent readings were added or subtracted. An arbitrary zero was used for all records, since the transmitted polarization was unknown. This zero was the same for any interval where there was no break in the record. The rotation angle was plotted and studied.

6.3 Power Spectra

Power spectrum analysis of scintillation from low orbit satellites and the geostationary satellite was carried out using the fast Fourier transform algorithm. The particular programme used was taken from the University Computing Centre library. The input to the programme was hand digitized data from chart records, run at a faster speed than was necessary for scintillation index. The reading interval for each record was chosen so that aliasing could not occur. The length was governed by three factors. Firstly, it should be stationary by visual inspection. Secondly, it had to be such that the number of points was a power of two. Lastly, no large very low frequency components should be present so that, if detrending was done, the "leakage" would not be large. Detrending was accomplished by fitting a parabola to the whole record and subtracting this before applying the fast Fourier transform. To smooth out the spectrum estimate, an 9-point mean was taken over the individual estimates.

7.0 Spaced Receiver Analysis

Records used by Parkin, 1967, were analysed for several extra quantities. Parkin was unable to obtain the random pattern parameter Vc (Fooks, 1965) due to a programme error. I also did

dispersion analysis on spaced receiver records already available. This used the subroutine that was written by Golley, 1970. Some extra programming was added to the spaced receiver analysis programme, to study the relationship between the half-width of the auto-correlation function, and the width to half maximum of the cross-correlation functions between receivers. The programme was the one used for all spaced receiver analysis in the research group at the time (Briggs, 1968).

CHAPTER 4

LARGE SCALE IRREGULARITIES IN THE IONOSPHERE

1.0 Introduction

"Large irregularities" will be defined as those whose scale is greater than 5 km. Irregularities of sizes from 100 km upwards have been known since Munro (1948) first observed them. They were first detected by variations in the apparent reflection height at a fixed frequency, Munro (1948, 1950, 1958) and in variations in direction of arrival of signals reflected from the ionosphere, Bramley (1953). The more intense disturbances produce characteristic effects on ionograms, due to non-vertical reflections, and vary the peak electron density (Heisler (1958)). They can also be detected by the changing frequency of continuous wave signals reflected from the ionosphere (Georges (1968); Chan and Villard (1962); Davies and Jones (1971)), and by the variation in the apparent position of radio sources, due to changes in ionospheric refraction (Lawrence (1961)). Observations of the total electron content of the ionosphere using radio transmissions from satellites also reveal irregularities. This type of technique is used in the present thesis. Such methods reveal irregularities of all sizes down to the arbitrary lower limit mentioned above (Alpert and Sinelikov (1966)), and up to an upper size

limit caused by a limited field of view (Titheridge (1963)).

By using spaced observing sites, information has been gained on the speed and direction of movement of the irregularities (Munro (1950); Munro (1958); George (1968)). Collectively these phenomena are all manifestations of a type of ionospheric disturbances known as "travelling ionospheric disturbances" (T.I.D.).

When satellites with radio transmitters in the upper HF and the VHF bands were launched it became possible to measure the total electron content between the observing point and the satellite, either by using the Faraday effect (Garriott (1960)) or the Doppler effect (De Mendonca (1962)), or a combination of both of them. The first observations were published by Little and Lawrence (1960), giving results for 3 transits of 1958 δ3 (Sputnik 3), using the Faraday effect. Irregular variations can be seen in their plots of total electron content against time. These are of the order of one percent in electron content and with a scale size of about 300 km. De Mendonca (1962) presented results for 68 transits, using the differential Doppler method. This technique involves finding the effect of the ionosphere by observing the Doppler effect on two harmonically related, phase locked radio transmitters. The Doppler effect due to the moving satellite is thus removed and ionospheric effects alone can be seen. De Mendonca's results showed that

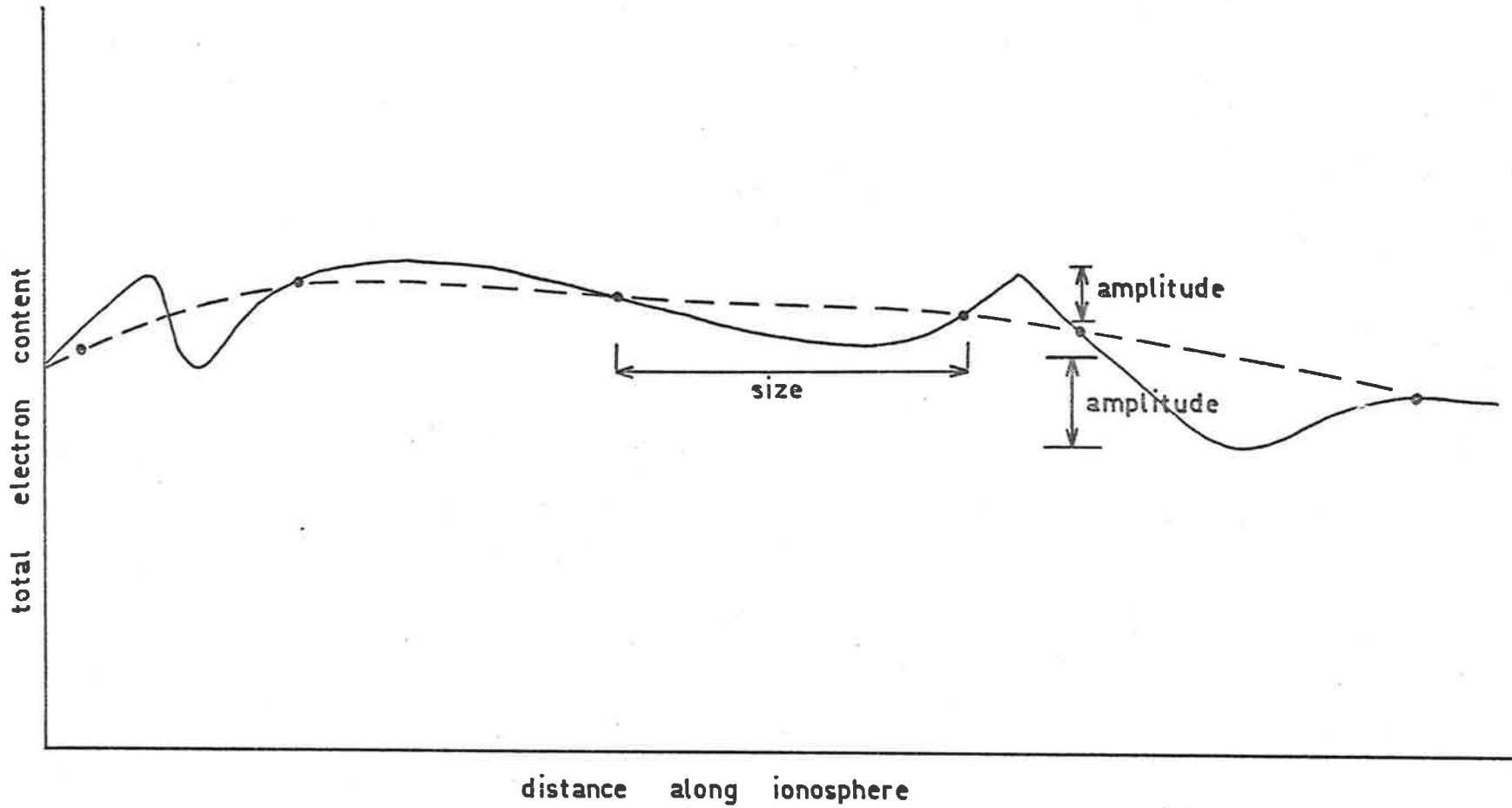

Figure 4.1 Illustrating the method of deriving irregularity size and amplitude.

irregularities were nearly always present because even when plotted at a 3 km spacing, values of the electron content showed more scatter than one would expect from measurement errors. Large scale irregularities can also be seen on his records. Titheridge (1963, 1968) observed fluctuations in the Faraday rotation rate from several satellites using frequencies near 20 MHz. Because of changing geometrical factors the amount of rotation imposed on a radio wave is constantly changing. This causes the signal strength pattern, recorded using a linearly polarized antenna, to show a modulus cosine pattern, whose frequency can be in the first approximation related to total electron content. The approximation assumes horizontal stratification. Thus irregular variations in electron content cause variations in the period of this fading. Titheridge (1963) shows how this can be used to derive some parameters describing the irregularities. The magnitude of the variations in total electron content was generally between 0.03 and 4.0 percent, with a median of 0.25 percent. The variation of irregular total electron content with size of the irregularity indicated that the change in electron density inside the individual irregularities was size independent, and was between 0.1 and 10 percent of the background ionization. Titheridge (1968a) also showed that the irregularities were not field aligned by observing that their amplitude did not depend on the angle between the direction to the satellite and the direction of the magnetic field.

He also presented evidence to support a model of the irregularities as discs, about 0.4 times as high as they are wide.

Bhonsle (1966) observed irregular total electron content variations at Stanford University, California, using Doppler measurements. He found the average gradient in electron content across an irregularity showed little diurnal change, but this was due to the well known diurnal change in the background total electron content.

Alpert and Sinelnikov (1966) describe Doppler measurements from two satellites in eccentric orbits (1964-6A and 1964 38A), using frequencies of 20 MHz and 90 MHz. They observe many irregularities, in all size ranges from 2 km to 400 km. Because of their assertion that the measurements refer to the immediate vicinity of the satellite, their sizes are calculated assuming the full satellite velocity, instead of the projected velocity inherent in other observations. They also state their sizes in wavelengths, a definition which gives numbers twice as large, for the same irregularity. These assumptions should result in their sizes being four times the size of other observers. Alpert and Sinelnikov (1966) find a maximum number of occurrence in the 20 km to 40 km size range (their measurement). Such sizes could not be seen by Titheridge (1968) although perhaps Rao (1967) observed them. However the size intervals chosen do not seem to have an obvious pattern and vary in width. The peaks in

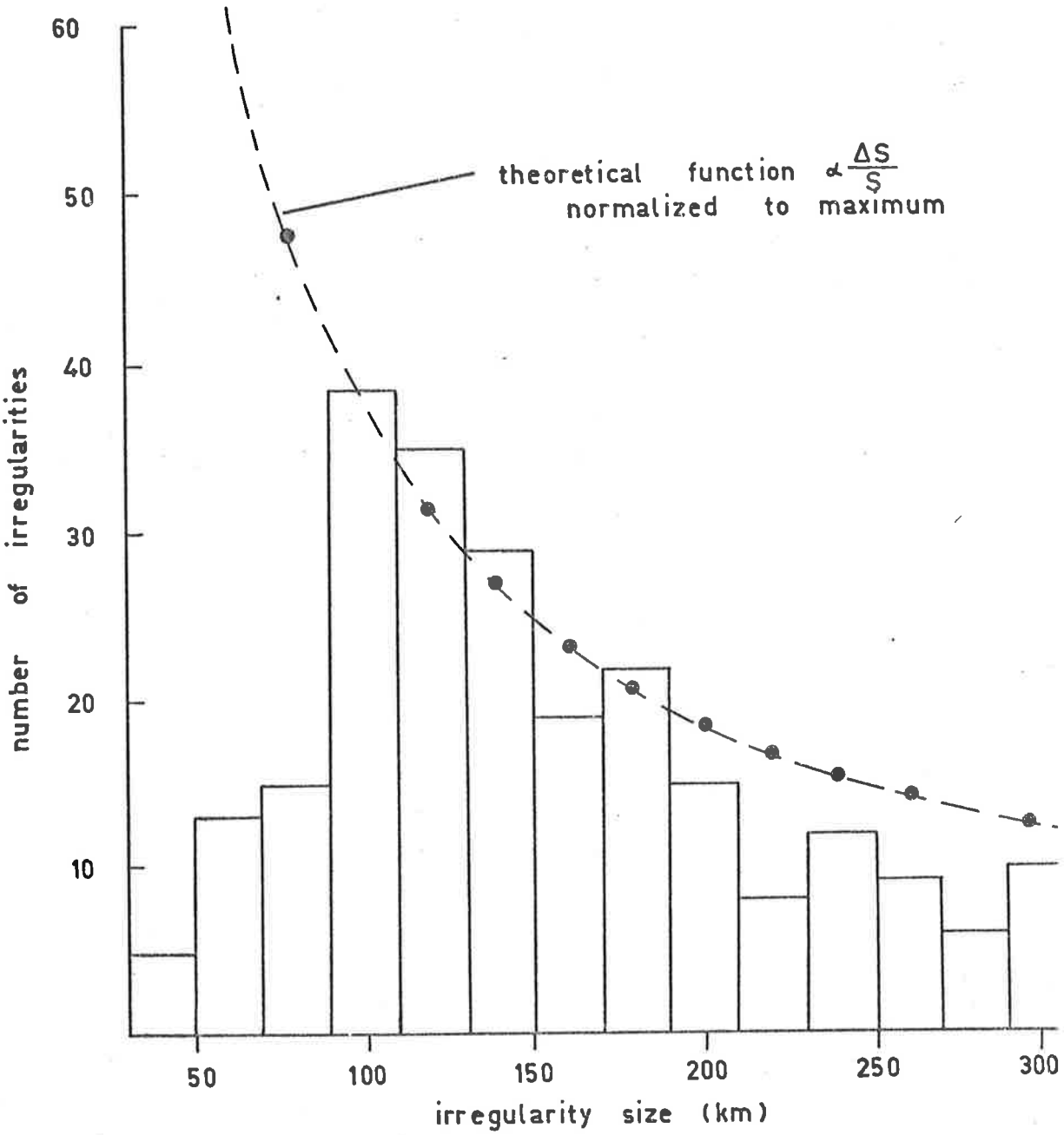

Figure 4.2 Histogram of irregularity size.

Alpert and Sinelnikov's Figures 11 and 12, could be due to that interval (20 to 40 km) being the widest interval, covering a size range of approximately two to one. A comparison with Titheridge (1968a) is not possible because of the irregular width of the interval. Their observations extend to smaller sizes but because Alpert and Sinelnikov do not use equal intervals like Titheridge, it is not possible to check Titheridge's hypothesis that there is no preferred irregularity size.

Rao (1967) observed irregularities in the total electron content curves, obtained using the satellite BEC, as seen from Urbana, Illinois, where the sub-satellite ionospheric point travels essentially west to east during a transit. Rao found by power spectrum analysis that the dominant east-west wavelength varied between 250 and 750 km. The longer wavelength dominated at night, with shorter wavelengths being more prominent between 0900 to 2100 hrs. local time. Rao gives no figures for direct comparison with Titheridge's (1963, 1968a) observations of probability of occurrence of an irregularity of a given size. However Rao's upper size limit would be similar, because all observations are limited by the finite length of record, which causes the long wavelength cut off in his power spectrum. The slope of the power spectrum of the irregular total electron content is linear near the origin. This implies, on

Figure 4.3 Irregularity content vs size for winter.

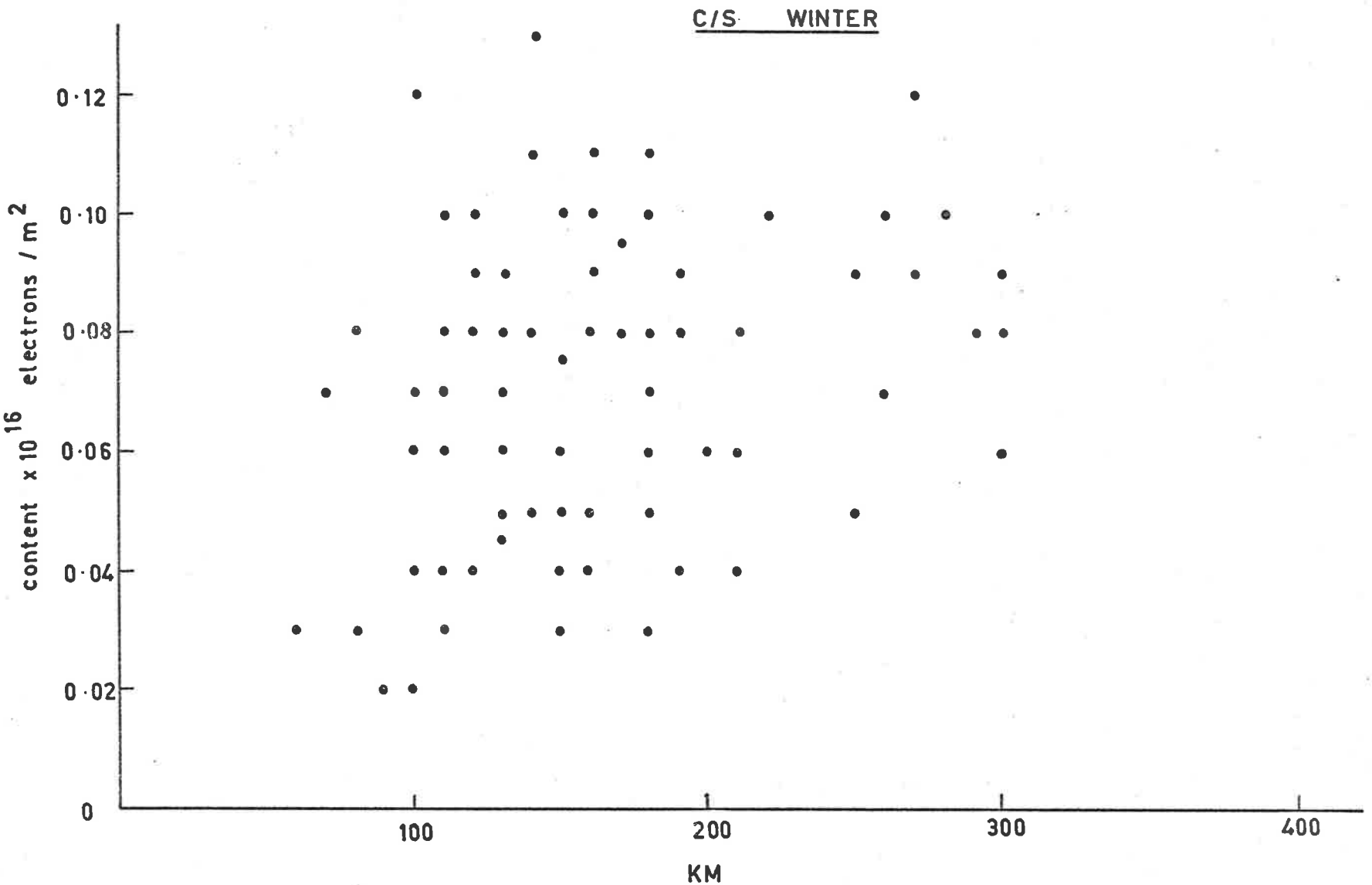

dimensional arguments, that irregularity content is proportioned to irregularity size, which is the same at Titheridge (1968a) shows, but different from Titheridge's (1963) results. This could be because of solar cycle changes in the ionosphere, since Titheridge's observations were at sunspot maxima and minima respectively.

Short period variations in total electron content can be observed using telemetry transmitters on geostationary satellites. Sometimes these variations are almost periodic (Titheridge 1968b). The first observations of total electron content by this method were reported by Garriott and Smith (1965). Irregularities or oscillations show up as deviations from a definite diurnal curve. These have periods ranging from 15 minutes to several hours. Further aspects of this will be discussed in another chapter of the present thesis.

2.0 Observations

Parkin (1967), observing at Adelaide, computed total electron content from observations of differential Faraday rotation of the 40 and 41 MHz transmitters of satellites 1964-64A and 1965-32A for all of 1965 and for January 1966. Parkin only used the results to derive seasonal and diurnal variations in total electron content.

Figure 4.4 Irregularity content vs size for summer.

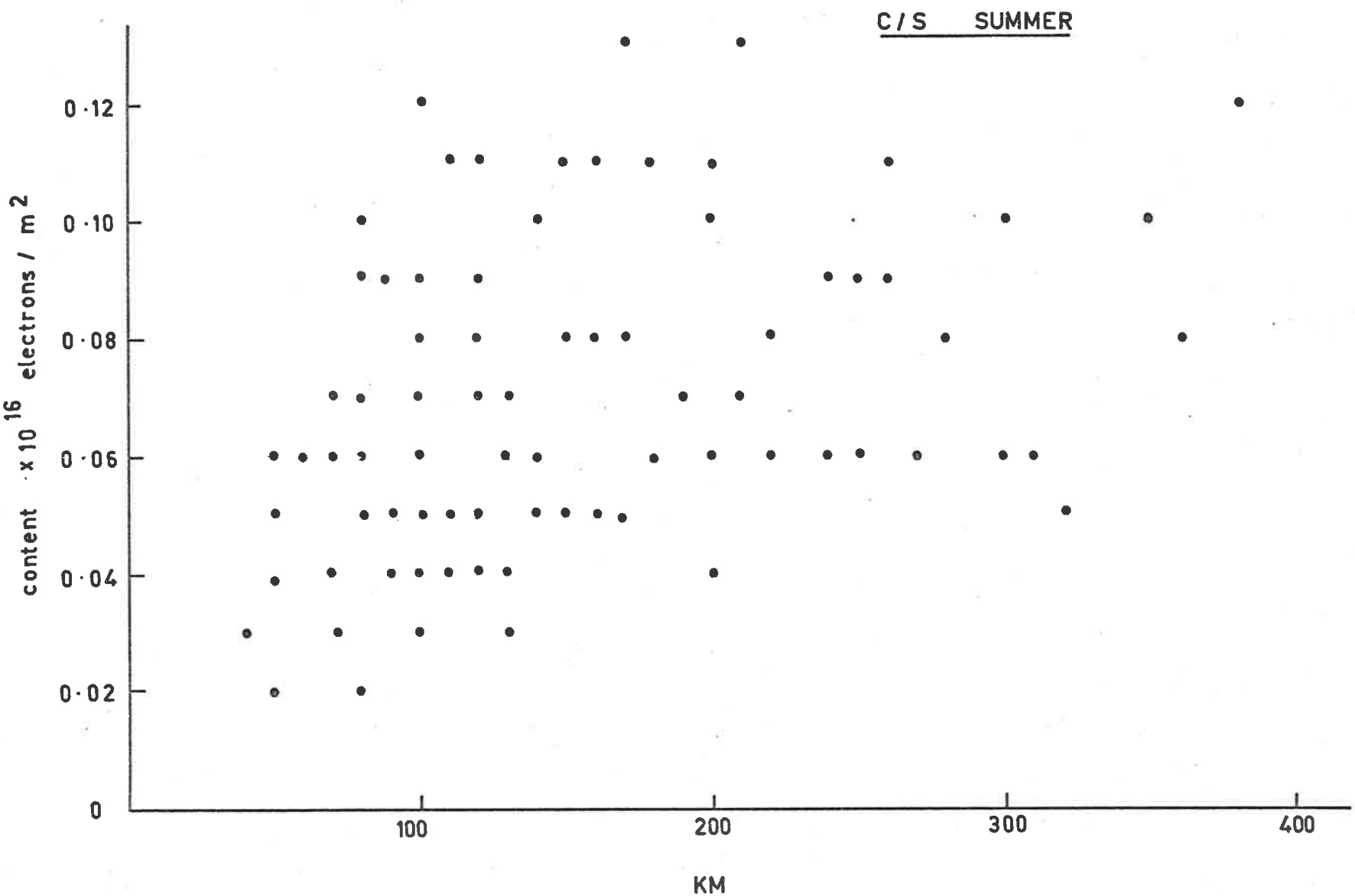

However the results for each pass usually exhibited irregular variations. Total electron content curves for two, three month intervals; May to July 1965 and November 1965 to January 1966, were studied to see how results compared with observations elsewhere.

The method used, was to plot the electron content against distance along a spherical shell 350 kms high. A smooth curve was estimated and drawn in. Irregularity size was defined as the distance between one crossing of the smoothed curve and the next, (Figure 4.1) and the total electron content deviation and percentage deviation recorded along with the size. The smallest size seen is limited by the Faraday rotation period of the 40 MHz signal. It is estimated to be the order of 40 kms, but this will vary from day to night and seasonally. The definition of size is equivalent to that of Titheridge (1963), if one assumes the greatest electron content gradient occurs at the crossing of the smoothed curve by the observed curve. In the following results the absolute value of the deviation was used, without any regard to sign.

3.0 Results

Histograms of the size distribution for summer and winter are

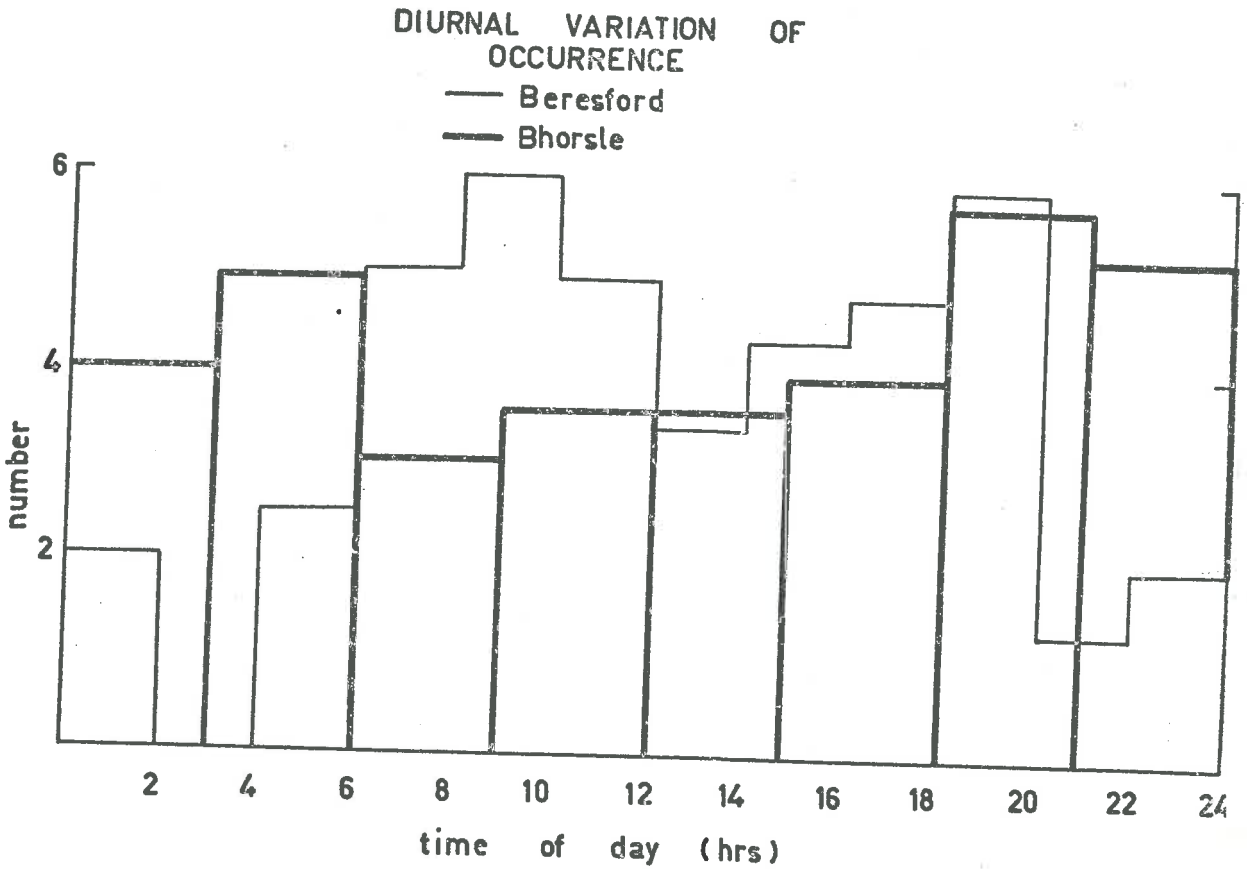

Figure 4.5 Diurnal variation of the number of irregularities observed.

shown in Figure 4.2. The distribution of the irregularity percentage deviation is shown in Figure 4.6. Figures 4.3 and 4.4 show scatter diagrams for electron content deviations against size, for comparison with Titheridge (1963). The diurnal variation in the probability of occurrence of the irregularities as measured by the number seen per satellite pass is shown in Figure 4.5,which also shows the number of passes which were used in each two hour interval. This includes all passes analysed, whether there were irregularities present or not.

4.0 Discussion

The size distribution is reasonably similar to the one found by Titheridge (1963, 1968a) in the range 100 to 180 km. Titheridge found that the distribution was such that the number in a range of sizes S to S+dS, N, was proportional to dS/S. The curve in Figure 4.2 is this function normalized to the number in the 100 to 120 km interval. Below 100 km the effect of the finite resolution drastically reduces the number of irregularities seen, while above 200 km, the total lengths of individual records limits the possibility of observing irregularities.

The histograms of percentage amplitude show that the median percentage amplitude changes from 0.4 - 0.6% in summer to 0.8 - 1.0%

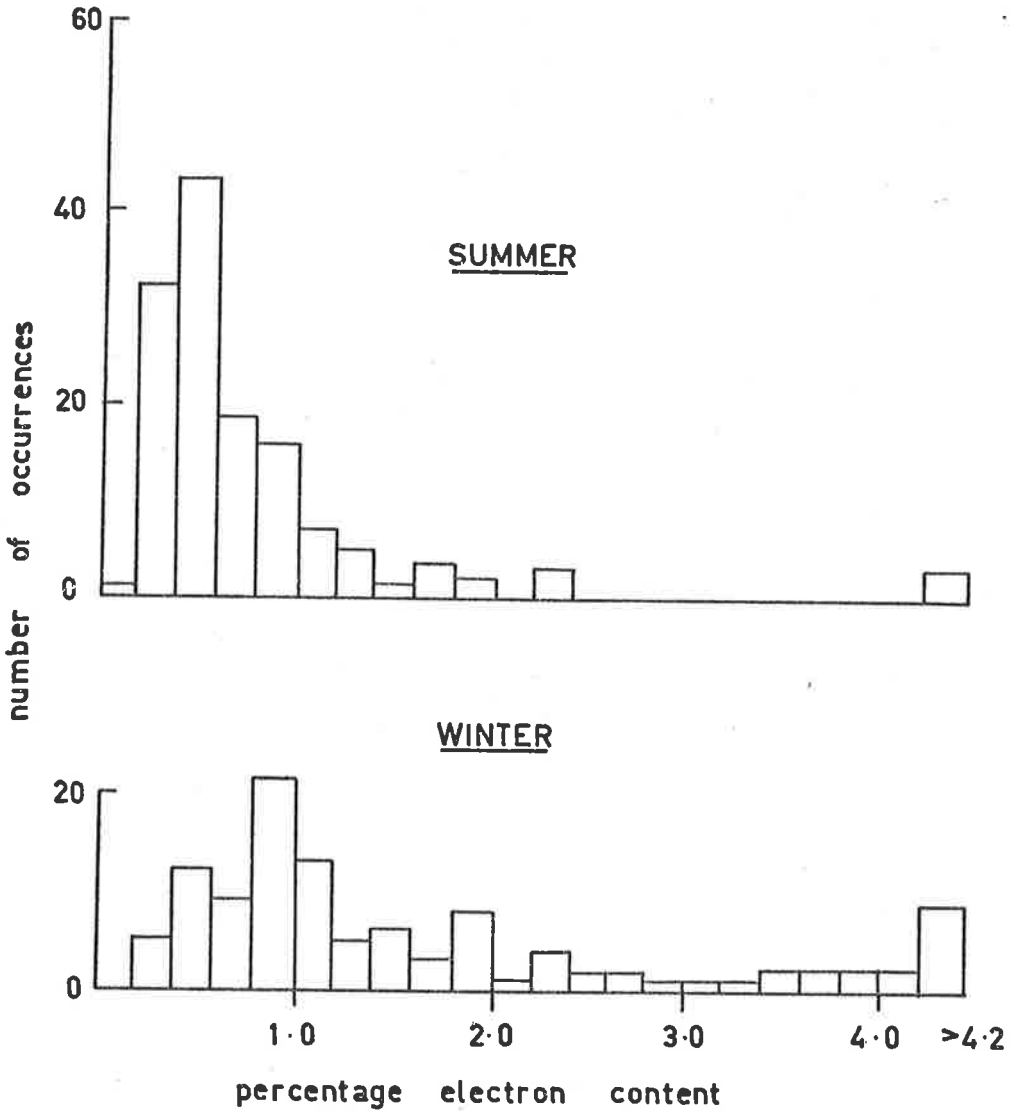

Figure 4.6 Histograms of percentage electron content of irregularities.

in winter. This change is more than the ratio of the total electron content in summer to that in winter. Average diurnal electron content curves were derived for the time concerned by Parkin (1967). These show a summer to winter ratio of maximum daytime total electron content of 1.5. Thus the average irregularity deviation must change from summer to winter, so as to account for the percentage change which is observed. This is supported by the fact that more large amplitude irregularities occur in winter.

The scatter plots of irregular electron content against size, show a definite trend, such that larger content irregularities are associated with larger size. However the scatter is too large to make any estimate of this relationship worthwhile.

The diurnal variation in the number of irregularities per pass shows a maximum in the daytime and early evening, dropping to a lower value at night. This variation is quite different from that of Bhonsle (1966), but similar to that of Titheridge (1968a). The small number of irregularities observed did not warrant a study of the diurnal variations in the irregular total electron content similar to that carried out by Titheridge (1968a) and Bhonsle (1966). The present observations are limited at night, because the increased Faraday rotation period lowers the probability of seeing the smaller scale irregularities. This factor affects

Titheridge's results also, but not those of Bhonsle (1966) or Rao (1967), because their measurements were at fixed time intervals. The results presented in this thesis are dominated by observations of a satellite in a polar orbit. The sizes therefore apply in a north-south direction. According to Titheridge (1968a) no field alignment is detectable, so the horizontal structure would be isotropic. The sizes found are in the range of wavelengths possible for internal gravity waves at F region heights, Hines (1960).

It is suggested that the observed irregularities are internal gravity waves. There are occasions when the appearance of the total electron content record is sinusoidal for several periods. Titheridge (1968b) gives some good examples. Such oscillations are better seen on records of Faraday rotation of geostationary satellite VHF radio transmissions. An example is given in Chapter 6 of this thesis.

5.0 Conclusions

The present results confirm that the number of irregularities in a given size interval S to S+dS, N, is related to that size interval by a relation of the form

$$N \propto dS/S$$

over the observed range when the effect of observational selection is allowed for. On the average, the irregularities have a larger magnitude in winter than summer (see Figure 4.6). The diurnal variation of occurrence shows a broad daytime maximum, with a slight dip at midday. This is similar to the diurnal variation of occurrence found by Titheridge (1968a).

It is assumed that the observed irregularities are the result of internal gravity waves perturbing the neutral atmosphere, and hence producing electron density perturbations. The observed size and magnitude are in the range of sizes and magnitudes possible for internal gravity waves.

CHAPTER 5

TOTAL ELECTRON CONTENT USING GEOSTATIONARY SATELLITES

1.0 Introduction

Total electron content measurements can be made using geostationary satellites as sources of the radio transmissions. The measuring technique can be based on a Doppler method or on Faraday rotation of the plane of polarization. Doppler measurements only give the rate of change of electron content. A means of finding the total electron content at some time during the observation must be used to enable continuous measurements of total electron content. Some variations of the Doppler method which rely on the group delay between low and high frequency, or on the rate of change of phase retardation with frequency, can give absolute values.

As the Doppler effect relies solely on the presence of free electrons, and not at all on the presence of a magnetic field, the measurement gives the total electron content between the observation point and the satellite, 35,000 km high above the equator. The Faraday effect depends on the presence of a magnetic field. Titheridge (1966) has shown that for any reasonable distribution of electron density, the ionosphere above 2000 km has only a very

small effect on the rotation of the plane of polarization, because of the rapidly decreasing strength of the magnetic field, and the decreasing electron density. The difference between the results of the two types of measurement can give information about the total electron content inside the plasmapause.

To deduce total electron content from the observations, it is necessary to know the original polarization of the transmitted signal. It is necessary to assume that at the time of day of lowest electron content, one can find out the integral number of half-rotations involved. This is usually possible, since the lowest electron content at mid-latitude stations causes a rotation of the plane of about Π radians. An estimate can also be obtained using ionosonde data. Both types of measurement result in values for the total electron content, as a function of time of day at the sub-ionospheric point. This is the point on the earth's surface directly beneath where the line of sight to the satellite intersects a spherical surface at a height of 300 to 450 km. In the present work as assumed height of 350 km has been used.

Plots of the total electron content show a diurnal variation upon which faster regular and irregular variations are superimposed. These are imagined to be produced at the position of the sub-ionospheric point, due to the same kind of irregularities studied

in Chapter 4. Thus with these observations, it is possible to observe time variations at a single point which complement the observations made at many points at essentially a fixed time, as obtained from orbitting satellites at lower heights.

2.0 Previous Studies

2.1 The Diurnal Variation

Garriott et al. (1965), who were the first to publish results of observations using the Syncom 3 satellite, give curves showing a typical diurnal variation. An outstanding characteristic is the consistency of curves for each day near sunrise, even though individual daily maxima may vary by a factor of two. Garriott and Smith (1965) showed that this similarity occurs because the slope of the curve is proportional to the electron production rate, integrated throughout the atmosphere. Since this is proportional to the solar XUV flux, which only changes slowly, the uniformity is explained. Garriott and Smith (1965) expand the simple theory to allow for more than one ionizable constituent. This is because although nitrogen is ionized, because of fast recombination reactions, such ionization does not contribute to the electron density. Smith (1968) further refined the theory to allow for the small effect of the loss of ionization. He developed a method involving an iterative

calculation, whereby both the integrated production and loss rates rates are calculated by a least squares fit to the observed curve, between solar zenith angles at the subionospheric point of 98° to 87°.

Garriott et al. (1965) also observed that the ratio of maximum to minimum electron content was 30 for observations at Hawaii and 10 for observations from California. Titheridge (1966) disputes these figures on the basis that the daily curves shown in the paper do not support the values quoted; he suggests figures of 15 and 5 for Hawaii and California respectively. The observations of Garriott et al. (1965) were made in autumn or winter. Later observations reported by Garriott et al. (1970) show both a seasonal and a solar cycle variation in the diurnal ratio over California. During the summer and at all phases of the sunspot cycle the ratio was 4. During winter months the ratio is greater and increases from 6 in 1965, to 12 for October 1967. Titheridge (1966) found that a similar seasonal variation occurred at Auckland. However the ratio was smaller, being 3.0 from October to January, decreasing to 2.1 in June and increasing again to 3.7 in September. Titheridge (1966) explains this difference as being due to the differing seasonal behaviour of the electron density in the northern and southern hemispheres. In mid-latitudes of the northern hemisphere the daytime total electron content is higher in winter than summer, and

there is little seasonal variation of the total electron content just before sunrise. This is not so for the southern hemisphere mid-latitudes, where Titheridge's observations show a strong seasonal variation in total electron content both before sunrise, and at the daily maximum. Total electron content at Auckland did not show any seasonal anomaly during 1965-1966. The observed seasonal changes in electron content were what would be expected if the temperature, and the loss coefficient at the F region maximum, were constant (Titheridge, 1966).

2.2 Loss Rate

Titheridge (1966) adopted a model for the F region whereby the equation of equilibrium is expressed in terms of the electron content.

$$\frac{\partial N_T}{\partial t} = Q - \beta' N_T$$

N_T is total electron content

Q is the integrated production rate

β' is the effective loss rate.

Titheridge (1966) derived values for β' at sunset and at some-time after sunset. He shows that differences observed in these

values are consistent with the known behaviour of the F region. For example β' decreases after sunset due to an increase in height of the F region. Titheridge (1966) deduced a value of β' at sunset of 1.4×10^{-4} sec^{-1} in winter, decreasing to 0.5×10^{-4} sec^{-1} for all seasons. Titheridge (1968c) extended this model, because observation showed that there were increases in total electron content on winter nights. He proposed a model whereby the total electron content decayed to a constant level in equilibrium with a constant source. Using the model he found that the seasonal behaviour of the night-time total electron content variation was due to the varying value of the total electron content at sunset. The base level was the same for all seasons but was reached in four hours in winter, but not in summer. The mean rate of change of electron content after midnight showed an increase with magnetic activity, due to an increase in the effective loss rate. This increase only slowly decreased after a period of high magnetic activity, a characteristic behaviour of changes due to magnetic storms, and already inferred from earlier measurements utilizing the rate of change of electron content near sunset (Titheridge and Andrews, 1967). Titheridge (1968d) later showed that his earlier model was unecessarily simplified. The average behaviour of the total electron content throughout the night was that of a decay after sunset and before sunrise with a value of β' that was in

accordance with the estimated value. This value was derived from the calculated loss rate near sunset, modified by two factors. These were, firstly the change in the molecular nitrogen density because of the drop in temperature, and secondly, the increase in the height of the F region peak electron density.

2.3 Night-time Behaviour

Around midnight a source of electron production was inferred (Titheridge, 1968d) causing total electron content to switch from one decay curve to another. This source of ionization produces about 3×10^{16} electrons/m^2 in summer and winter at 34°S but is reduced at the equinoxes. The differing seasonal behaviour is still explained, because of the higher electron density at night in summer and the equinoxes. The low values of electron density in the winter allow the source of ionization to actually increase the total electron content on about 50% of winter nights. Titheridge found that with this model of the night-time behaviour, the source of ionization did increase with magnetic activity, and there was an annual variation of the ionization produced. He studied the night-time behaviour of the F region maximum electron density for places in both the southern and northern hemispheres, and showed (Titheridge, 1968d) that there was a night-time source of ionization at latitudes 15° - 40° latitude in summer, and from 25° - 50° in winter. This

ionization had a flux of about 2 x $10^{16}/m^2$ in mid-latitudes. The source is less at the equinoxes, and shows an annual variation in flux, being 50% greater in December than June. It also shows a sunspot cycle variation of 2.5%.

All the above effects can be explained by diffusion of ionization from the exosphere if the number of protons in a tube of force does not change during the day or night. It is as though the protons are floating on top of the ionized oxygen atoms that provide the ionization for the ionosphere below 500 km. As the midlatitude ionosphere cools at night, the height where O^+ exceeds H^+ decreases from 1000 km to 500 km. This causes the observed ionization below 1000 km to increase sufficiently to satisfy the observations. The limited latitude range is caused by two factors. At low latitudes, the lines of force of the magnetic field do not go above 1000 km. At high latitudes the transition height does not get below 1000 km. In winter the lower temperate causes this region to extend to higher latitudes. It is possible to imagine the main flux of ionization from this source to occur mainly around midnight. Any other source would have to be constant all night, because of the observed effect on electron temperature. The annual and sunspot cycle variations are also explained, as variations in the electron density in the plasmasphere of this phase and magnitude are already known (Titheridge, 1968d).

The results so far apply to the average behaviour of the total electron content. Young et al. (1970) show that at Hawaii increases in night time total electron content occur over rather small areas, sometimes ionospheric points 500 km apart showing no correlation. These observations also show increases in summer and winter, a different behaviour from the night time variation reported by Titheridge (1968b). The average value of the total flux is also considerably larger than the flux reported by Titheridge. It seems to be too large to be supplied by the same mechanism, as Hawaii is too near the equator. However the value of the flux is calculated differently from that of Titheridge, so direct numerical comparisons could be misleading. The results of Young et al. (1970) show a strong occurrence peak in the northern hemisphere winter for these events, with a smaller peak in the summer and minima at each equinox. They are able to show that the disturbance has a westerly motion, because it occurs earlier at the most easterly sub-ionospheric point.

Titheridge (1969) reports a form of disturbance observed in the summer night in New Zealand. By using several observing points, he shows that the average disturbance propagates toward the north west at 140 $m.sec^{-1}$ and is weaker south of 40°S. The disturbance has a particular form of a small decrease, followed by a large increase. Titheridge shows that these disturbances have a front of at least 1000 km and a thickness perpendicular to the front of about 350 km

on average. The factor which distinguishes these disturbances from ordinary travelling ionospheric disturbances is the fact that they are of smaller amplitude in the south. They also occur too frequently to be associated with the disturbances known to occur during substorm activity in the auroral oval.

The comparisons Titheridge (1969) reports with ionosonde observations show that they occur predominantly in the topside ionosphere, since the percentage disturbance in the peak electron density is less than the percentage variation in total electron content. These disturbances seem to be the same kind of disturbance that Young et al. (1970) observed at Hawaii. If this is so it is notable that the peak of occurrence occurs at the same time of year in both hemispheres. The other distinguishing characteristic is that they often cause increases of 50% in total electron content. This is much larger than the irregularities and waves reported by Titheridge (1968a; 1968b).

In summary, the night-time total electron content behaves differently in summer and in winter. During the summer the higher electron content causes the ionization to decay until sunrise. This decay is interrupted around midnight by a source of ionization which lasts for several hours. In summer this source is not enough to reverse the decay. During the equinoxes the behaviour is similar

except the effect of the night-time source is less. During winter the ionization decays to a constant level several hours after sunset. This is because an equilibrium is maintained for several hours between the loss processes and the apparent production of ionization. On occasions, the total electron content increases. On top of this behaviour in summer and winter are superimpposed short (2 hours or less) large (40 to 80%) increases in total electron content. These increases occur around midnight. They occur mainly in northern hemisphere winter with a secondary peak in northern hemisphere summer. Titheridge's (1968a) observations show that the disturbances he detected occurred in the topside ionosphere. These disturbances seem too large to be formed by influx of ionization by the changing level of the transition between a O^+ ionosphere and a H^+ ionosphere. Titheridge (1968e) showed that this could not produce a flux greater than 3×10^{16} el/m^2, while the disturbance is often more than this.

2.4 Irregularities and Waves

Irregular behaviour in total electron content curves has been observed using satellites in medium altitude orbits, as shown in Chapter 4. Irregular variations have also been observed using stationary satellites; they are detectable in the earliest observations, and have been most extensively studied by Titheridge (1968),

using observations during 1965 and 1966. He showed that 30% of irregularities observed showed periodic behaviour, having a period constant within 15%, and an amplitude constant within 50%. Sometimes this almost sinusoidal behaviour continued for up to 12 cycles. Similar phenomena are reported from observations of the Faraday rotation period of the 20 MHz transmissions from Cosmos 5. Observations of total electron content from Invercargill, as well as Auckland, show that these periodic disturbances occur more often in the south at all times of the year. Both stations show a semi-annual occurrence of the disturbance, with maxima in November and June. The summer peak shows more irregularities. The periods of the oscillations are between 15 and 80 minutes. Longer periods were not seen because of difficulty in reading the chart record for such long periods, due to the diurnal changes in the ionosphere. Such difficulties can be removed by applying a high pass digital filter to the digitized data. Observations from Invercargill in the winter (subionospheric point 42°S geographic) showed a concentration of the observed periods towards 20 minutes. Titheridge deduced that the observed seasonal and diurnal variations were caused by two independent variations, possibly two separate processes for producing the variations. These were, firstly, day time irregularities occurring more frequently in winter, and more common at 42°S than 34°S and of small percentage amplitude, and, secondly, night-time irregularities,twice as common in summer and slightly more common near the

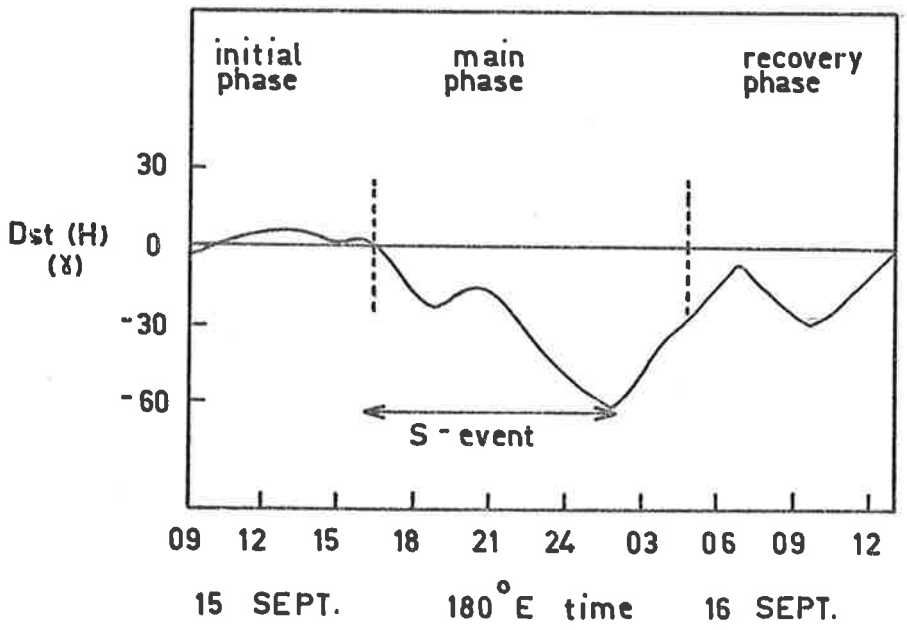

Figure 5.1 D_{st}(H) for 15-16 September, 1967.

equator, and of larger percentage amplitude. The day-time oscillations were almost the same period in winter and at 42°S. This is shown by the fact that 86% of oscillations occurred with periods between 16 and 24 minutes, as observed at 42°S latitude. The night-time oscillations were spread in period from 15 to 100 minutes, and only experienced the aforementioned seasonal variation. Some of this separation into distinct variations is prompted by the lack of observations of any variations during sunset and sunrise apart from the regular variations. This lack of observations may be more apparent than real, however. It is much harder to detect small irregularities in a line which is steeply sloping, as is the line of total electron content against time during sunrise and sunset.

These phenomena are almost certainly produced by the ionospheric effect of internal gravity waves propagating in the neutral atmosphere. The ions are forced into motion along the magnetic field lines by collisions with neutral atoms. Some of the observed variations in occurrence could be due to the geometrical effects which affect the observation of waves in the total electron content (Georges and Hooke, 1970). From their paper it can be seen that travelling ionospheric disturbances would be most easily detected when moving so that the surface of constant phase contained the observer to satellite path. Other differences could be caused by variations in the percentage electron density perturbation imposed,

because of the variation of the response of the F region with the direction of motion of the wave (Hooke, 1970). Other phenomena can be expected because of the filtering effect of wind systems in the stratosphere, mesosphere and the E region. These can act because vertical shear in the background wind affects the propagation of internal gravity waves. The occurrence of sinusoidal oscillations implies strong filtering and modification because most sources of internal gravity waves would give a wide spectrum, not a narrow one. In connection with a lack of disturbances near sunset and sunrise, it should be noted that travelling ionospheric disturbances do occur near sunset (Davies and Jones, 1971) and these have been shown to have the phase characteristics of internal gravity waves.

Large long period disturbances in total electron content have been noted, the most extensive study being by Davis and da Rosa (1969). These disturbances show a marked similarity over distances of 1000 km, have periods between 60 minutes and 180 minutes, and last usually 10 to 15 hours. Davis and da Rosa (1969) used spaced station observations to show that these disturbances propagate at about 500 m/sec along the direction away from the midnight section of the auroral oval. The speed also shows a diurnal variation, with a maximum near local noon. These factors point to the T.I.D. being the ionospheric effect of a gravity wave in the neutral atmosphere.

Similar disturbances have been observed using incoherent scatter (Thome, 1968; Georges, 1968). They are of the type Georges classifies as large scale travelling ionospheric disturbances. Testud (1970) shows, by analysing observations of the vertical velocity and ion temperature of the plasma, using the incoherent scatter sounder in France, that such disturbances can be produced by an auroral substorm, causing Joule heating of the neutral atmosphere.

Chimonas (1968) showed that the Lagrangian $\underline{J} \times \underline{B}$ force could also produce gravity waves. The evidence is not yet complete in that nobody has produced a satisfactory model. This would involve modelling the auroral electrojet as well as the atmospheric response more exactly.

2.5 Transient Phenomena

Certain large solar flares have been observed to cause increases in total electron content (Garriott et al. 1967). Such increases must be due to increases in the extreme ultraviolet radiation, and not in increases in the X-ray emission, which are known to occur in solar flares. This is because the X-ray enhancement only causes increased ionization in the D region. Garriott et al. (1967) showed that such an increase in D region ionization could explain neither the magnitude of the change of total electron

content or its time behaviour. Only the largest flares cause detectable effects. Such events are best observed using spaced stations so as to eliminate travelling ionospheric disturbances. Measurements of the magnitude of the electron content increase and of the associated sudden frequency deviation, combined with X-ray flux measurements, would be useful in estimating both the ionizing flux, and perhaps in studying the F region chemistry.

2.6 Annual and Semi-annual Variation

Garriott et al. (1970) present results for Stanford and Hawaii of total electron content measurements from September 1964 to June 1969. The observed daily maxima show a strong semi-annual effect during sunspot maximum, the largest values occurring near the equinoxes. However if the results are normalized for an overhead sun by multiplying by the secant of the minimum zenith angle, the variation becomes annual, with a minimum in June. This suggests that the seasonal anomaly occurs because the summer values are low. During sunspot minima no variation is detectable. The average night-time variation in electron content shows an annual variation with a maximum around June. The amplitude increases as sunspot number increases, and the amplitude is greater for Hawaii than for Stanford. The solar cycle variation is less marked than for the maximum total electron content. Garriott et al. note that during winter of 1965-1966, there was little variation in total electron content from

night to night. During summer nights there is a greater spread of values, although from their Figure 4 it seems the percentage variation is much the same in winter as in summer. From the description it seems that days of large total electron content, associated with ionospheric storms, have not been eliminated before taking the running means. This could bias the data at the equinoxes. No longer series of data is available at this time to study the solar cycle variations using geostationary satellite measurements. Bhonsle et al. (1965) using total electron content measurements from lower orbiting satellites, for 1958 to 1962, plotted values of the noon electron content against smoothed sunspot number. It was observed that the data grouped itself along three straight lines of progressively smaller slope. One group consisted of values at equinoctial times, one for winter values and another for summer values. Garriott et al. (1970) state that similar plots of the available Stanford data show more scatter and the seasonal effects are less clear. Walker (1971) gives results derived from measurements using nonstationary satellites, and these show a behaviour at Hong Kong similar to that at Hawaii.

2.7 Ionospheric Storms

An association between magnetic activity and changes in the F region electron density have been known for many years (Hafstad

and Tuve, (1929, Appleton and Piggott, 1952). The effects are stated relative to a zero time which starts at sudden commencement. The most common way of describing the magnetic activity is illustrated in Figure 5.1, taken from Jones (1971). The main phase begins when Dst(H) goes through zero. The recovery phase begins when Dst(H) starts to increase. The main phase usually lasts 18-24 hours, while the recovery phase can last several days, (Rishbeth and Garriott, 1969). In Mid-latitudes, superposed epoch analysis on many storms, using storm commencement time as zero epoch, shows that there is an increase in electron concentration at the beginning of the main phase, followed by a decrease at the end of the main phase which tapers off during the recovery phase. Such effects are observed using either the maximum electron density (Appleton and Piggott, 1962) or the total electron content (Hibberd and Ross, 1967). Thomas and Venables (1966) showed that the effect of a storm depended on the local time of the beginning of the main phase. If this occurred during the night, an immediate decrease in the maximum electron density was observed. Recently Jones (1971) has observed a similar effect in the total electron content over Auckland. If main phase occurs during the time interval 0800 to 1200 local time, an increase in total electron content is observed. Jones postulates that a separate effect causes the decrease in electron concentration, probably an increase in the loss rate due to compositional changes.

Because the 72 storms which Jones studied show a distinctly non-uniform distribution in Universal Time, the local time effects are longitude dependent. Thus storms which cause large increases in total electron content at Auckland, can cause large decreases in the F region electron density at Mundaring four hours to the westward. In another paper, Jones and Rishbeth (1971) show that this phenomenon could be caused by heating in the auroral zone during an auroral substorm. They use as a model of this heating an increase in the latitudinal gradient of temperature. The heating causes a change in the neutral atmosphere winds, due to the increase in the pressure at the poles. This increases the equatorward wind during the night, and decreases the poleward wind during the day. Both these changes increase the height of the F layer and thus decrease the loss coefficient, thus increasing the electron concentration. Papagiannis et al. (1971) studied a selection of magnetic storms, which do not overlap Jones' selection to an appreciable extent. They studied the deviation from the monthly mean of the hourly averages of the total electron content observed using ATS-3, at a subionospheric point of 30°N, 70° W. They showed that the predominant storm effect was an increase in total electron content near sunset. This occurred even when the storm started after sunset, the increase being delayed until the next day in most cases. This seems to indicate a somewhat different behaviour from that observed

at Auckland, but since the storms considered also show non-uniform time distribution, local time effects may be a reflection of such a distribution. Since Papagiannis et al. do not put their data on quite the same basis as Jones, exact comparison of the two sets of observations is not possible. Papagiannis et al. also show that the magnetic field observed nearby exhibits a similar peak near 1800 local time. Using this fact they develop a model to explain both phenomena, involving the contraction of the plasmasphere in the dusk region, and the dumping of electrons into the ionosphere. This dumping occurs because an increased electric field opposes the co-rotation of the plasmasphere with the earth. This causes a compression of both the plasma, which flows down into the ionosphere, and a compression of the field, which is frozen in the plasma. The observed effect seems distinct from the type of increase mentioned by Jones (1971). The percentage effect is also smaller. The arguments for the plasmaspheric model are rather vague and non-quantitative. Perhaps the effects are caused by neutral wind, but the timing is different because of differences in the neutral wind pattern relative to the geomagnetic field. The marked decreases in total electron content observed could be due to many factors, for example; the increase in the loss coefficient during magnetic disturbance as mentioned earlier, a change in the composition of the ionosphere, due to an increase in the molecular nitrogen concentration, or changes

in the neutral atmosphere winds caused by the longer term effects of magnetic storms.

CHAPTER 6

OBSERVATIONS OF TOTAL ELECTRON CONTENT

1.0 Introduction

Observations of the rotation of the plane of polarization of the telemetry transmitter of the geostationary satellite A.T.S.1 (1966 110A) were made during August and September, 1970 using the rotating aerial system described in Chapter 3.

Two difficulties were experienced because of the low angle of elevation of the satellite. These were both caused by ground reflections. Some difficulty would have occurred whatever the antenna height chosen. Because of the low elevation of the satellite an antenna of beamwidth less than five degrees would have been needed to exclude the ground reflected ray. The originally chosen height of 2m was retained because any lower height would have influenced the antenna impedance, while any higher would have made the coupling coils inaccessible. The problems arose because of the combination of the ground reflected ray with the direct ray. For the antenna height used, the resultant signal received when the field was vertically polarized was small compared with the signal when the plane of polarization was horizontal. This caused some problems in the phase measuring equipment. Secondly at any

position other than horizontal or vertical the observed plane of polarization was not quite the same as the plane of polarization of the direct ray. The errors were of the order of twenty degrees. The effect caused spurious oscillations in the apparent rate of change of total electron content derived from the rate of change of the plane of polarization. This meant that the variation of total electron content for individual days could not be used to determine the change in the rate of change as the sun rose. It was necessary to average the total electron content over several days and to use these averages to calculate $d N_T/dt$ and d^2N_T/dt^2. The errors were most obvious near sunrise, because of the high rate of change of total electron content at that time.

At other times of the day T.I.D.'s masked any observable effects due to ground reflection. The effect of such errors on T.I.D.'s would be to distort the waveform of the T.I.D.

Observations without any break were obtained from August 13 to August 18 and from August 28 to September 2. Another period of unbroken observation extended from September 3 to September 8. However in this period interference shortly after ground sunrise due to radio emission from the sun made deduction of the total number of rotations impossible. The results in this chapter involve the two intervals mentioned above. The various studies are reported

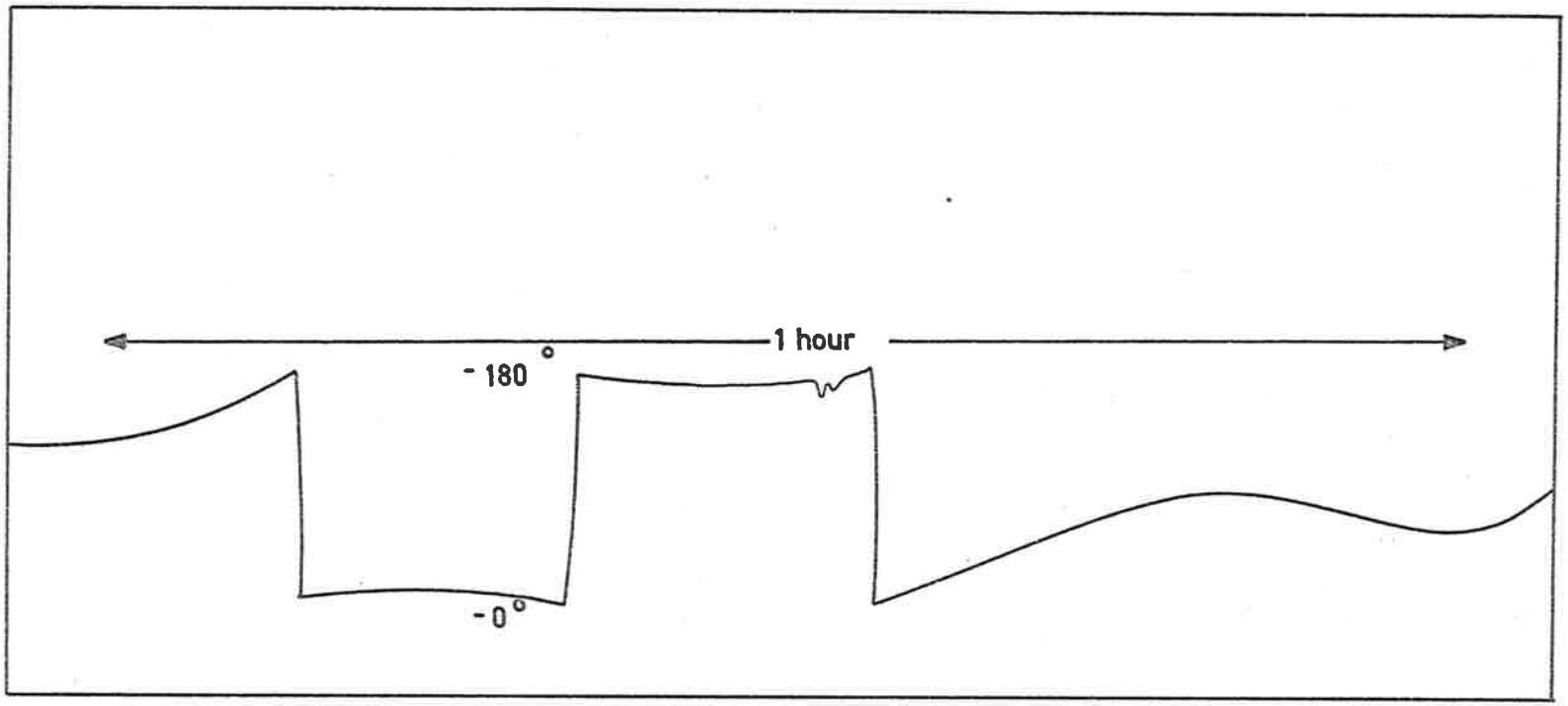

Figure 6.1 A sample of the recorded angle of polarization.

in the following sections.

2.0 Reduction

The angle of the recorded plane of polarization recorded on a chart, a sample length of which is given in Figure 6.1, was read at 18 points to the hour. The discontinuities at 0° and 180° were removed by considering whether the angle of polarization was increasing or decreasing. The particular reading interval was chosen so as to give no aliasing of high frequency components in T.I.D.'s. In addition it represented a convenient length of the chart recorder paper.

At this stage the smallest angle recorded during an interval was arbitrarily assigned the value of zero. Using an average value for the field factor for the whole day, calculated at a fixed height, the rotation was converted to total electron content with an arbitrary zero. Thus it was necessary to find the total electron content corresponding to the smallest rotation in each interval. This could not be attempted by two of the methods usually used. The elevation angle of line of sight was too low to observe a satellite in a lower orbit to calibrate the observed total electron content because one could not apply adequate theory to the lower satellite observation at such low angles. The stationary satellite only transmits on one

frequency so that the method of Garriott et al. (1965) could not be used. The only other technique is that of Smith (1969). However plotting the observed angle of the plane of polarization against the F region critical frequency at Brisbane or Norfolk Island did not produce a sensible result. This is probably because these ionosondes are not near enough to the sub-ionospheric point. Any method used must also allow the transmitted polarization to be determined, since it cannot be deduced from knowledge of the spacecraft. Thus any method to calibrate must either use a measurement of total electron content, or make use of an assumption about the number of rotations of the plane of polarization and a knowledge of the transmitted polarization. It is a fair assumption that the day after a magnetic storm the minimum total electron content is such that the rotation of the plane of polarization is less than Π radians (Titheridge, private communication). It would be of advantage for future observations of total electron content, if satellites carried antennae whose transmitted polarization was known, such as a dipole, rather than the turnstile antenna used on A.T.S.1.and the Syncom satellites. An alternative would be some of the frequency independent antennae, mentioned in I.E.E.E. (1971). It is possible to have the polarization parallel to the spin axis of the satellite which is usually aligned with the axis of rotation of the earth.

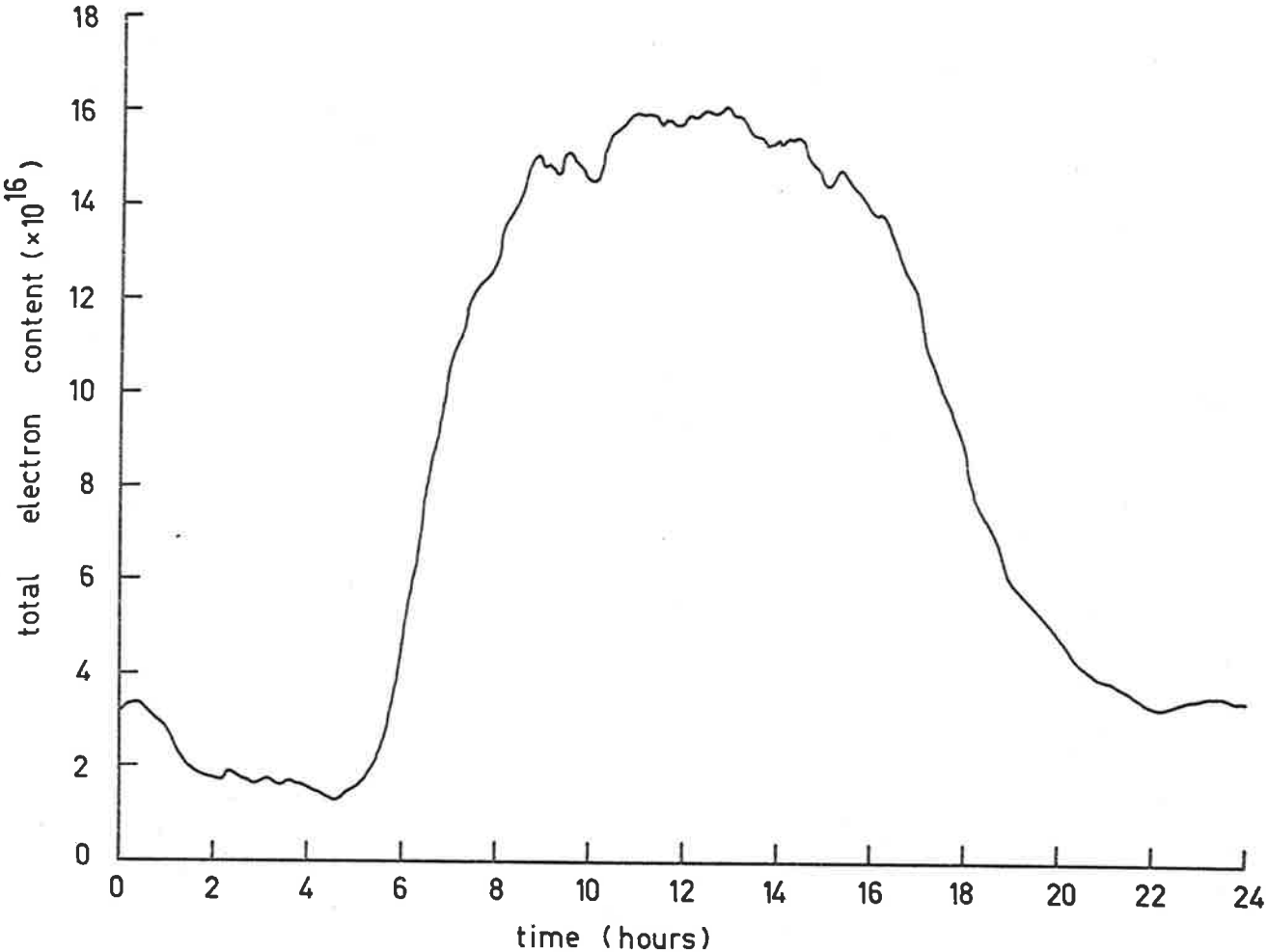

Figure 6.2 The average diurnal variation of total electron content.

Because none of the above methods could be used, total electron content for the two intervals had arbitrary and different zeroes. Therefore no studies were attempted where absolute values of the total electron content were necessary. The total electron content for the two intervals was tabulated and plotted.

3.0 Rate of Change Near Sunrise

Titheridge (1966) derived values for the integrated production rate for an overhead sun using the relation $Qo = 15 \frac{dN_T}{dt} = (\chi = 90°)$ where χ is the solar zenith angle. The results of applying this to individual days is shown in Table 4. The value is corrected for changes in total electron content before sunrise. The average value is 2.85×10^{13} electrons $m^{-2} sec^{-1}$.

Garriott et al. (1965) derived the formula

$$Qo = \frac{d^2 N_T}{dt^2} \int \left(\frac{d\eta}{d\chi} \frac{d\chi}{dt} \right)$$

where η is the reciprocal of the Chapman function and χ is the solar zenith angle, and all quantities evaluated when $\chi = 90°$. This formula is more accurate because it is almost independent of the value of scale height used to calculate the Chapman function. However due to the sinusoidal fluctuations produced by ground

TABLE 4

Date	dN/dt(χ=90°) $e/m^2/sec$	+Loss Rate	Qo $e/m^2/sec$	S $(10^{-26}_{wm}{}^{-2}_{sec}{}^{-1}$
August 14	2.04×10^{13}	$.09 \times 10^{13}$	3.19×10^{14}	167
15	2.11×10^{13}	0	3.16	169
16	1.86×10^{13}	.09	2.92	163
17	1.89×10^{13}	0	2.83	152
18	2.48×10^{13}	.525	4.52	149
28	1.406×10^{13}	0	2.11	139
29	1.580×10^{13}	0	2.37	146
30	2.61×10^{13}	0	3.02	146
31	2.14×10^{13}	0	3.21	152
September 1	1.09×10^{13}	0	1.64	151
2	1.55×10^{13}	0	2.33	154
Average	2.85×10^{13}			

reflections, $\frac{d^2N}{dt^2}$ could not be calculated for individual days. The values calculated using the averages for the two longest intervals are shown in Table 5. The average value is 2.06×10^{14} electrons $metre^{-2} sec^{-1}$. Considering the change in solar activity the average value from the slope method, which is probably the most accurate, is in reasonable agreement with the value for Qo measured by Titheridge (1966).

TABLE 5

Time Interval	Qo ($e/m^2/sec$)	β' ($second^{-1}$)
Aug 14 - Aug 18	3.0×10^{14}	$.49 \times 10^{-4}$
Aug 28 - Sep 2	1.11×10^{14}	$.88 \times 10^{-4}$
Average	2.06×10^{14}	$.69 \times 10^{-4}$

4.0 The Diurnal Variation

The dominant diurnal variation was a steep rise after sunrise, levelling off during the day, followed by a fall after sunset. This is shown in Figure 6.2 which is the average of the variations on August 14, 15, 16 and 18. The residual fluctuations are due to the small number of days averaged. Only 3 days, August 17, 28 and 29 were significantly different. They exhibited a sharp peak at about 1100 LT and a decrease after this. August 17 was definitely atypical

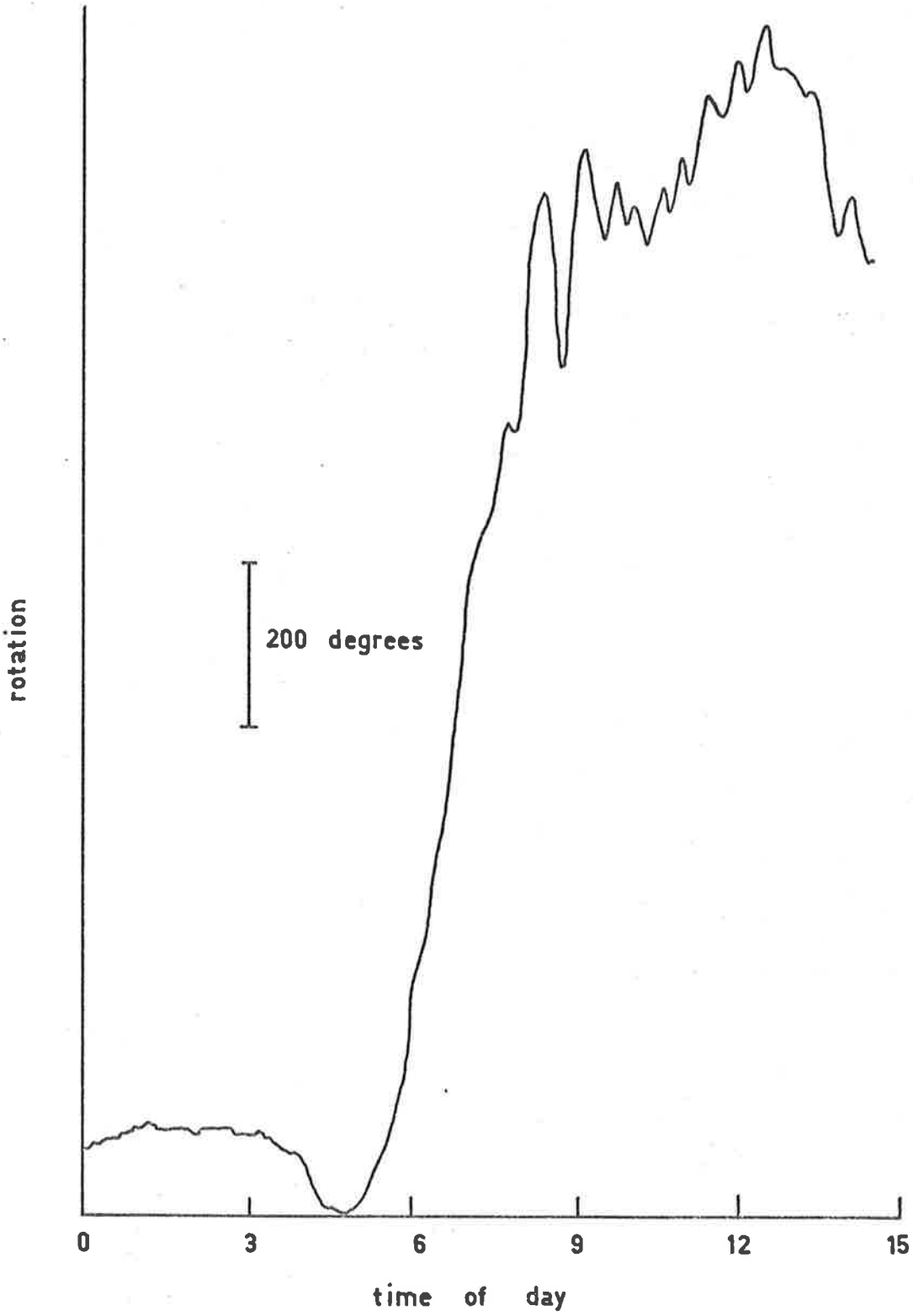

Figure 6.3 Total electron content record showing quasi-sinusoidal variation.

because there was a magnetic storm at that date, and the electron content recorded was the highest during the series of measurements.

5.0 Night-time Variation

Three varieties of behaviour occurred. The first was a monotonic decay until sunrise at the subionospheric point. The second was a decay to a constant value of total electron content, reached around 2400 LT, and maintained until the sunrise increase. The third type of behaviour was again a decay to a constant value at about midnight and then another decrease at around 0200 LT. This last type is also illustrated in Figure 6.2.

These last two forms of behaviour suggest a night-time source of ionization, the variation occurring because of a variation in the time the source ceases to supply electrons. Some short term increases in total electron content were observed. These can be attributed to travelling ionospheric disturbances, as the excursions were similar to variations in total electron content during daytime. The loss rate in the simplified model of the ionosphere was calculated using the average rate of change of total electron content one hour after ionospheric sunset. The model, used by Titheridge (1966) leads to the equation

$$\frac{dN_T}{dt} = Q - \beta' N_T$$

where N_T is the total electron content,

Q is the production rate,

and β' is the effective loss rate.

When Q is zero, $$\beta' = \frac{dN_T}{dt} / N_T \quad .$$

Table 5 shows the result for the two intervals of measurement, using the averaged diurnal curves, and a linear least squares fit to the curves from one to three hours after ionospheric sunset. The average value may be compared with the value 0.5×10^{-4} found by Titheridge (1966).

6.0 Travelling Ionospheric Disturbances

Irregular and quasi regular disturbances are visible on plots of the total electron content. A non-typical example is shown in Figure 6.3. Usually the variation is more irregular. The power spectrum of the time series formed by the values of total electron content from August 13 to August 18 is shown in Figure 6.4. No filtering was performed, and the maximum at zero frequency is due to the diurnal variation. No significant peaks occur at any particular period. The logarithm of the power shows an almost exponential form.

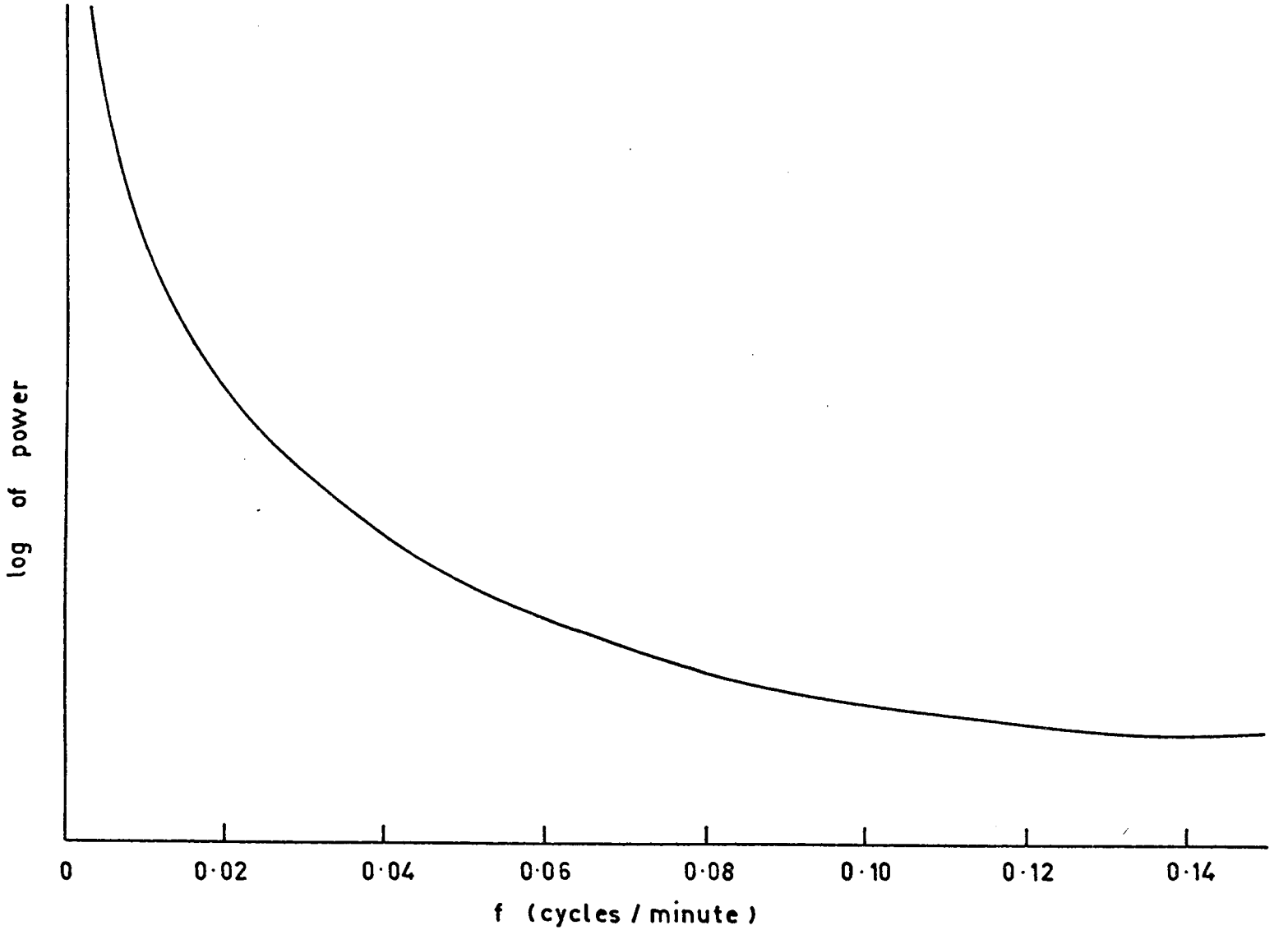

Figure 6.4 Power spectrum of total electron content. August 13 to August 18, 1970.

A more detailed analysis was carried out by applying a numerical filter to the time series. The filter had a form in the frequency domain of:

$$T(f) = \frac{(f/fo)^4}{1+(f/fo)^4}$$

where f is the frequency, and fo is the cut off frequency. This is a high pass filter. The cut off frequency was chosen so that disturbances with a period of four hours were reduced in power by six decibels. A plot of the output of such a high pass filter is shown in Figure 6.5. This shows that the observed T.I.D.'s were of longer period and smaller amplitude during the night-time. All the T.I.D.'s have periods greater than twenty minutes. This can be explained by the geometry of the observing situation and the response of the ionosphere (Georges and Hooke, 1970). From Figure 7 in their paper (reproduced as Figure 6.6 here) it can be seen that the longer period T.I.D.'s would be favoured because of the low elevation angle. The same diagram (the one for satellite elevation 80°) indicates that T.I.D.'s travelling in the direction of the line of sight and in the north eastern quadrant would be favoured.

The amplitude of the T.I.D.'s during the daytime did not exceed 15% of the daily maximum total electron content.

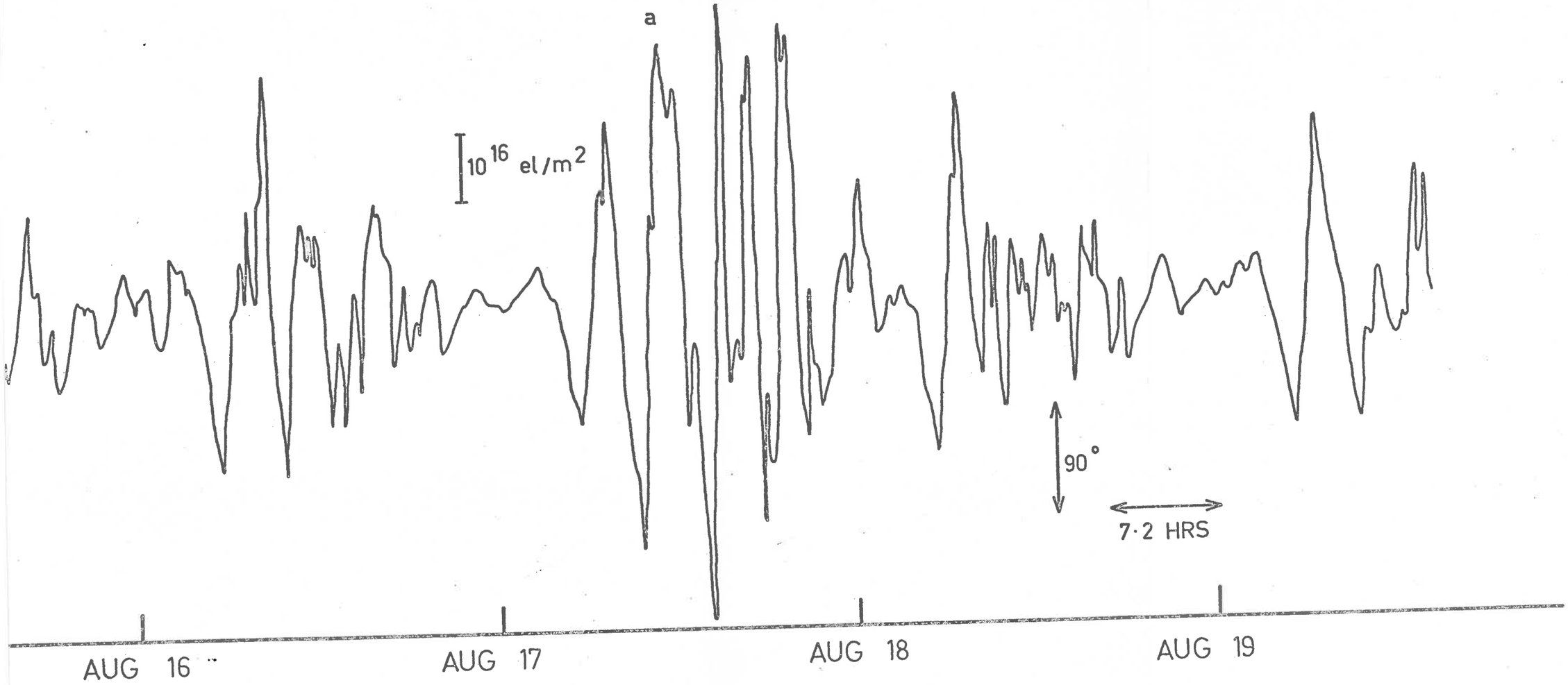

Figure 6.5 Result of applying a high pass filter to total electron content record

7.0 Ionospheric Storms

The magnetic storm which began on August 17 (local time) showed two significant effects. Firstly, the largest total electron content observed, 20 percent higher than any other, and secondly a long period, very large amplitude T.I.D. which would appear to be a large scale travelling ionospheric disturbance associated with the geomagnetic storm which had a sudden commencement on August 16 at 2204 UT. This T.I.D. is included in the section of filtered record shown in Figure 6.5. The first peak, marked "a" in the Figure 6.5 would be the increase in total electron content due to the storm. This peaked at about 0158 UT on August 17 (1214 LT). The main phase as seen on magnetograms in the Solar-Geophysical data bulletins, appeared to begin about 0300 UT, which is 1316 LT at the subionospheric point. Thus Jones' (1971) criterion is not quite met, since he says the main phase must include the 0800-1200 LT interval to give an enhancement. However it should be noted that, without the $D_{st}(H)$ values for the storm, an exact time for the start of the main phase cannot be given. Also, the enhacement is not very large, so perhaps the effects would have been larger if the storm had started a little earlier.

8.0 Solar Flare Effects

No readily recognizable solar flare effects were detected during the observations. It is rather difficult to separate out any such effects from travelling ionospheric disturbances using observations at a single station. If one had observations at several stations the simultaneous occurrence of solar flare effects would make them obvious.

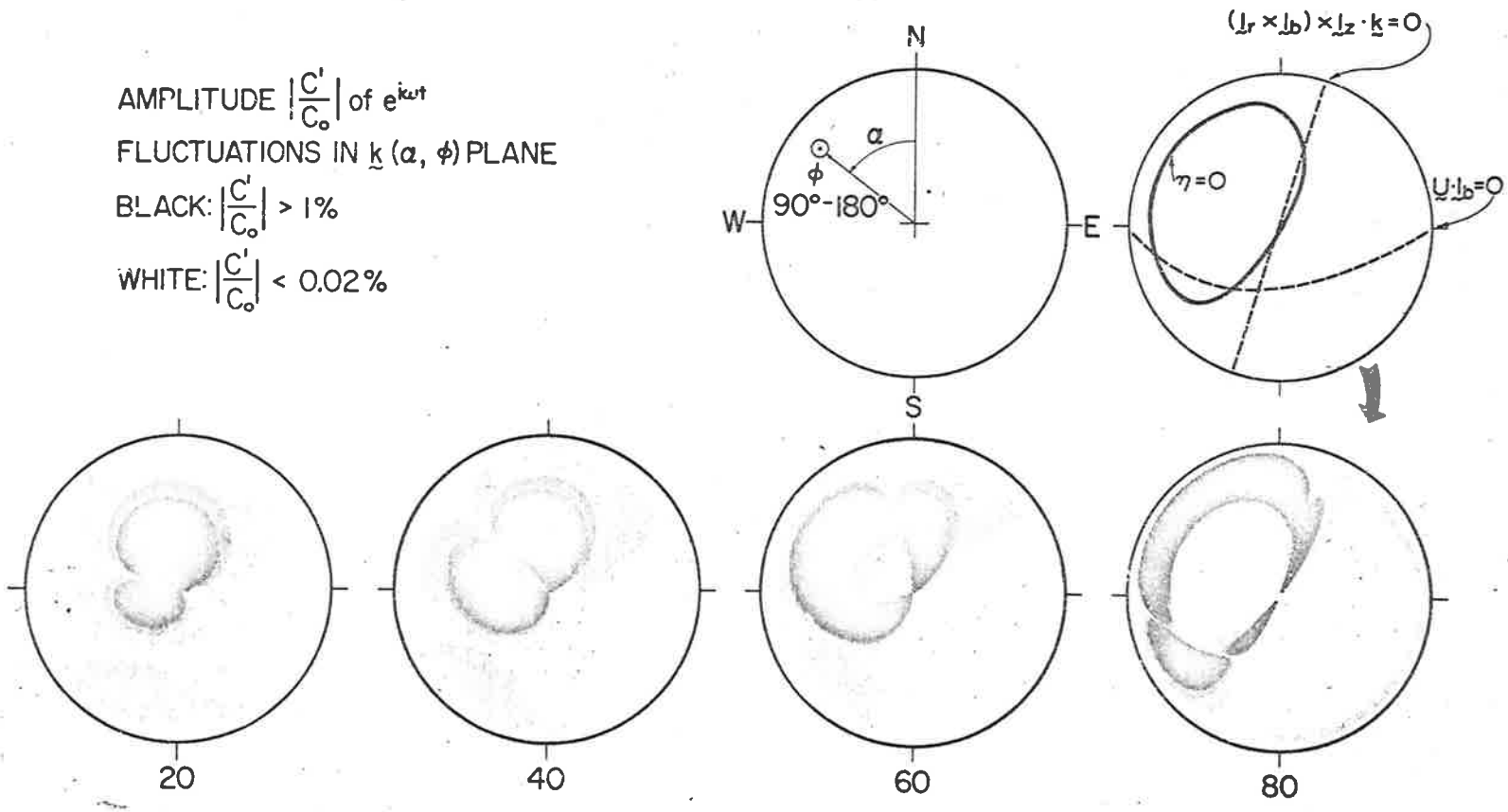

Figure 6.6 Plane gravity waves in α-Chapman layer. Intensity plots of the amplitude of fractional content fluctuations in the k plane for four fixed satellite locations. These plots indicate the spectral biases of given satellite geometries. I is 40°, λ is 100 km, U is 10 m/sec, H is 50 km.

CHAPTER 7

STUDIES OF DIFFRACTION EFFECTS DUE TO IONOSPHERIC IRREGULARITIES

1.0 Introduction

This chapter comprises three topics, which are not very closely related except that they are all concerned with studies of the diffraction pattern produced a radio wave after it has passed through irregularities in the ionosphere.

2.0 Regular Scintillation

This is a term applied to certain regular patterns seen on records of radio star or satellite scintillation. An example obtained during the course of the present investigations (a recording of the ATS1 telemetry transmitter) is shown in Figure 7.1. Similar events have been seen in radio star scintillation where they are known as broad band scintillation because of the large frequency range over which they are detected (Wild and Roberts, 1956; Warwick, 1964). It has been usual to assume that the scintillation normally observed using satellites and radio stars can be explained by diffraction due to an irregular phase screen. That is,

irregularities are separated by a distance less than the size of the first Fresnel zone. This means that the observed diffraction pattern is caused by the scattering from several irregularities. Titheridge (1971) has discussed several examples where this is not true. The amplitude pattern and the pattern of total electron content can exhibit related peaks. This shows that single irregularities can cause scintillation effects.

Elkins and Slack (1969) observed quasi-regular amplitude patterns on records of the amplitude of signals from several geostationary satellites. They were able to measure ground speed using spaced receiver observations. Assuming a model of reflection from a moving discontinuity in refractive index they made use of the observed interference pattern to determine the height of the irregularity. Heights in the F region were found. Titheridge (1971) shows that a model of a drifting elongated irregularity of sufficiently large phase deviation will produce a similar pattern. He also can determine the height if the velocity is known. For lower satellites it is not necessary to know the velocity of the ground pattern, only the satellite velocity and height.

Another cause of regular scintillation appears to be sporadic E layers with "sharp" edges (Basu, 1969; Ireland and Preddy, 1969).

Since the height can be calculated from the diffraction

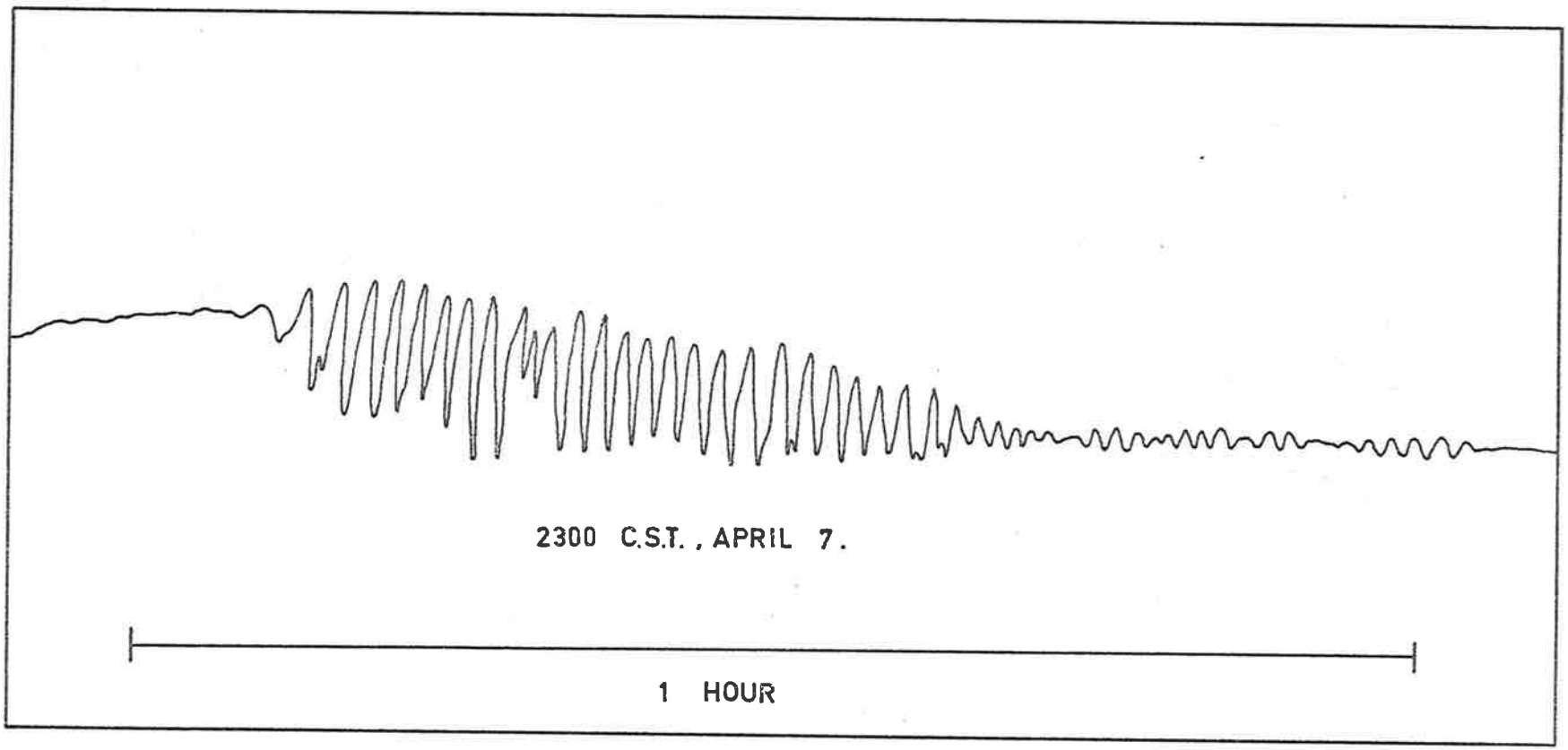

Figure 7.1 Example of regular scintillation

pattern, it is possible to distinguish such effects from the similar patterns due to F region irregularities.

3.0 Strong Individual Irregularities

Titheridge (1971) shows that isolated Gaussian irregularities of electron density show focussing behaviour when

$$\phi \geq \frac{37fd^2}{h}$$

where ϕ = maximum phase deviation in radians

f = frequency in MHz

d = Gaussian half-width in km

h = height in km

since $\phi = 0.81 \times 10^{-14} \Delta I$ for f = 137 MHz.

If ΔI is the line-integrated electron content of an irregularity, then for focussing the total electron content required is

$$\Delta I \geq 2.08 \times 10^{15} d^2 \quad (d \text{ in km})$$

for the frequency of A.T.S.1.

For an elongated irregularity, of Gaussian form which falls to e^{-1} 0.5 km from the centre, focussing will occur if $\Delta I > 5.2 \times 10^{16}$. This is about 300 degrees rotation of the plane of rotation. Such

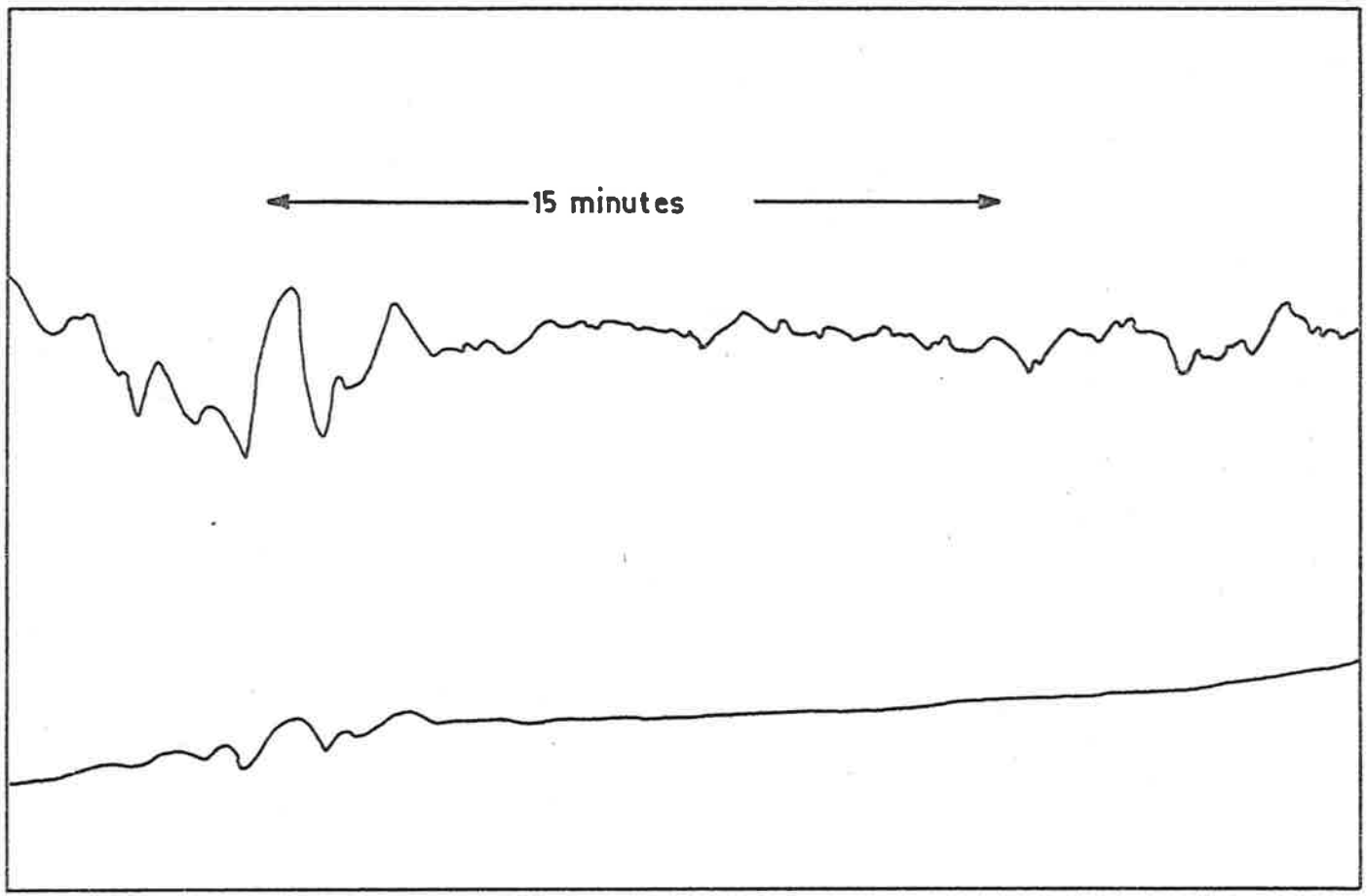

Figure 7.2 The top trace shows focussing effects on the amplitude record. The bottom trace shows the variation in total electron content.

irregularities would be detectable, but none of such a size were observed with such amplitude in the course of the present work. However if we reduce the size to 2 km, the critical limit becomes 4.3×10^{15}, which is nearer the perturbations observed.

Several times perturbations in the total electron content accompanies regular scintillation. An example of focussing is shown in Figure 7.2, with accompanying record of the total electron content. The irregularity appears as a large decrease in electron content flanked by two smaller decreases. A wave packet is vaguely suggested by the form. The amplitude of the irregularity is 10^{15} electrons m^{-2}.

The width of the main irregularity, using a Gaussian model, is about 50 seconds. If a drift velocity of 50m sec^{-1} is assumed this gives a width of 1 km. Since full regular scintillation has not occurred, the criterion for it should not be satisfied, which it is not. The agreement is probably fortuitious, considering the method by which Titheridge (1971) worked out the critical phase. Sharper gradients in electron density than would be given by a Gaussian irregularity can occur for other forms of electron density variation. This would cause a larger refraction, and hence interference could occur with an irregularity of smaller total electron content than the criterion gives.

It is concluded that small irregularities can exist by themselves in the ionosphere. They are such that they cause a change in total electron content of the order of 10^{15} electrons m^{-2}.

For a Gaussian variation of electron density along the ray path this implies a central density about 0.5×10^{12} electrons m^{-3} relative to the background. This density is a very appreciable fraction of the background density. Irregularities of 30 percent above or below the background seem quite possible. If the present estimate of the size is too small, as it could be, then the irregularities would be a smaller percentage of the background.

It is concluded that regular scintillation is caused by irregularities of size the order of 2 km, and of density such that they differ from the background ionization by about 50 percent.

4.0 Power Spectrum of the Amplitude Diffraction Pattern

It is commonly assumed that the observed random variations in amplitude of radio star and satellite signals are due to diffraction by an irregular phase screen produced by random variations in electron density. Diffraction of a normally incident plane wave by a think weak, one dimensional phase screen has been analysed by Hewish (1951), Bowhill (1961) and others. They show that the power

spectrum of the amplitude pattern on the ground. V(X), is related to the power spectrum of the phase fluctuations of the wave emerging from the screen, W(X), by the relation

$$V(X) = W(X)\sin^2(\Pi\lambda h X^2) \qquad (1)$$

where X is the spatial frequency

λ is the wavelength of the radiation,

and h is the height of the screen.

This function has zeroes whenever

$$X^2 = n/(h\lambda) \quad (\ = 1,2,3) \qquad (2)$$

To apply to the satellite case h must be transformed to Hh/(H-h) where H is the height of the satellite. This is because the radio waves from the satellite are not plane but spherical. Also for a satellite in a low orbit the spatial frequencies are converted to temporal frequencies, f, by the motion of the satellite with velocity v. Thus finally,

$$X = \frac{(H-h)f}{hv} \qquad (3)$$

The temporal spectrum then has the form

$$V(f) = W\left|(H-h)f/hv\right| \sin^2\left|\Pi\lambda \frac{(H-h)}{h} H \left(\frac{f}{v}\right)^2\right| \qquad (4)$$

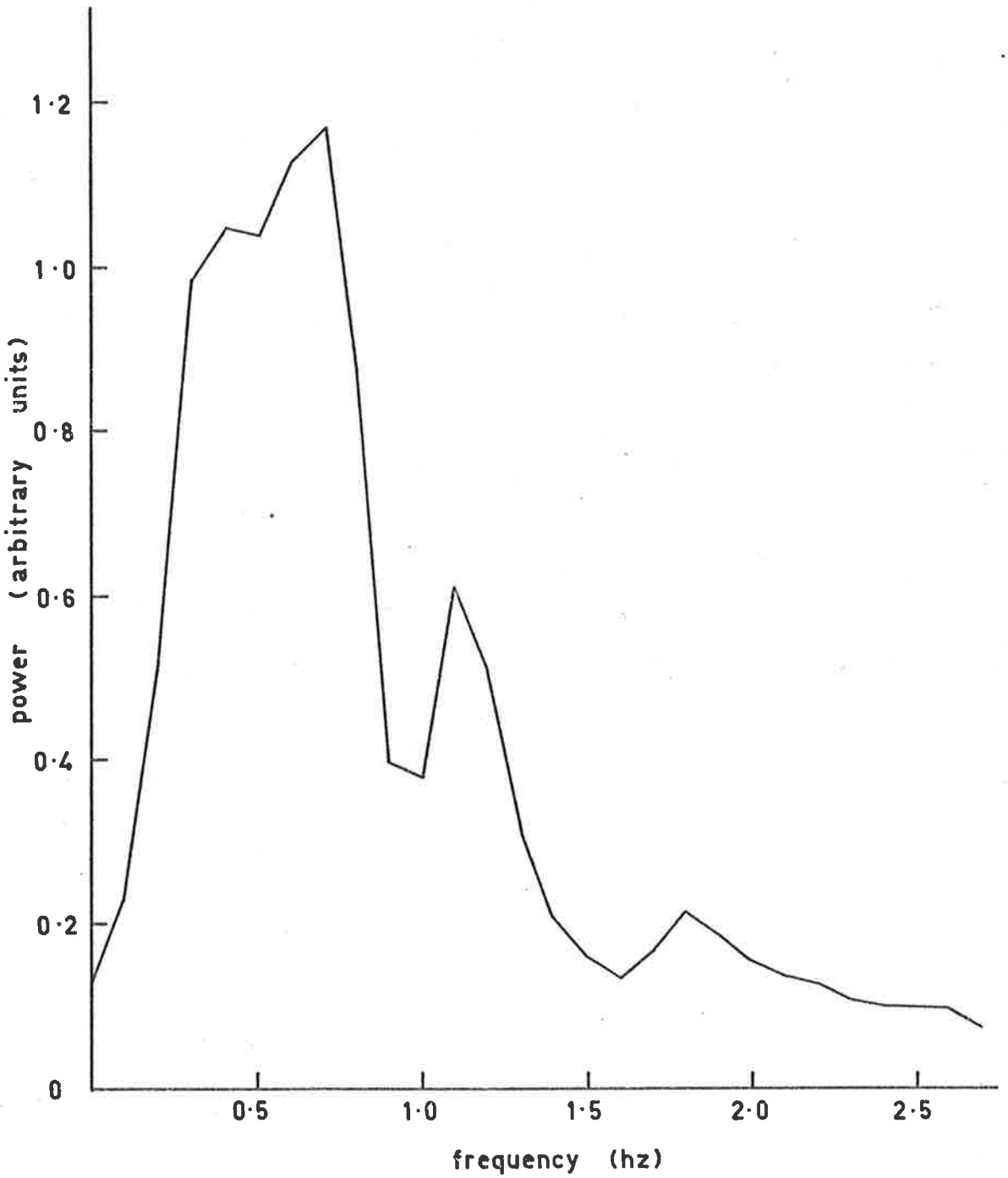

Figure 7.3 Power spectrum of a scintillation record.

Thus if the position of the first zero is observed in the power spectrum of an amplitude record, the height of the diffracting screen can be calculated. It should be noted that the velocity of the ground pattern need not be known explicitly.

In practice of course the spectrum of phase fluctuations of the emerging wave is two dimensional. Parkin (1967) shows that the power spectrum obtained from sampling with a single receiver an amplitude pattern which has a 2-D spatial power spectrum $V(X,Y)$ is proportional to $\int V(X,Y)dY$, for motion of the pattern along the direction Y. This function will not generally show the fringe structure which $V(X,Y)$ shows. If $V(X,Y)$could be observed directly this problem would not exist. However such an experiment would require an array of antennas spaced several hundred metres apart up to a maximum distance of several kilometres, and such an array would seem to be too costly to be worthwhile. However there are conditions where the two dimensional case approximates to the one dimensional result. This is when the pattern on the ground is greatly elongated, say along the y direction, and the pattern is moving along the x direction, that is, perpendicular to the direction of elongation. Then Parkin (1967) shows that $\int V(X,Y)dY \doteq V(X,0)$. In such a case the observed spectrum would show the same fringing as a cross-section of the two dimensional spectrum. The above discussion is based on a thin screen model. For a thick

screen Budden (1965) and Parkin (1967) show that the effect on V(X,Y) is to fill in the zeroes of the spectrum to some extent.

Parkin (1967) derived an expression to test whether the first zero of the fringing function, $\sin^2(\Pi\lambda h X^2)$, fell on a useful part of the spectrum. This was defined by saying that the zero had to occur before the value of the function W(X,Y) had fallen to $1/3^2 (\doteq .15)$, assuming that W(X,Y) is normalized to have a maximum value of 1.0. For the satellite case this requires

$$\frac{\lambda h}{\Pi^2 r_o^{\,2}} \geq \frac{H}{2(H-h)} \qquad (5)$$

where $2r_o$ is the length of the correlation function of the irregularities. For the values of these variables chosen by Parkin (1967) the quantity on the left hand side $\doteq .45$ and this is less than the right hand side $\doteq .7$. Parkin thus concluded that any detection of the zeroes in the power spectrum would be marginal and would rely on oblique angles and the use of the 20 MHz transmitter on the satellite BE-C. He also found no spectra showing zeroes in practice, using records of the signal strength on 40 MHz. It was not possible to use the 20 MHz transmissions because the Faraday fading on 20 MHz was too close in frequency to the frequency of the scintillations.

Parkin (1967) made measurements of the ground pattern size,

shape, and velocity using three spaced receivers in conjunction with full correlation analysis. The results show that the pattern is usually highly elongated, and that a better estimate of the size of the irregularities is r_o = 0.5 km not r_o = 1 km. This means that the zeroes in the power spectrum should be quite detectable on 20 MHz and occasionally seen even on 40 MHz when the propagation is oblique and the irregularities small. As some later measurement using the equipment and programmes constructed by Parkin, with some modifications by the author, indicated in one case a value of r_o = 0.3 km, a search was instituted among the recordings of satellite passes to see whether there were occasions when distinct zeroes or minima did occur in the spectra. Two passes of the satellite BE-C were observed in which the power spectrum of the scintillations showed minima other than the one at zero frequency. The power spectrum for the pass on 17th October 1967 is shown in Figure 7.3. This feature was seen in spectra from non-overlapping records on either side of the section of record used, so its reality is not in doubt. The formula for working out the height was derived for the oblique situation using the formulae given by Parkin (1967). The two results are shown in Table 6. The computed angle between the projected direction of the magnetic field and the direction of motion, θ is given. The estimate error is about $\pm$ 30 km, that is about ten percent. The height calculated for February 10, 1966

compares reasonably with the height, computed from the pattern motion by Parkin (1967), of 307 km. The reason why he did not see this minima was because he used too short a length of record to calculate the power spectrum in this particular case.

TABLE 6

Time of Pass	θ	Height
Sept 17, 1967	25°	326 km
Feb 10, 1966	5°	334 km

It is interesting to note that the sizes of irregularities in the F region get smaller both towards the south pole (Clark, 1971) and towards the equator (Koster, 1966). Perhaps if power spectra were obtained from equatorial or auroral stations, minima would be detected which could give the height of the irregularities. Such observations would have to be at times of moderate scintillation index, so that the weak screen assumption is still reasonably valid. The above statement applies to transmissions at 40 MHz. However if r_o is ever as low as 0.2 km, then $\frac{\lambda h}{\pi r_o^2} = 1.5$ for $\lambda = 2m$, and $h = 300$ km. This suggests that the power spectra of scintillation due to F region irregularities might sometimes show the minima sought for, even in the 136-138 MHz telemetry band. Such observations would seem particularly useful since the ground pattern is always

greatly elongated. Since one important condition is that the ground pattern must be moving perpendicular to its elongation, observations would not be successful on low satellites in polar orbits. There are however a few satellites in near equatorial orbits that would be useful, if it is feasible to use them. Two in particular are PEOLEI (1970-109A) and Uhuru I (1970_107A). For observations of geostationary satellites, as a strong east-west drift exists most of the night, no problem would be encountered. If observations of the drift velocity were made, as well as spectral observations, then it would be possible to determine irregularity height. There are non-ionospheric applications to this principle, in other diffraction problems, interplanetary scintillation in particular. Lovelace et al. (1970) has shown that if the zeroes can be detected in the power spectrum of the interplanetary scintillation, or rather the Bessel transform of the power spectrum, then the solar wind velocity can be determined, from observations with a single receiver. The Bessel transform comes in because it can be assumed that the pattern is isotropic. Parkin (1967) showed that the two dimensional spatial spectrum and the observed spectrum are related by a Bessel transformation in this case.

3.0 Study of Full Correlation Analysis

The method of full correlation analysis is that most fully outlined by Fooks (1965). The method was applied to the ground pattern of satellite scintillation by Parkin (1967) and Koster (1966) (in a slightly modified form). The correlation between two points on the ground separated by distances x and y in the two co-ordinate directions, and time t, can be imagined as a scalar field in a three dimensional co-ordinate system. The axes are X, Y and T. Then full correlation analysis assumes that surfaces of equal correlation are ellipsoids of revolution, formed by rotating an ellipse about its major axis. The auto-correlation at any receiver is given by a path along the T axis. The cross-correlation between two receivers separation x, y, is similarly a vertical line parallel to the T axis and going through the point x, y. From geometric reasons this implies that the half width of the auto and cross correlations should be the same. Many things could alter this result, either the assumptions about time and space correlations implicit in full correlation analysis, or the change in one of the parameters during the length of record analysed. For example, if the velocity changes during the length of record analysed, this would tend to increase the width of the cross-correlation function more than the width of the auto-correlation function. In general the ratio of the half-widths is

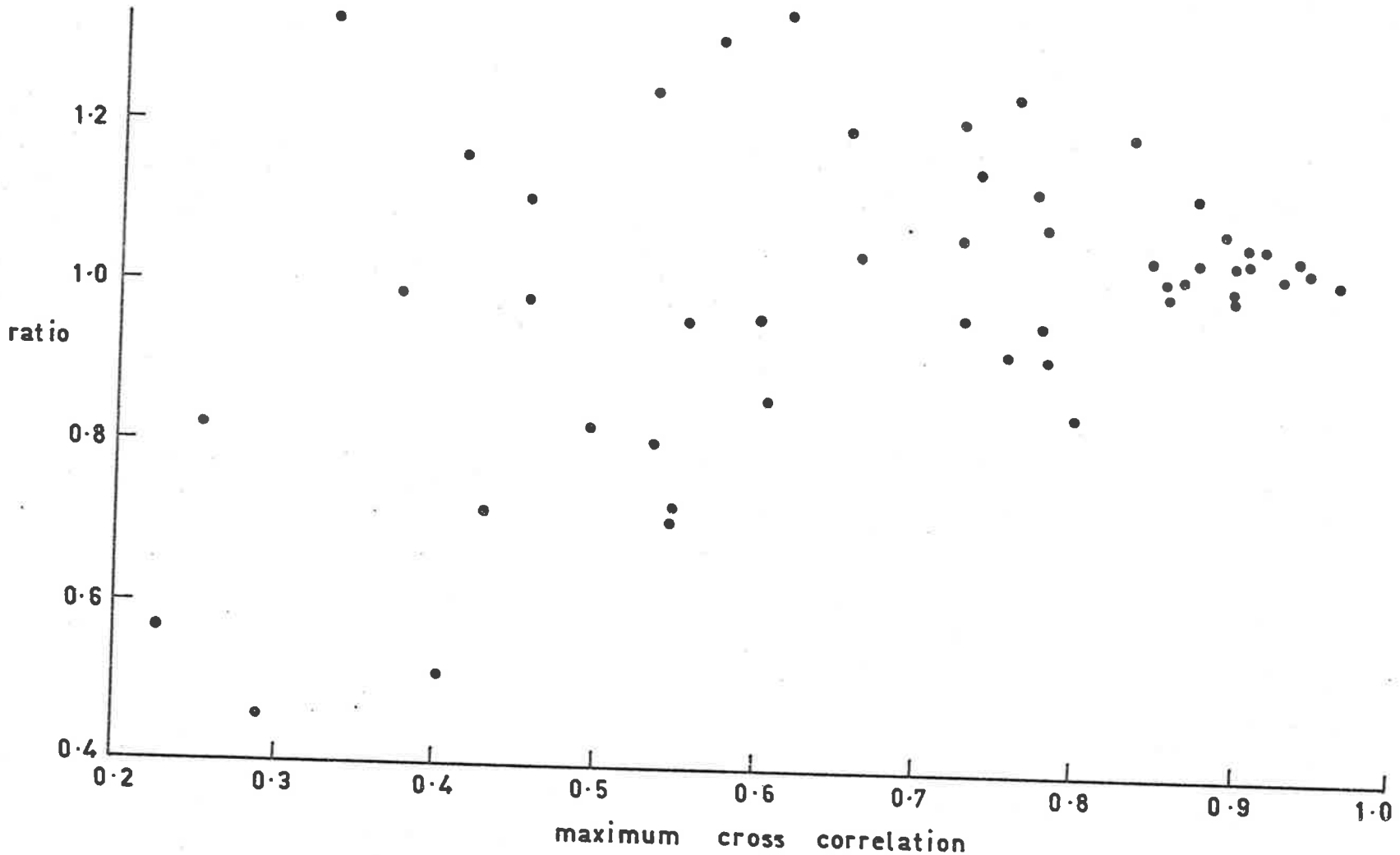

Figure 7.4 Ratio of the half-widths of the cross and auto-correlations against the maximum cross correlation.

a test of whether the pattern on the ground fulfils the assumptions of full correlation analysis.

An examination of the ratio was carried out using all available spaced receiver data. Most of this was data collected by Parkin (1967). About ten percent of it was collected by the author. A plot of the result is shown in Figure 7.4, with the ratio plotted against the maximum cross-correlation. Rather more than two thirds of the cross-correlation studied fall into the range $1.0 \pm .2$, which seems a reasonable interval to cover random errors. The scatter is also much less for high maximum cross-correlation, a not unexpected result. Therefore it may be concluded that full correlation analysis should only be attempted on spaced satellite receivers when the maximum cross-correlation is greater than 0.7.

CHAPTER 8

SCINTILLATION OBSERVATIONS: DIURNAL AND SEASONAL VARIATIONS

1.0 Introduction

This chapter will be concerned with observations of the diurnal and seasonal variations of scintillation index and the occurrence of scintillations. Variations in scintillation index are assumed to represent variations in the average difference in electron density between the irregularities and the background ionization. Mid-latitude observations are emphasized because the results to be given apply to these regions of the globe.

2.0 Radio Star Observations

The first observations of scintillations used radio sources. Results such as those presented by Briggs (1964), showed that for Cambridge, England observing the circumpolar source Cassiopeia A, scintillation was predominantly a night time phenomena. There was no seasonal variation. This question of seasonal effects is impossible to study properly using a single radio star because of the seasonal variation in the zenith angle at a fixed solar time.

Briggs also noticed that daytime scintillation occurred during sunspot maxima. He suggested that this was due to the southward extension of the auroral zone irregularities. Earlier, in the southern hemisphere, Bolton et al. (1953) showed by combining observations from three sources low in the northern sky, that the diurnal variation was doubly peaked and that a seasonal variation also occurred with minima at the equinoxes. The second diurnal peak at midday was confirmed by Smerd and Slee (1966) using observations of sources over 1955-1959 at a range of zenith angles. They found however that little seasonal variation was observed. They attribute the earlier observation to the spurious effects of the diurnal variation. Wild and Roberts (1956) had observed this double peak. They found that the daytime scintillation occurrence was related to sporadic E layers.

3.0 Satellite Observations

Observations of scintillation on low orbit satellite transmitters give a good picture of the spatial variations. However the diurnal and seasonal effects can only be obtained by averaging. Most satellite orbits precess in such a manner that the local time of observation gets earlier every day. The time for a complete diurnal cycle depends on the inclination. It is possible to put satellites

in such an orbit that the local time at which the equator is crossed stays the same. Meteorological observation satellites use such orbits. However no transmitters on a low enough frequency have been put into such an orbit.

The diurnal variation of occurrence of irregularities using satellite transmissions shows a small but definite occurrence of daytime scintillation. This is not as definite during sunspot maxima as the results of Yeh and Swenson (1964) show, but appears in their results for 1962. They also show that a seasonal variation in the average index occurs, with a maximum at the autumnal equinox and a minimum during the summer for night time indices, and a winter maxima and summer minima for daytime scintillation. They were observing at Urbana, Illinois (40°N, 88°W). Aarons et al. (1964) using observations of Transit 4A on 54 MHz, showed that scintillation was predominantly a night time phenomenon but that a secondary peak of occurrence occurred near noon in summer. Winter average scintillation was down, compared with other seasons.

The most extensive study of the morphology and occurrence of scintillation was done by Preddey and Mawdsley (1969). For stations in the Australasian region plus Alaska, they show both latitudinal and seasonal and diurnal variations. For a position corresponding to the sub-ionospheric point of the stationary

satellite observations, the daytime scintillation shows minima during the equinoxes. Night time scintillation shows two peaks in early summer and in winter. The ratio of mean scintillation index for day and night was greater than five for all seasons.

Observations by the joint satellite studies group (1968) showed that during March to July, 1965, at two northern hemisphere stations near the edge of the mid-latitude region, daytime scintillations were also noticed. Jones (1968) presents the results of mean scintillation indices for October 1964 to October 1965 for S-66 (1964 64A) observations from Brisbane. They show the same effects observed in New Zealand. The only other results are those of Singleton (1969) who showed the diurnal and latitudinal changes in scintillation and bottom and topside spread F and topside ducting. On examination his results show the same results as quoted above, that is night time and daytime scintillation is lower at the equinoxes than at other times.

Observations of scintillations of stationary satellites show that for North America daytime scintillation only occurs in the summer. It has been reported by Aarons et al. (1969) and Checcacci (1966). Observations reported by Allen (1969) for Hamilton, Mass., for 1967 and 1968 show a daytime peak in winter as well. During summer the two peaks were about of equal size while the winter daytime peak in mean scintillation index was only a quarter the height

of the night time peak. This was mainly because the winter night-time scintillation was much more than the summer. This is different from results for a similar geomagnetic latitude in the southern hemisphere.

There is a strong relationship between the presence of sporadic E and the day time scintillation. Jones (1968) showed that the best correlation was achieved by using the difference between the sporadic E critical frequency and the frequency at which sporadic E obscures the observation of higher layers. This is a measure of the range of electron density in the sporadic E layer. So much daytime scintillation is probably due to irregularities at E region heights. Jones finds a significant correlation between sporadic E and night time scintillation also. But the correlation between a spread F index and night time scintillation index was higher.

4.0 Observations (Data Handling)

The hourly values of scintillation index were found for days from September 15, 1969 to May 24, 1970, with gaps for various breakdowns. The method of assigning the index is given in Chapter 3. The night-time period was arbitrarily defined as 21 hours to 04 hours Eastern Australian standard time (E.A.S.T.). Daytime was

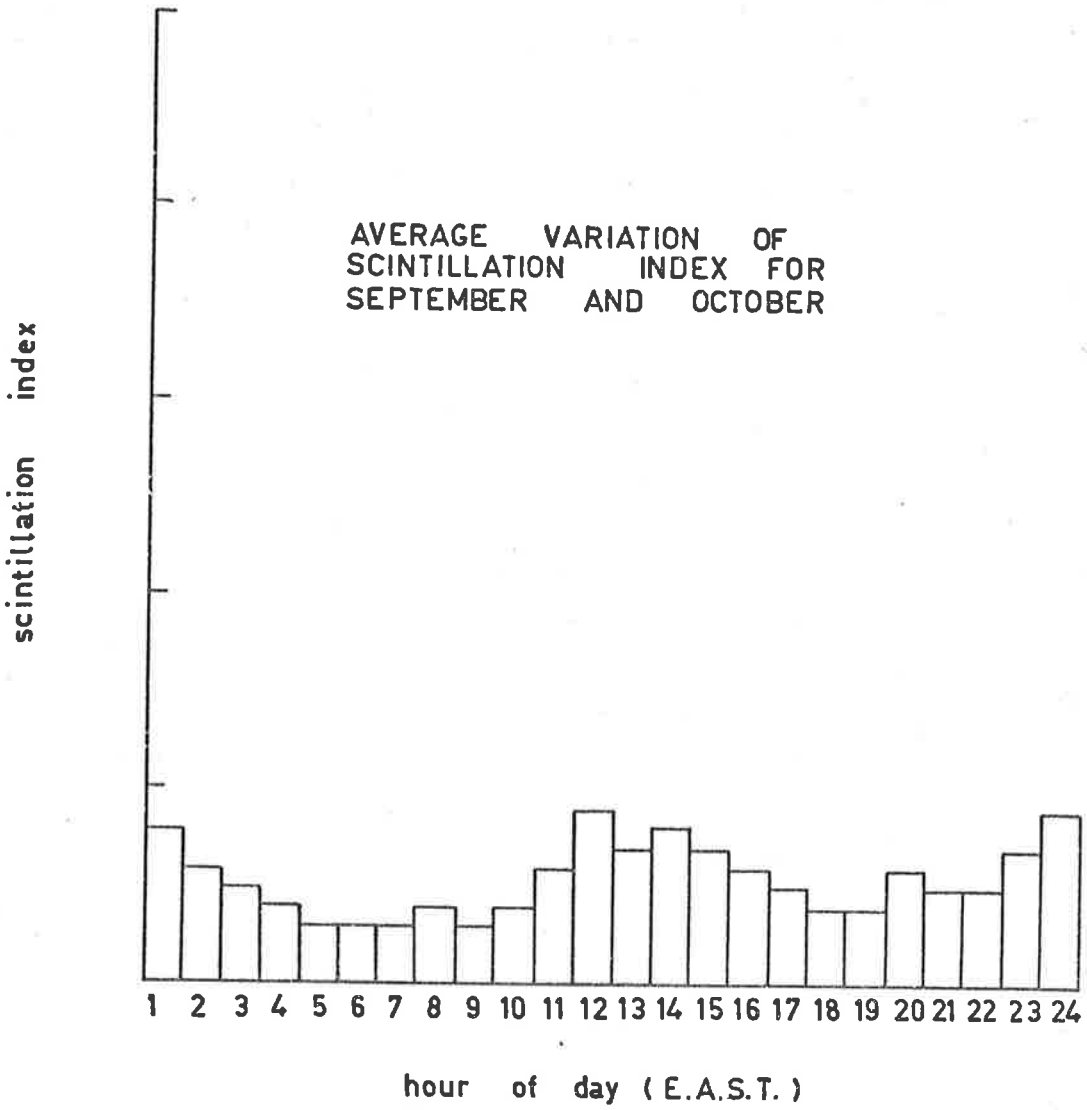

Figure 8.1 Average diurnal variation of scintillation index for September and October, 1969.

defined as the hours between 08 hours to 17 hours E.A.S.T. Average daily night time and daytime indices were calculated by averaging the hourly indices in the above intervals. Also average monthly and longer averages of the diurnal variation were taken. The 3-hourly K index from the Toolangi magnetic observatory were summed over a day to derive an index of daily magnetic activity. Because no ionosonde is within 200 km of the sub-ionospheric point no correlation with spread F or sporadic E was attempted.

5.0 Results

The diurnal variation of scintillation index for September and October combined is shown in Figure 8.1. Two peaks occur at midnight and midday. They are of nearly equal height with the peak average index at night just a little greater than the daytime peak. The results for January and December, Figure 8.2, also show two peaks, with the daytime peak being distinctly lower. These results show the two distinct types of diurnal variation.

The average night time and daytime index, taken from the montly curves are shown in Figure 8.3. They show a maximum for December for both day and night indices, and another peak in May. From visual examination of the scintillation records for June, it could be that the scintillation index in June peaks, but no

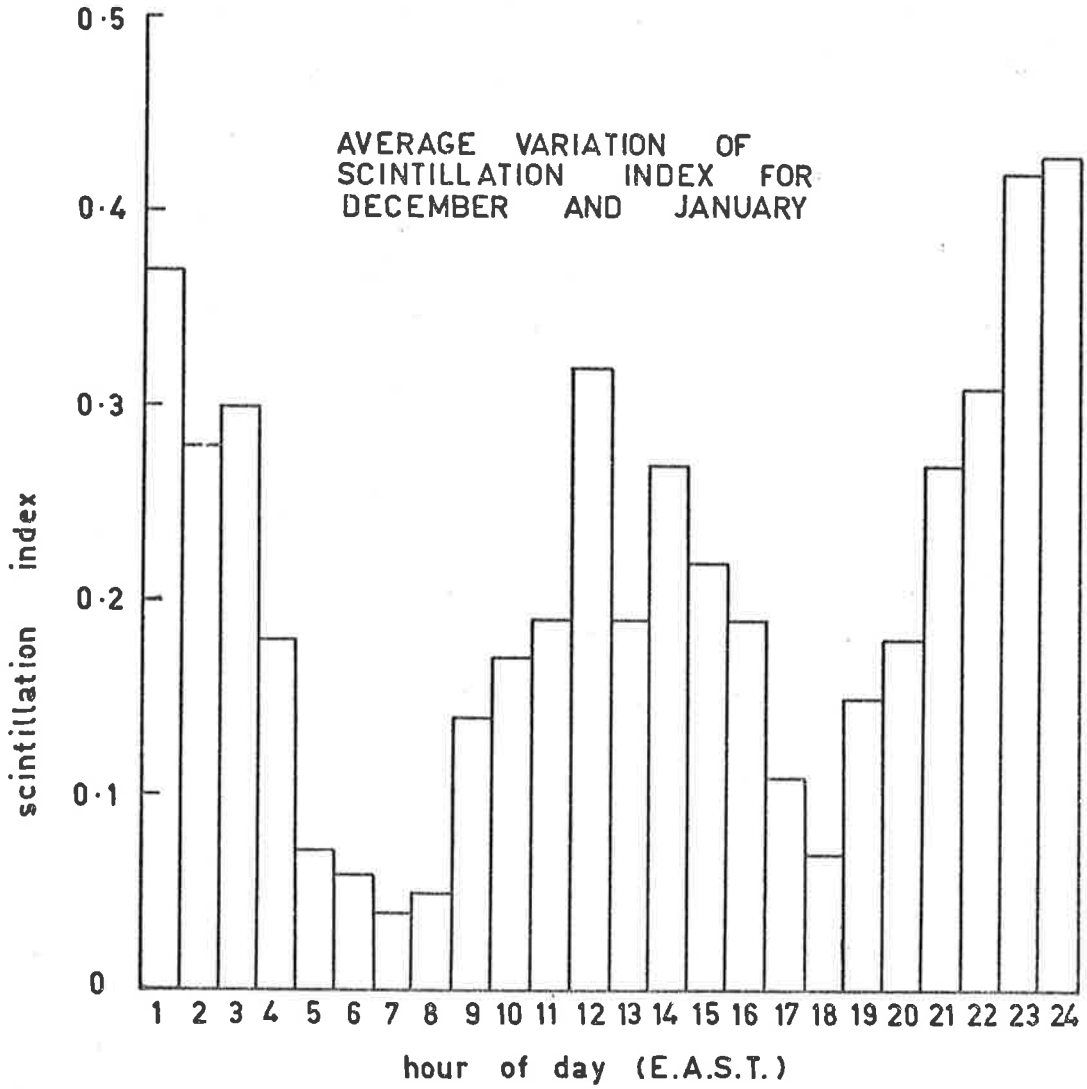

Figure 8.2 Average diurnal variation of scintillation index for January, 1970 and December 1969.

figures can be given.

The cross correlation between daytime and night time indices is shown in Figure 8.9. This shows that daytime and night time indices are correlated at the one percent level of significance. The maximum occurs such that night time indices are best correlated with scintillation for the previous day. The auto-correlation functions for night and day are given in Figure 8.5. Both show the fact that the indices show an alternating characteristic. This has never been noted before.

A cross correlation between the indices and magnetic activity was carried out. The result was that there was no significant correlation for either day or night.

6.0 Discussion

The semi-annual variation in indices is as reported by Jones (1968). It would also seem to be similar to the results of Preddy and Mawdsley (1969). The results show that the daytime scintillation shows a distinct maximum around noon for both summer and early winter, and the two equinoxes. However the peak is sharpest and highest in summer. This suggests a correlation with sporadic E. The night time scintillations seasonal variation is different from

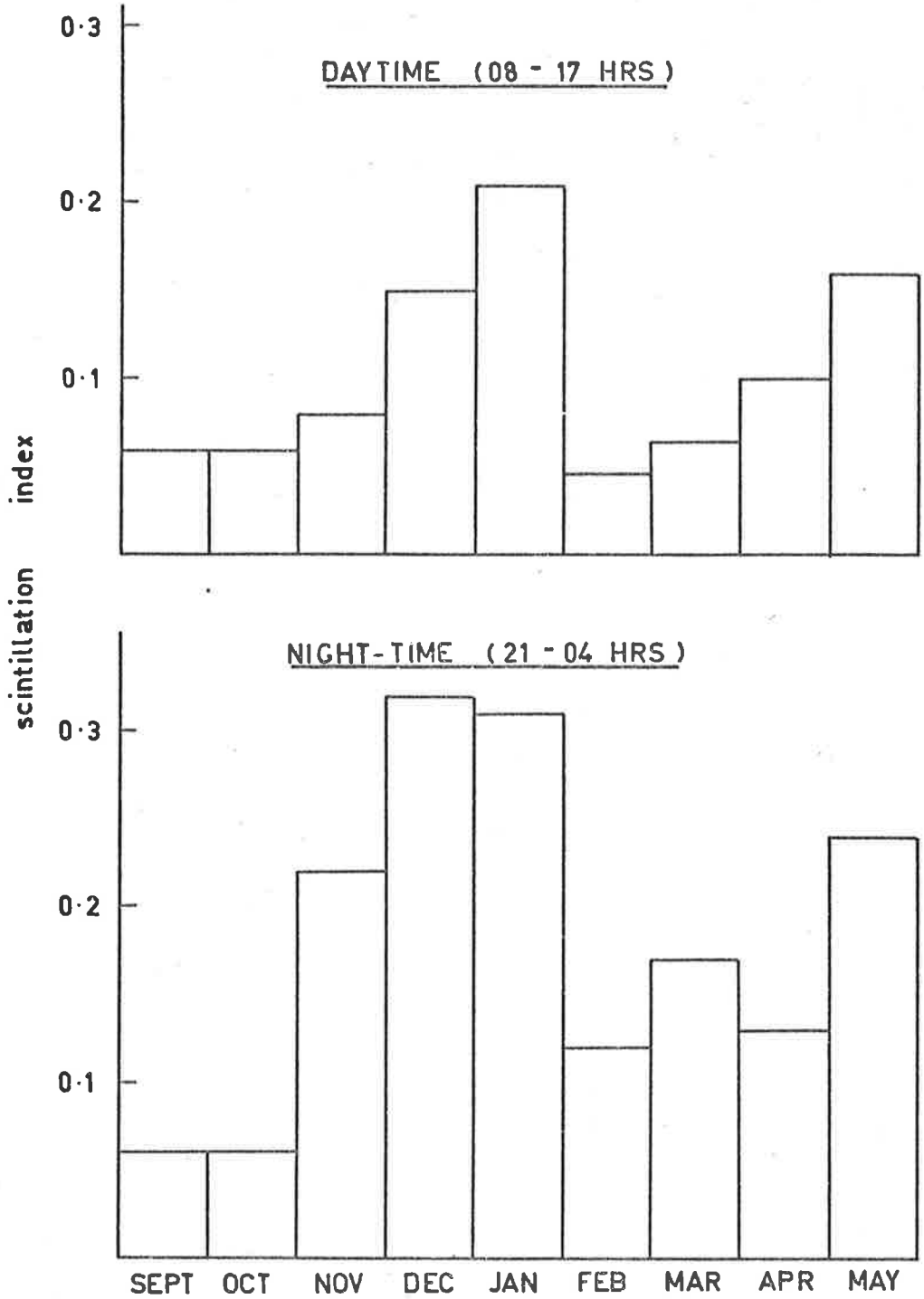

Figure 8.3 Night-time and day-time averages of the average monthly diurnal variation.

that of spread F, which is often suggested as a related phenomena. This may be caused by height variations causing blanketing effects in summer, or the two phenomena may not be directly related. It should be noted that for years of low solar activity, spread F at Brisbane, the nearest ionosonde, does exhibit a semi-annual variation in occurrence.

This seasonal variation is in contrast to the lack of seasonal effects found by Smerd and Slee (1966). However their results were indirect so that these much more direct results take precedence. The diurnal variation reported agrees with their result, and with the result of Bolton et al. (1953), to which it is more exactly comparable, both observations being at a low angle.

The lack of correlation with magnetic activity fits in with what Jones (1968) found for Brisbane also. It also agrees with the result in Chapter 2 where no correlation was found between spread F at Woomera and magnetic activity. As scintillation and magnetic activity are positively correlated at and just below the auroral zone, and negatively correlated near the equator, there must be a region where no correlation can be found. The result here suggests it is at about geomagnetic latitude 41°S in the Australasian region.

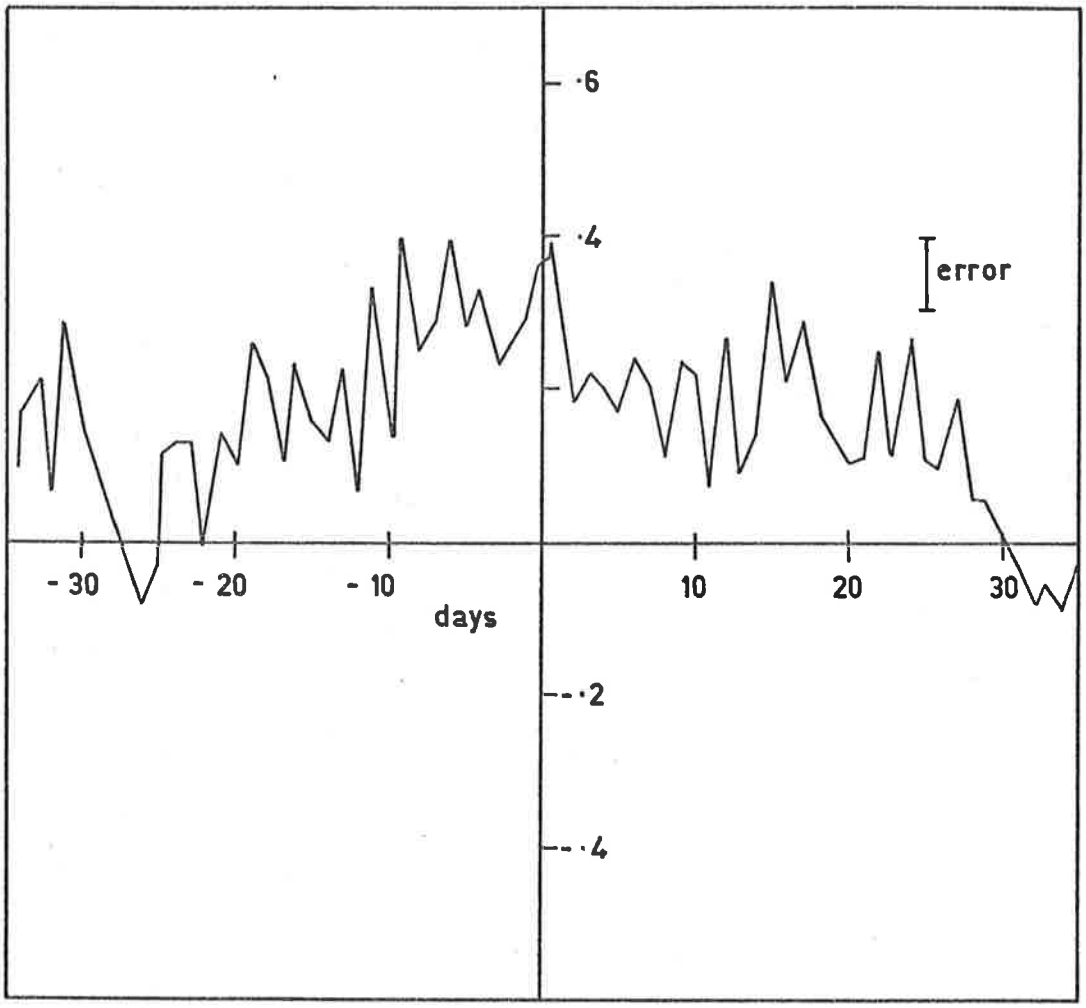

Figure 8.4 Cross-correlation between day-time and night-time indices.

7.0 Conclusion

At the declining part of the sunspot cycle, scintillation in the Australian region shows a daytime peak as well as a night time peak in the average diurnal variation of scintillation index. There is also a strong seasonal variation with peaks during winter and summer and minima at the equinoxes, and no correlation with magnetic disturbances.

Figure 8.5 Auto-correlation functions for night-time and day-time indices.

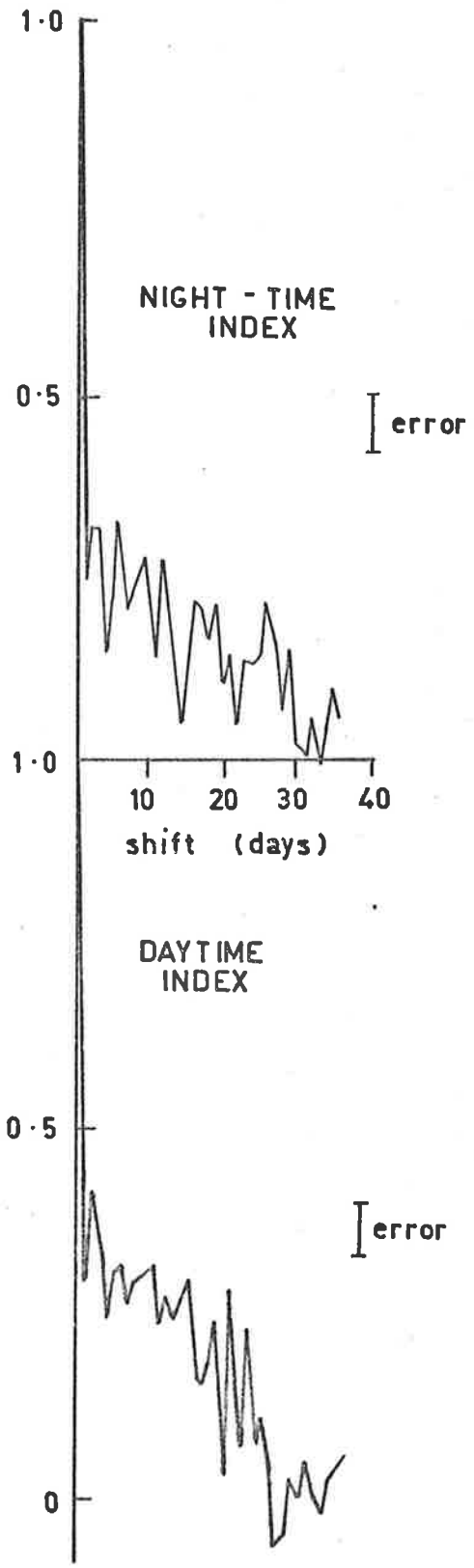

CHAPTER 9

SUMMARY OF CONCLUSIONS

1.0 Introduction

Here I summarise the conclusions of the various sections and make some broad conclusions and some suggestions for further work.

2.0 Summary of Conclusions

Spread F at Woomera has no significant correlation with magnetic activity. Woomera seems to be in the transition region between the equatorial and mid-latitude zones of spread F. No correlation was found between spread F at Woomera and changes in atmospheric density. The seasonal variation of spread F occurrence at Woomera has two peaks, a variable one in summer and a strong one in winter. Minima occur near the equinoxes. The variation of spread F at Canberra, the next most southerly location at which there is an ionosonde, is different, showing no summer peak. Spread F at Brisbane shows a variable summer peak of occurrence. It is suppressed during sunspot maximum.

The number of larger scale irregularities in a size interval S to S + dS, satisfies the rule that it is proportional to dS/S

over the observed range km to km when the effect of observational selection is allowed for. The large irregularities are stronger in winter. The diurnal variation is similar to that found by Titheridge (1968a). The observed sizes and magnitudes are in the range possible for internal gravity waves.

The average value for Qo, the overhead sun integrated production rate is in reasonable agreement with previous observations. The form of the diurnal variation in total electron content was similar to other observations. The form of the night-time variation suggested a source of ionization for several hours either side of midnight.

T.I.D.'s were observed, some of which were quasi-sinusoidal. The periods of oscillations observed were in the range expected for the geometrical situation involved. A suspected aurorally caused T.I.D. was seen and a large increase in total electron content was detected during the magnetic storm of Aug 17, 1970. No solar flare effects were seen.

Small very dense irregularities exist in the ionosphere. They are only a few kilometres across, and are usually at least 50% above or below the ambient electron density.

Sometimes it is possible to calculate the height of the

irregularities which cause satellite scintillation by a method only involving one receiver. This involves finding the first minimum of the "fringing function" in the power spectrum of the amplitude fluctuations. A restriction to the general applicability of this method arises because usually the irregularity size is too large.

Full correlation analysis should only be attempted on spaced satellite receivers when the maximum cross-correlation is greater than 0.7.

Lastly from Chapter 8 the following properties of satellite scintillation are deduced. There is a daytime peak as well as the well known night time peak in the average diurnal variation. A strong seasonal variation exists with minima at the equinoxes.

3.0 General Conclusions

While the observations reported in this thesis cannot be used to decide directly between one theory and another, it is hoped that they will provide a contribution to the general body of observational knowledge about ionospheric irregularities which is continually being built up, and that this body of knowledge will eventually lead to a decision as to the mode of formation of the irregularities.

4.0 Suggestion for More Observation

Firstly work should be carried out on the power spectrum of satellite scintillation near the magnetic equator to see whether the minima suggested in Chapter 7 does show up.

Secondly more spaced receiver work should be done on daytime satellite scintillation using orbitting satellites, so as to determine whether these irregularities are in the E region.

BIBLIOGRAPHY

Aarons, J., Mullen, J., Basu, S. (1964) J. Geophys. Res. 69, 1785.

Aarons, J., Whitney, H.E., Allen, R.S. (1969) AFRCL Environmental Research report No. 296.

Allen, R.S. (1969a), J. Atmos. Terr. Phys. 31, 289.

Allen, R.S. (1969b) AFCRL Agardograph Report 1.

Alpert, Ya.L., Sinelnikov, V.M. (1966) Plan. Space Sci. 14, 313.

Appleton, E.V., Piggott, W.R. (1952), J. Atmos. Terr. Phys. 2, 236.

Basu, S. (1969) J. Geophys. Res. 74, 1294.

Bhonsle, R.V., Da Rosa, A.V., Garriott, O.K. (1965) Radioscience 69D, 929.

Bhonsle, R.V. (1966), J. Geophys. Res. 71, 4571.

Bolton, J.G., Slee, O.B., Stanley, G.J. (1953) Aust. J. Phys. 6, 34.

Booker, H.G. (1956) J. Geophys. Res. 61, 673.

Bordeau, R.E. (1962), Goddard Space Flight Centre Report X-615-62-99.

Bowhill, S.A. (1961), J. Res. NBS 65D, 275.

Bowman, G.G. (1960a), Plan. Space Sci. 2, 133.

Bowman, G.G. (1960b), Plan. Space Sci. 2, 150.

Bowman, G.G. (1964), Nature 201, 4919.

Bowman, G.G. (1971), Nature 229, 117.

Bramley, E.N. (1953), Proc. Roy. Soc. A 220, 39.

Briggs, B.H. (1958a), J. Atmos. Terr. Phys. 12, 34.

Briggs, B.H. (1958b), J. Atmos. Terr. Phys. 12, 89.

Briggs, B.H. (1964), J. Atmos. Terr. Phys. 26, 1.

Briggs, B.H. (1965), J. Atmos. Terr. Phys. 27, 991.

Briggs, B.H. (1963), J. Atmos. Terr. Phys. 30, 1777.

Budden, K.G. (1965), J. Atmos. Terr. Phys. 27, 155.

Checcaci, P.F. (1966), Radio Science 1, 1154.

Chan, K.L., Villard, J.R. (1962), J. Geophys. Res. 67, 973.

Chimonas, G. (1970), Plan. Space Sci. 18, 591.

Clark, D.H., (1971), J. Atmos. Terr. Phys. 33, 1267.

Davies, K., Jones, J.E. (1971), J. Atmos. Terr. Phys. 33, 39.

Davis, M., Da Rosa, A.V. (1969), J. Geophys. Res. 74, 5721.

Elkins, T., Slack, F.F. (1969), J. Atmos. Terr. Phys. 31, 421.

Fooks, G.F., (1965), J. Atmos. Terr. Phys. 27, 979.

Garriott, O.K. (1960), J. Geophys. Res. 65, 1139.

Garriott, O.K. Da Rosa, A.V., Davis, M., Villard, O.G. (1967), J. Geophys. Res. 72, 6099.

Garriott, O.K. Da Rosa, A.V., Ross, N.J. (1970), J. Atmos. Terr. Phys. 32, 705.

Garriott, O.K., Smith, F.L., Yuen, P.C. (1965), Plan. Space Sci. 13, 829.

Garriott, O.K., Smith, F.L. (1965), Plan. Space Sci. 13, 839.

Georges, T.M. (1968), J. Atmos. Terr. Phys. 30, 735.

Georges, T.M., Hooke, W.H. (1970), J. Geophys. Res. 75, 6295.

Heisler, L.H. (1958), Aust. J. Phys. 11, 79.

Hewish, A. (1951), Proc. Roy. Soc. A209, 81.

Hibberd, F., Ross, W.J. (1967), J. Geophys. Res. 72, 5331.

Hines, C.O. (1960), Can. J. Phys. 38, 1441.

Hooke, W.H. (1970), J. Geophys. Res. 75, 5535.

Hunsucker, R.D. Tveten, L.H. (1967) J. Atmos. Terr. Phys. 29, 909.

I.E.E.E. (1970), Conference Proceedings No. 77.

Ireland, W., Preddey, G.F. (1967), J. Atmos. Terr. Phys. 29, 137.

Jacchia, L.G. (1965), Smithson Contr. Astrophys. 8, 215.

Jacchia, L.G., Slowey, J. (1963), Smithson. Contr. Astrophys. 8, 1.

Joint Satellite Studies Group (1968), Plan. Space Sci. 16, 1277.

Jones, K.L. (1968), Plan. Space Sci. 16, 1475.

Jones, K.L. (1971), J. Atmos. Terr. Phys. 33, 379.

Jones, K.L. Risbeth, H., (1971), J. Atmos. Terr. Phys. 33, 391.

King, G.A.M. (1970), J. Atmos. Terr. Phys. 32, 209.

Koster, J., Kent, G.S. (1966), Ann. de Geophys. 22, 405.

Lawrence, R.S. Jesperson, J.L. (1961), Space Reserach II, p277, North Holland Pub. Co.

Little, G.C., Lawrence, R.S. (1960) Space Research I, p340, North Holland Pub. Co.

Lovelace, R.V. Saltpeter, E.E., Sharp, L.E., Harris, D.E. (1970), Ap. J. 159, 1047.

McNicol, R.W.E., Webster, H.C., Bowman, G.G. (1956), Aust. J. Phys. 9, 247.

de Mendonca, R. (1962), J. Geophys. Res. 67, 2315.

Munro, G.H. (1948), Nature 162, 886.

Munro, G.H. (1950), Proc. Roy. Soc. A202, 208.

Munro, G.H. (1958), Aust. J. Phys. 11, 91.

Papagiannus, M.D., Mendillo, M. Klobuchar, J. (1971), Plan. Space Sci. 19, 503.

Parkin, I.A. (1967), Ph.D. Thesis, University of Adelaide.

Preddey, G.F., Mawdlsey, J. (1969), Plan. Space Sci. 17, 1161.

Rao, N.N. (1967), J. Geophys. Res. 72, 2929.

Raju, P.T.S., Rao, B.R. (1969), J. Atmos. Terr. Phys. 31, 869.

Reber, G. (1965), J. Geophys. Res. 61, 157.

Shimazaki, T. (1969), J. Rad. Res. Lab. 6, 669.

Singleton, D.G. (1962), Aust. J. Phys. 15, 242.

Singleton, D.G. (1969), J. Geophys. Res. 74, 1772.

Slee, O.B. (1962), Aust. J. Phys. 15, 568.

Smerd, S.F., Slee, O.B. (1966), Aust. J. Phys. 19, 427.

Smith, D.H. (1970), J. Geophys. Res. 75, 823.

Smith, F.L. (1968), J. Geophys. Res. 73, 7385.

Testud, J. (1970), J. Atmos. Terr. Phys. 32, 1793.

Thome, G. (1968), J. Geophys. Res. 73, 6319.

Titheridge, J.E. (1963), J. Geophys. Res. 68, 3399.

Titheridge, J.E. (1966), J. Atmos. Terr. Phys. 28, 1135.

Titheridge, J.E. (1968a), J. Atmos. Terr. Phys. 30, 73.

Titheridge, J.E. (1968b), J. Geophys. Res. 73, 243.

Titheridge, J.E. (1968c), J. Geophys. Res.7 3, 2985.

Titheridge, J.E. (1968d), J. Atmos. Terr. Phys. 30, 1857.

Titheridge, J.E. (1968e), J. Atmos. Terr. Phys. 30, 1843.

Titheridge, J.E. (1969), J. Geophys. Res. 74, 1195.

Titheridge, J.E. (1971), J. Atmos. Terr. Phys. 33, 47.

Titheridge, J.E. (1971a), J. Geophys. Res. 76, 6955.

Titheridge, J.E., Andrews, M.K. (1967), Plan. Space Sci. 15, 1157.

Warwick, J.W.C. (1964), J. Res. N.B.S. 68D, 179.

WDC-A (1970), World Data Centre A, Report UAG-15.

Webster, A.R. (1967), J. Atmos. Terr. Phys. 29, 793.

Wild, J.P., Roberts, J.A. (1956), Nature 178, 377.

Yeh, K.C., Swenson, G.W. (1964), J. Res. NBS 68D, 881.

Young, D.M.L., Yuen, P.C., Roelofs, T.H. (1970), Plan. Space Sci. 18, 1163.